UNIVERSITÀ DEGLI STUDI DI MILANO

PhD Course in Veterinary and Animal Sciences (Cycle XXXIII)

Department of Veterinary Medicine

Identification of tumor-associated molecules as suitable biomarkers of cancer in dogs using OMIC approaches

(VET/03)

VALENTINA ZAMARIAN

R12073

SUPERVISOR: PROF. CRISTINA LECCHI

PHD PROGRAM COORDINATOR: PROF. VALERIA GRIECO

Academic Year 2019 – 2020

Index

Index of Figures

Abbreviations

ACVR2A: Activin A Receptor Type 2A

ADAMTS2: ADAM metallopeptidase with thrombospondin type 1 motif 2

AF4: asymmetric flow field-flow fractionation

AKT: AKT Serine/Threonine Kinase

APOBEC3A: Apolipoprotein B MRNA Editing Enzyme Catalytic Subunit 3A

ARHGEF: Rho Guanine Nucleotide Exchange Factor

ASV: amplicon sequence variant

ATP: Adenosine triphosphate

AUC: area under the curve

BLC2: BCL2 Apoptosis Regulator

BMP4: Bone Morphogenetic Protein 4

CAF: cancer associated fibroblast

CCDC80: coiled-coil domain containing 80

CLEC: C-type lectin domain

CLEC: C-Type Lectin Domain Containing

c-MYC: MYC Proto-Oncogene, BHLH Transcription Factor

COL: collagen

CRISPLD2: cysteine rich secretory protein LCCL domain containing 2

ctDNA: irculating tumor DNA

CuMM: cutaneous malignant melanoma

CXCL12: C-X-C Motif Chemokine Ligand 12

DE-miRNA: differentially expressed miRNA

DGCR8: DGCR8 Microprocessor Complex Subunit

Dicer: Dicer 1, Ribonuclease III

Drosha: Drosha Ribonuclease III

EV: extracellular vesicle

Exp5: Exportin 5

FC: fold change

FERMPD: a gene encodes a multi-domain (WW, PDZ, FERM) containing protein

FF: fresh frozen

FFPE: formalin-fixed paraffin-embedded

FOS: Fos Proto-Oncogene

HDAC: Histone Deacetylase

HOM: healthy oral mucosa

HS: healthy skin

HSPA9: Heat Shock Protein Family A (Hsp70) Member 9

HTR: Hydroxytryptamine Receptor

Ki-67: Marker of Proliferation Ki-67

KIT: KIT Proto-Oncogene, Receptor Tyrosine Kinase

KLHL: Kelch Like Family

LC: liquid chromatography

LOX: lysyl oxidase

MAC: macrophages

MALDI: matrix-assisted laser desorption/ionization

MCT: mast cell tumor

miRNA: micro-RNA

MMP9: Matrix Metallopeptidase 9

MMPs: matrix metallopeptidase

MS: mass spectrometry

mTOR: Mechanistic Target of Rapamycin Kinase

NDRG2: NDRG Family Member 2

NF: normal fibroblasts

NF2: Neurofibromin 2

NF-kB: Nuclear Factor Kappa B

NGS: next generation sequencing

NRAS: NRAS Proto-Oncogene, GTPase

NTA: Nanoparticle tracking analysis

OMM: oral malignant melanoma

p53: Tumor Protein P53

PACT: protein activator of PKR

PAX9: Paired Box 9

PDIA3: Protein Disulfide Isomerase Family A Member 3

PI3K: Phosphatidylinositol 3-kinase

PIK3RA: Phosphoinositide-3-Kinase Regulatory Subunit 3

PTMs: posttranslational modification

qPCR: quantitative PCR

RAN-GTP: RAN, Member RAS Oncogene Family

RISC: RNA-induced silencing complex

ROC: Receiver operating characteristic

rRNA: ribosomal RNA

SCFAs: short-chain fatty acids

SEC: size exclusion chromatography

SENP7: SUMO Specific Peptidase 7

SGIP1: SH3 domain GRB2-like endophilin interacting protein 1

SOCS: suppressor of cytokine signaling

SPRY: Sprouty RTK Signaling Antagonist

STRN: Striatin

TCP1A: T-Complex 1 alpha subunits

TCP1E: T-Complex 1 epsilon subunits

TGF-β: Transforming Growth Factor Beta

TLR4: Toll Like Receptor 4

TNM: Tumor, node and metastasis staging

TOF: time-of-flight mass spectrometer

TRBP: TARBP Subunit of RISC Loading Complex

UTR: Untranslated region

WHO: World Health Organization

Abstract

Omics techniques have been widely applied to veterinary science, although mostly on farm animal productions and infectious diseases. In canine oncology, on the contrary, the use of omics methodologies is still far behind. This thesis aims to fill in the gap in the molecular background of canine cancer tumors and to apply this new knowledge for the identification of suitable biomarkers mainly based on the identification and quantification of microRNAs. The thesis applied next generation sequencing (NGS) to investigate onco-miRNome and skin microbiota of one of the most relevant, highly metastatic canine malignant tumor, the mast cell tumor. The results of miRNomic have been validated by RT-qPCR to develop molecular tools to enhance the robustness of clinical decision-making. To elucidate the host-tumor interaction, the skin and dermis microbiota of MCT-affected dogs has been investigated as well. This thesis aims also to characterized the proteomic profiles of exosomes purified from plasma of MCT-affected dogs. Due to the pandemic situation, the protocol for exosome purification has been developed, while the proteomic analysis is still ongoing. Finally, a very preliminary evaluation of miRNA dysregulation in canine oral and cutaneous melanoma was carried out.

To characterize the epigenetic modulation of MCT microenvironment and to identify a panel of miRNAs dysregulated during the neoplastic process and suitable as biomarkers, the miRNome of canine MCT was profiled on FFPE samples using an NGS approach; the result was then investigated also in saliva samples of MCT-affected dogs. The NGS findings revealed that 63 miRNAs were differentially expressed between MCT and healthy adjacent margins (45 down-regulated and 18 up-regulated). A panel of nine miRNAs was validated by qPCR, of which five were dysregulated in the tumor. Specifically, miR-21 and miR-379 were up-regulated while miR-885, miR-338 and miR-92a were down-regulated in the MCT compare to the healthy margins. A further analysis including the variable of the lymph node involvement in the tumor, revealing that a panel of three miRNAs, miR-

21, miR-379, and miR-885, was able to discriminate metastatic from non-metastatic MCTs. The diagnostic potential of the panel was also explored in the saliva of MCT-affected dogs, showing that miR-21 and miR-885 discriminated tumor-affected from healthy dogs; miR-885 could also discriminate the metastatic from the non-metastatic MCTs with good diagnostic potential, make this miRNA attractive for a future diagnostic purpose starting form a less-invasive matrix.

The microbiota of the MCT associated with the skin surface and dermis was characterized for the first time investigating alpha diversity which describes the differences of taxa by qualitative and quantitative approaches and beta diversity which describes the differences between groups generating distance matrices between samples. The data showed that a reduction of taxa was present in the tumor skin surface compared with the healthy contralateral part with an increase of Firmicutes phylum and *Corynebacteriaceae* family. A similar reduction of taxa found out in the tumor dermis compared with the overlying tumor skin surface. These differences exerted an impact also in beta diversity, which highlighted the differences between the samples. The characterization of the core microbiota of the tumor and healthy skin surface and the tumor dermis showed that the healthy skin was characterized by a higher number of ASVs (27 ASVs) compared to the tumor skin surface (12 ASVs) and dermis (16 ASVs) and that 10 ASVs were present only in the tumor site. The data proved that the presence of the tumor interfered in some way with the microbial population, paving the way for further investigations on host-microbiota interaction. Moreover, the reduction of microbiota diversity and taxa was seen to be associated with an unhealthy status.

A protocol for the purification of plasmatic exosome from dog affected by MCT was developed to obtain samples with a good degree of purity and suitable for proteomic analysis, that may elucidate the cell-to-cell communication strategy used by MCT to prepare the metastatic niches, and may promote the identification of suitable biomarkers for the MCTs diagnosis and prognosis. The Size Exclusion Chromatography purification approach was identified as the best approach to obtain

samples depleted from the most abundant plasmatic protein, including albumin, and exosomes in the right size range and with concertation feasible for further proteomic analysis.

Finally, the potential of a target miRNAs panel was also evaluated in canine cutaneous and oral malignant melanoma. The data showed that, among six miRNAs selected from the bibliography, miR-145, miR-365, miR-146a, and miR-425 were differentially expressed in canine melanoma. In detail, miR-145 was down-regulated in cutaneous and oral melanoma and miR-365 was down-regulated in cutaneous melanoma. On the other hand, miR- 146a and miR-425 were up-regulated in cutaneous melanoma. The gene ontology analysis suggested that these miRNAs may have a role in tumor progression and cell proliferation.

Chapter 1. The multi-omics approaches in cancer research

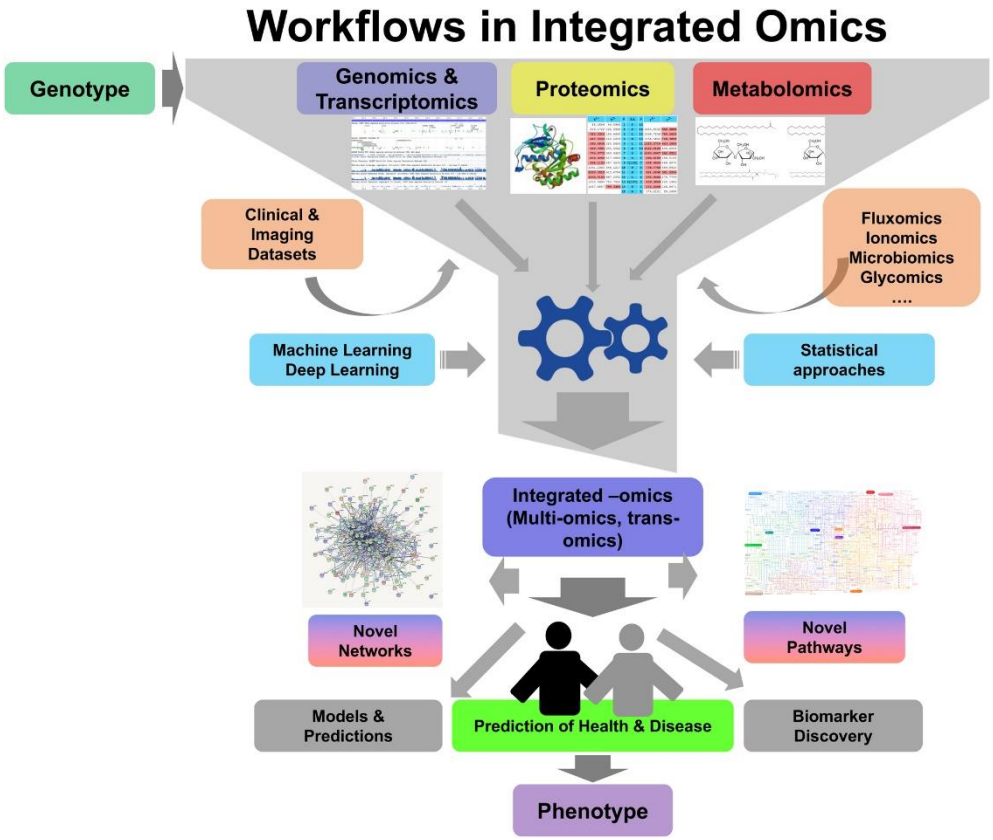

Figure 1 The multi-omics approaches. The integration of the OMICs sciences, including genomics, transcriptomics, proteomics and metabolomics, contributes to the identification and prediction of novel pathways, networks, and biomarkers.
From (Misra et al., 2018)

The new frontier of cancer research is the application of an integrative multi-omics approach to figure up the molecular changes linked to the neoplasm to characterize the tumor features and behavior and at the same time to identify new biomarkers for diagnosis, prognosis, and patient follow-up (Figure 1). The carcinogenic process triggers changes at different molecular levels affecting genome, epigenome, and transcriptome, and protein expression and metabolites production; the modulation of these pathways is exerted by different modulatory players, including non-coding RNAs, such as micro RNAs (miRNAs) (Chakraborty et al., 2018; Lu and Zhan, 2018), and host-microbiota community (de Anda-Jáuregui and Hernández-Lemus, 2020). The number of

information increases in complexity from genome to metabolome and microbiome (Figure 2) due to the increase of output of information.

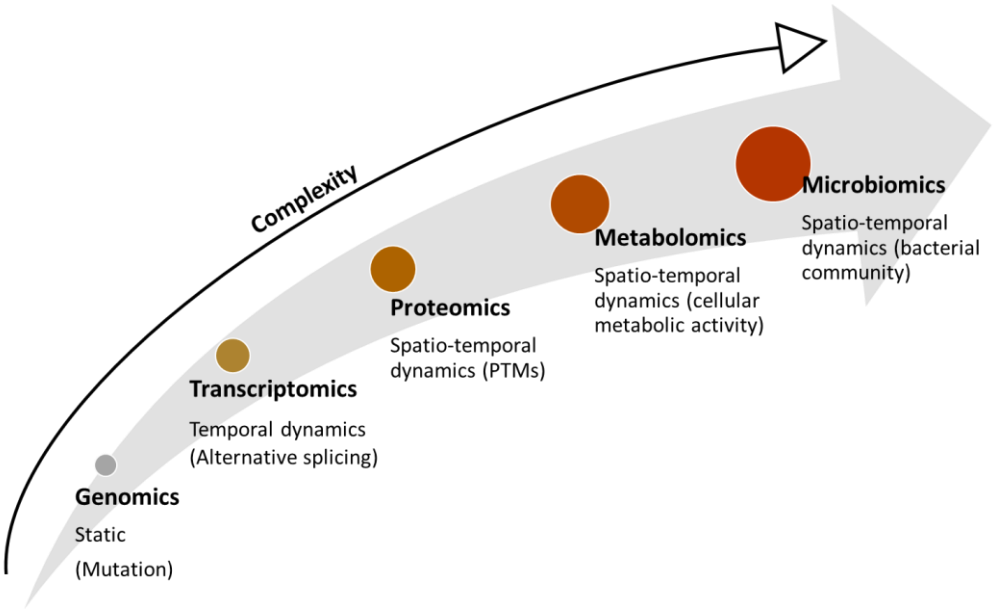

Figure 2 OMICs science in order of complexity due to the increase out-put of information from genomics to microbiomics.
PTMs= post translational modification

The information presents in the genome, like mutations, are largely static but the complexity increases with the gene expression and the introduction of the temporal dynamic and alternative splicing accompanied by transcriptomic, and with the spatio-temporal dynamics in proteomics due to different posttranslational modification (PTMs) and different subcellular localizations of the proteins. The complexity still increases in metabolomics, in which different types of metabolites (amino acid, carbohydrates, and lipids) (Chakraborty et al., 2018) are characterized, and in microbiomics, where alterations of the microbial population are characterized in relation with the tumor (de Anda-Jáuregui and Hernández-Lemus, 2020). The development of new analytical techniques such as next generation sequencing (NGS) and new computational tools allows the application of an integrative omics approach which provides new findings in scientific research (Ohashi et al., 2015; Misra et al., 2018).

1.1 miRNomic

Micro RNA (miRNAs) are small non-coding RNAs (19–25 nucleotides) involved in post-transcriptional regulation of different pathways, including cell cycle, differentiation, proliferation, apoptosis, stress tolerance, energy metabolism, and immune response (Giovannetti et al., 2012). The first miRNA was discovered in *Caenorhabditis elegans* in 1993 (Lee et al., 1993). MiRNA biogenesis is illustrated in Figure 3. In brief, pri-miRNA is transcribed by RNA polymerase II into the nucleus, where the complex Drosha/DGCR8 processes pri-miRNA in the intermediate precursor pre-miRNA, which is transported into the cytoplasm by Exp5/Ran-GTP complex. In the cytoplasm the complex Dicer/TRBP/PACT cleaves the pre-miRNA into double-stranded RNA and is unwound into single strands by the action of helicase. At this point, only one of the two single-strand RNA will be integrated into the RNA-induced silencing complex (RISC) to become a mature miRNA and the other strand will be degraded (Si et al., 2019). Then, miRNAs can be released in vesicles such as exosomes or microvesicles or associated with proteins such as ribonucleoprotein complex (Cui et al., 2019) to mediate cell-to-cell communication and play their role outside of the cell (Wang et al., 2010).

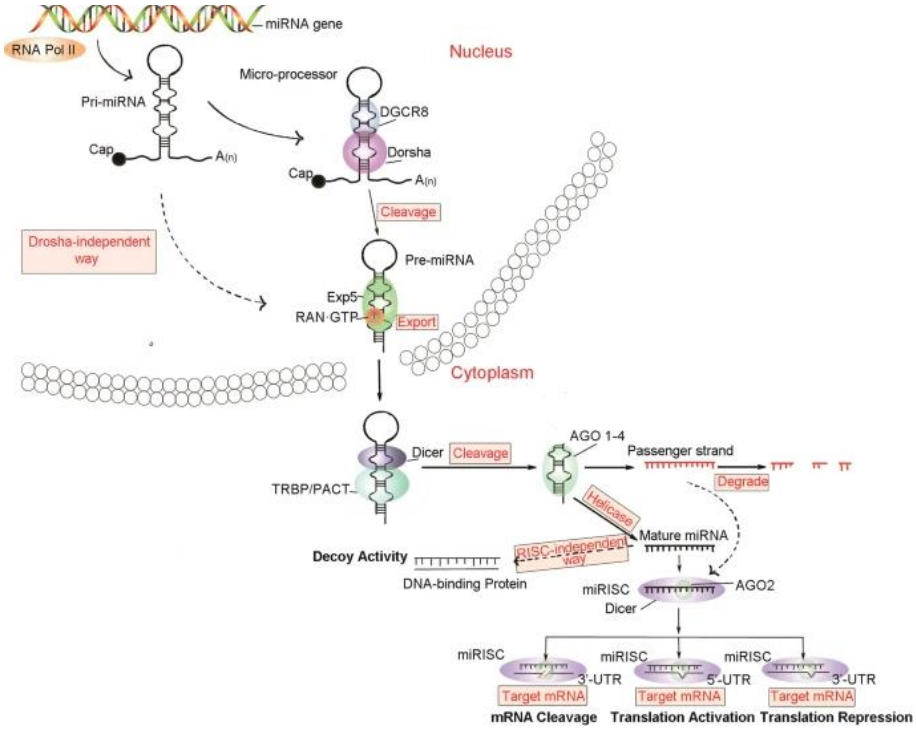

Figure 3 miRNA biogenesis and post-transcriptional regulation. The solid and the dotted arrows represent the classical and non-classical pathways, respectively. The pri-miRNA is transcribed by RNA polymerase II into the nucleus. Drosha/DGCR8 complex processes pri-miRNA in the pre-miRNA, transported into the cytoplasm by Exp5/Ran-GTP complex. The complex Dicer/TRBP/PACT cleaves the pre-miRNA into double-stranded RNA and is unwound into single strands by the action of helicase. One of the two single-strand RNA will be integrated into the RNA-induced silencing complex (RISC) to become a mature miRNA and release to mediate cell-to-cell communication and play their role outside of the cell. The type of binding of the mature miRNA with the target mRNA will define its role. A full complementary binding in the 3'UTR region will lead to the cleavage of target mRNA and a partial binding will lead to repression of translation. On the other hand, a binding in the 5'UTR region will activate the translation.
From (Si et al., 2019)

The interaction of miRNAs with the 3'UTR region of the target mRNA leads to the block of its translation or the mRNA cleavage (Bartel, 2004; Si et al., 2019). In some cases, the binding of miRISC complex with the 5'UTR region of a target mRNA leads to the activation of the translation (Vasudevan et al., 2007; da Sacco and Masotti, 2013).

MiRNAs regulate more than 50% of human genes, among which half are involved in tumorigenesis or located in fragile loci (Calin et al., 2004; Krol et al., 2010). During cancer, miRNAs are dysregulated (Ortiz-Quintero, 2016), acting as tumor-suppressor- or onco-miRNAs (involved in tumor progression), implicated in onset, progression, and metastasis (Di Leva et al., 2014; Sahabi et al., 2018). The ability of the extracellular miRNAs to reach a recipient cell and affect its metabolism is an important strategy in tumorigenesis (Figure 4), especially in the interaction with the immune cells (Gong et al., 2012; Lässer, 2012).

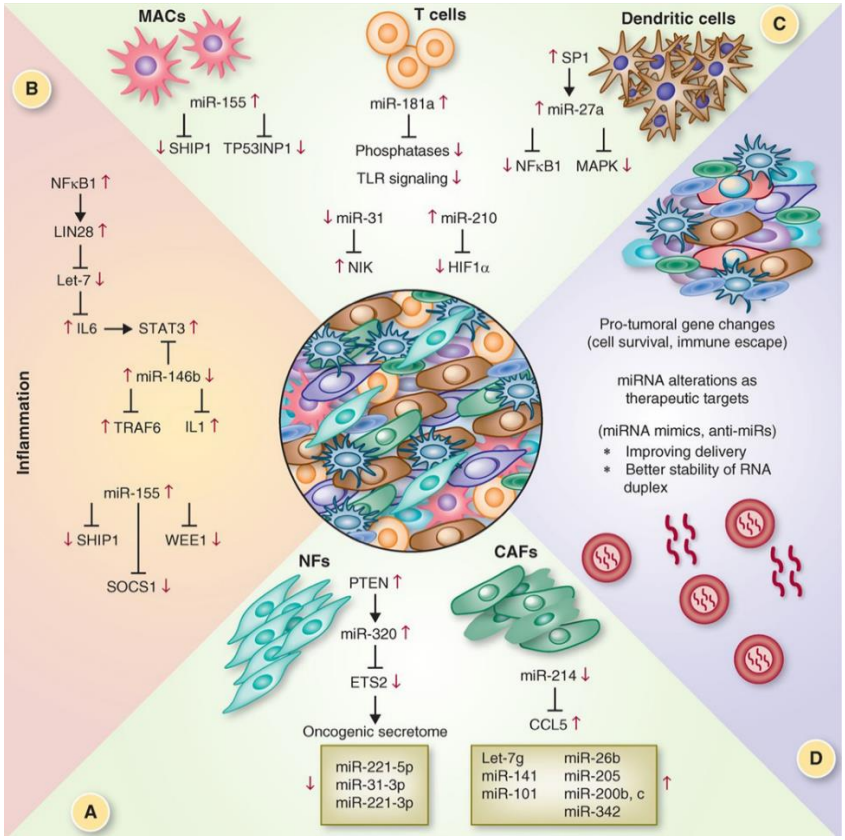

Figure 4 Role of miRNA and target networks in cancer and in tumor microenvironment
(A) miRNAs have a role in normal fibroblasts (NF) to cancer associated fibroblast (CAF) transformation. (B) The inflammatory microenvironment is able to alter the miRNAs expression profile involved in a pro-inflammatory signaling; and (C) the immune cells, such as macrophages (MAC), T cells, and dendritic cells are able to influence the miRNA expression in a tumor promoting phenotype. (D) Nowadays, the new challenge is the developing of miRNA-based cancer therapy finding stable miRNA mimics or anti-miRNAs and stable delivery systems.
From (Rupaimoole et al., 2016)

The characterization of the miRNomic profile associated with the neoplasia by a NGS approach allows to better understand the tumor strategies to reach a diagnosis at the early stage of the disorder and a more precise prognosis. Moreover, the identification of new biomarkers can be used to develop new therapeutically approaches and to predict the response to treatments (precision medicine) (Cui et al., 2019). The role of miRNAs in carcinogenesis has been studied in human and canine cancer as well (Wagner et al., 2013). The quantification of miRNAs differentiates different cancer subtypes, grades, and stages in humans (Chen et al., 2014; Stückrath et al., 2015), and dogs (Bulkowska et al., 2017; Craig et al., 2019) as well. The differences in miRNAs panel were able to characterize the tissue of origin of unknown origin cancers (Rosenfeld et al., 2008). Therefore, miRNAs can play a prognostic and predictive role in disease monitoring, since their expression

change in association with physiological status (Condrat et al., 2020); miRNAs can be also used to predict drug and therapy sensitivity (Jacob et al., 2013; Franchina et al., 2014). To conclude, the new frontier of miRNAs is their application against the tumor applying a miRNA-based cancer diagnosis, prognosis, and therapy monitoring. The therapeutic approach exploits their role as tumor-suppressor or antisense miRNAs delivered in carriers (Cui et al., 2019).

1.2 Proteomic

The characterization of protein profiles and structures demonstrated that different proteoforms are present as a result of combinations of genetic variations. Alternative mRNA splicing and posttranslational modifications (PTMs) result in different protein variants or isoforms starting from a single gene.

The proteomic approach has the ultimate goal to disclose the real products resulted from gene transcription and translation process and also to quantify the amount of proteins (Pardanani et al., 2002). Different methods for protein identification are available, but the most accurate and reliable is the mass spectrometry approach, which characterizes proteins based on their mass and charge (McCormack, 2005). In combination with mass spectrometry, different bioinformatics tools are present for protein identification and functional predictions (Villavicencio-Diaz et al., 2014; Calderón-González et al., 2016).

The ability to identify the proteomic profile in a specific pathophysiological status makes it attractive in cancer research since carcinogenesis is the result of dysregulation of cellular pathways and metabolism (Zhang et al., 2009). A branch of proteomic, the oncoproteomic, explores the proteins profile and their interaction in cancer, with the final aim to identify cancer-associated protein networks suitable for the discovery of new biomarkers and in early diagnosis and precise prognosis (Veenstra et al., 2004; Cho, 2007). Besides this, the proteomic profile could in-depth describe the

molecular network of the tumor, from onset to spread, potentially identify candidate pathways for therapy (Yarbrough et al., 2006).

Before mass spectrometry analysis, protein should be digested (bottom-up approach) (Figure 5) or used intact (top-down approach). In the first case, different protocols for protein separation after digestion, such as liquid chromatography (LC) or gel electrophoresis, are usually applied in combination with mass spectrometry to identify high- and low-abundant proteins (Morris, 2016). The conventional "bottom-up" proteomics, based on the analysis of small peptides originated from protein digestion, gives the entire protein profile but with a limited sequence coverage and incomplete information about the PTMs. A new "top-down" proteomics approach, analyzing intact proteins, provides information about intact proteoforms and the localization of PTMs and sequence variants. Top-down proteomics is nowadays used to discover, characterize and quantify the disease associated-proteoforms (Gregorich et al., 2014; Chait, 2006).

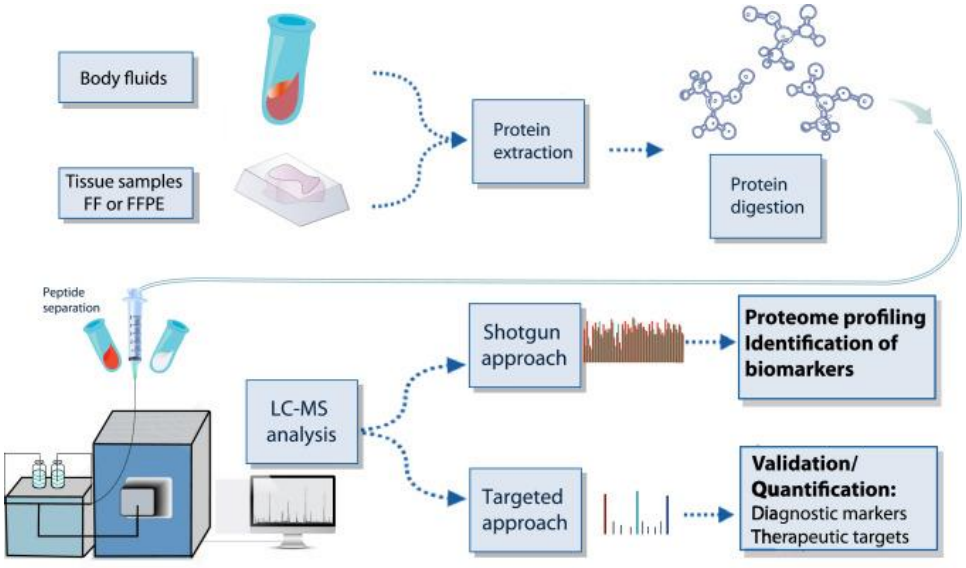

Figure 5 Representation of a bottom-up mass spectrometry (MS) analysis
FF, fresh frozen;FFPE, formalin-fixed paraffin-embedded; LC, liquid chromatography
From (Mardamshina and Geiger, 2017)

The application of proteomic science is becoming relevant also in veterinary oncology for the detection of new biomarkers and diagnosis. By now, the proteome in different biological matrices was profiled in a limited number of canine tumors, including lymphoma, mammary tumor, prostate

tumor, and mast cell tumor (Gaines et al., 2007; Leroy et al., 2007; McCaw et al., 2007; Wilson et al., 2008; Ratcliffe et al., 2009; Klopfleisch et al., 2010; Klose et al., 2011; Schlieben et al., 2012; Zamani-Ahmadmahmudi et al., 2014).

In conclusion, proteomics may elucidate cancer pathogenesis and promote the discovery of new tools to support prognosis, diagnosis, and therapeutically application.

1.3 Microbiomics

The whole microbial community inhabiting a specific body district defines the microbiota and constitutes a complex biosystem able to interact between its members and with the cells of the host.

The most used approach to study the microbiota composition is the sequencing of a region of the 16S rRNA (~250 bp) even if nowadays the sequencing of the entire gene (~1500 bp) allows to reach a higher taxonomic resolution (Johnson et al., 2019). The 16S rRNA gene is present in all bacteria and archea and the sequencing is performed on the nine hypervariable regions (V1 – V9) useful to identify different taxa (Figure 6) (Clarridge, 2004).

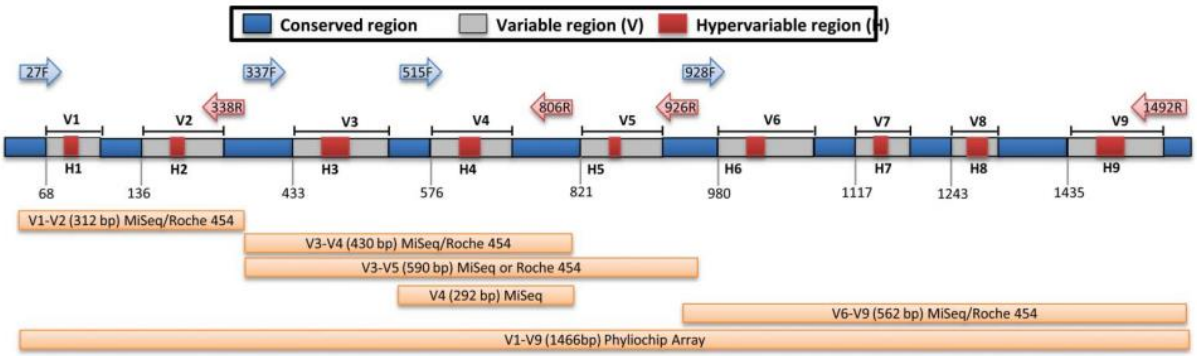

Figure 6 The 16S rRNA gene with the conserved, variable and hypervariable region. The red bars represent the primers paired design in a conserved region used for metagenomics sequencing. From (Shahi et al., 2017)

The 16S rRNA gene can be sequenced using a second or a third-generation sequencing approach. The second-generation sequencing allows to obtain a reads length of 35-700bp with a low error rate (from 0.1 to 1%) but the DNA requires a pre-amplification step (PCR) and it is based on a dense array of DNA features (Goodwin et al., 2016). The third-generation sequencing instead doesn't

require a pre-amplification step, but consists of the single-molecule real-time sequencing. It allows to obtain an output of longer reads length (1Mb for oxford Nanopore technology) but with a higher error rate (up to 15%) (Quick and Loman, 2017).

Besides the use of 16S rRNA to characterize the microbial community, another approach call metagenomics, based on a shotgun sequencing approach, is becoming more popular improving the taxonomic resolution, the identification of single nucleotide polymorphisms (SNPs) and other variants. Moreover, a functional analysis of the microbial community can be performed using the online database as KEEG (Morgan and Huttenhower, 2012).

The role of the microbiota in cancer is still to be well elucidated to disclose its influence on cancer progression and treatment response. Microbes can play a harmful or beneficial role, direct or indirect interacting with the host (Figure 7).

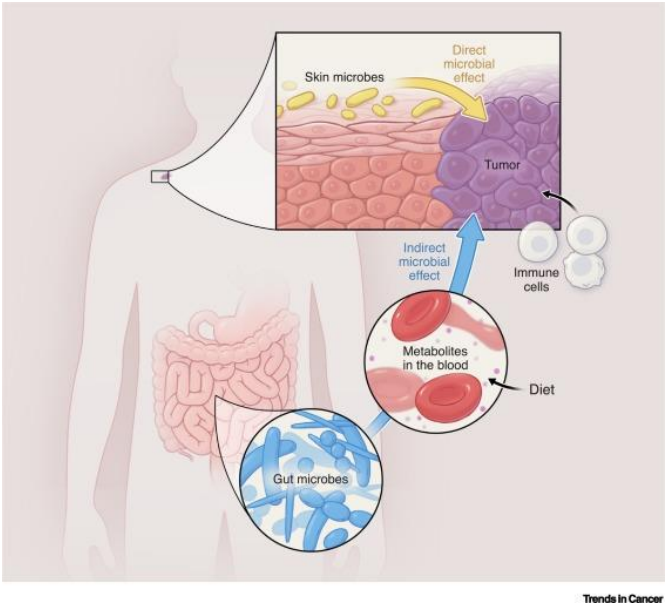

Figure 7 Microbiome and possible direct and indirect interaction with a tumor
From (Xavier et al., 2020b)

Indirect interaction describes the ability of the microbial community to influence cancer by metabolite-products (Ma et al., 2018), which can be affected by external agents, like antibiotics (Xavier et al., 2020b). Bacteria can promote cancer, or an antitumor immunity like Bifidobacterium genus (Sivan et al., 2015). A study performed on a mouse mastocytoma tumor model (P815),

demonstrated that the butyrate, an intestinal microbial metabolite, was able to modulate mast cells, inhibiting P815 cell proliferation, inducing cell-cycle arrest and apoptosis, and decreasing c-Kit activation (Zhang et al., 2016).

The direct impact is related to the body district colonized by the bacteria which can directly interact with the host. Some examples are the effect of gut, lung, and skin microbiome on colorectal cancer (Wong and Yu, 2019), lung cancer (Ramírez-Labrada et al., 2020), and melanoma (Mrázek et al., 2019), respectively. However, also the presence of bacteria in an unusual site can exert an effect on tumor progression; it has been reported that in colorectal cancer *Fusobacterium nucleatum* is carried by cancer cells to metastatic sites; the presence of this bacteria played a crucial role in malignancy (Bullman et al., 2017).

The bacterial population can also interact with the host immune system influencing the response to immunotherapy. Changes in microbiota composition, a compromised skin barrier (Prescott et al., 2017), a local immune response (Abdallah et al., 2017), and a decrease in microbiota diversity (Bradley et al., 2016) are associated with skin disorders (Zeeuwen et al., 2013), such as dermatitis (Bradley et al., 2016). An example of an antitumor-effect carried out by the microbes is the promotion of the memory potential of antigen-activated CD8+ T cells by the production of short-chain fatty acids (SCFAs) (Bachem et al., 2019). The microbiota of the skin can modulate the immunity response (Naik et al., 2012). A study confirmed that the skin microbiota of mice enhances the recruitment of mast cells, promoting their maturation in the dermis via stem cell factor production in mice (Wang et al., 2017). These studies highlighted that microbiota is an integral part of the organism able to communicate and react to several stimuli and to modify the host response. This has been already observed in the case of *Helicobacter pylori*, the etiological agent of the 89% of gastric cancer (Plummer et al., 2016), and of *Bifidobacterium* genus, which has a role in promoting an antitumor immunity (Sivan et al., 2015).

Chapter 2. Less-invasive biological matrices for biomarkers detection and tumor follow up

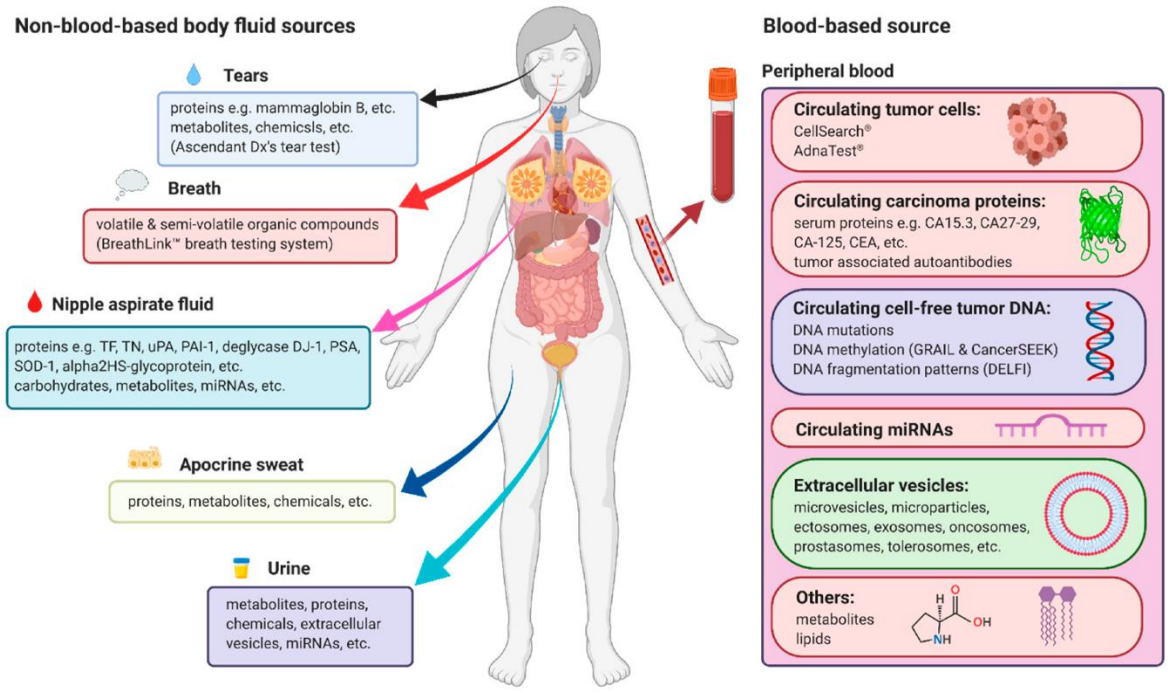

Figure 8 Sources of non-invasive biomarkers for early detection of cancer
From (Li et al., 2020)

To reduce the discomfort of the patient during sample collection and to allow for routine early tracking for recurrence or therapy resistance and minimal residual disease, a new frontier of medicine is the identification of biomarkers in less-invasive matrices suitable for cancer detection over time. Although surgical biopsies are the gold standard for diagnosis and tumor treatment, circulating biomarkers identified in biological fluid samples are particularly valuable. Tissue biopsy is invasive, sometimes gives only a partial representation of tumor heterogeneity, is not repeatable over time after surgery, and it is very difficult to do longitudinal monitoring (Gerlinger et al., 2012; Li et al., 2020).

NGS techniques arise the use of less/non-invasive matrices for the identification of promising panels of biomarkers available for the early diagnosis and prognosis, such as in human breast cancer (Li et al., 2020). Figure 8 summarizes the sources of less invasive biomarkers, including blood and blood-based source, tears, breath, urine, and saliva. The detectable molecules are cell-free DNA/RNA, miRNAs, proteins, metabolites, and chemicals in a free form bind to proteins or carried in extracellular vesicles (microvesicles, exosomes) (Li et al., 2020). The liquid biopsy (LB) approach is becoming more and more used for the detection of tumor-associated biomarkers in different biological fluids (Fernández-Lázaro et al., 2020). Among them, the use of saliva is gaining popularity because it is a non-invasive, repeatable and economic procedure that does not require trained personnel suitable as biomarker source. The high permeability of salivary glands and the proximity to the capillaries promote the free exchange of blood-based molecules into the saliva for the detection of oral and systemic diseases. Although the saliva may seem a matrix easy to be collected, it has some issues related to salivary flow rate, circadian rhythm, type of salivary gland, type of salivary stimulus, diet, age, physiological status, and method of collection (Yoshizawa et al., 2013).

The most promising sources of LB biomarkers are ctDNA and miRNAs (Domínguez-Vigil et al., 2018), which are released into the circulation also by tumors and reach up to 1000ng/ml in the blood of human patients with cancer and up to 100ng/ml in the blood of healthy subjects (Schwarzenbach et al., 2011). Studies pairing plasma and tumor tissue in humans demonstrated a concordance of more than 80% in tumor DNA aberrations, suggesting that the blood sample may provide a more complete tumor profile than the solid biopsy, targeting the heterogeneity of primary tumors and metastasis (Forshew et al., 2012; Reinert et al., 2016).

The same number of metabolites, 89, was identified in tissue, serum, and urine of tumors of the kidney (Ganti et al., 2012). Another study discovered that tumor associated-miRNAs were present in primary tumor mass, plasma, and saliva of patients with head and neck cancer (Salazar et al.,

2014) and oral squamous cell carcinoma (Liu et al., 2012), respectively (Rapado-González et al., 2018). Mutation of a primary tumor mass can be detected by a liquid biopsy approach as well (Schwartzberg et al., 2020). To conclude, the identification of candidate reliable biomarkers in less/non-invasive biological matrices is important to improve clinical approaches for early cancer detection, classification, and prognosis.

Chapter 3. Skin tumors in dogs

Skin tumors arising from the epidermis, dermis and associated structures can be define based on their differentiation into specific skin components (Goldschmidt, 1998). The incidence of skin tumors in dogs and cats is 25.5% to 43%, among them up to 40% are malignant forms. An overview of the most relevant canine neoplasms is reported in Figure 9; the top ten includes mast cell tumor (16.8%), lipoma (8.5%), histiocytoma (8.4%), perianal gland adenoma (6.5%), squamous cell carcinoma (6.0%), melanoma (5.6%), fibrosarcoma (5.4%), basal cell tumor (5.0%) and malignant peripheral nerve sheath tumor (4.3%) (Hauck, 2012).

TUMOR TYPE	OVERALL (NO.)	OVERALL (%)
Mast cell tumor	1494	16.8
Lipoma	758	8.5
Histiocytoma	752	8.4
Perianal gland adenoma	692	7.8
Sebaceous gland hyperplasia/adenoma	577	6.5
Squamous cell carcinoma	531	6.0
Melanoma	500	5.6
Fibrosarcoma	478	5.4
Basal cell tumor	445	5.0
Malignant peripheral nerve sheath tumor	381	4.3
Papilloma	251	2.8
Sweat gland adenocarcinoma	101	1.1
Sebaceous adenocarcinoma	42	0.5
Miscellaneous	1899	21.3
TOTAL	8901	100

Figure 9 Skin tumor incidence in dogs determined from the collection of 10 worldwide studies
From (Hauck, 2012)

The identification of tumor malignancy is based on two recognized and standardized systems the World Health Organization (WHO) grading, completed for the first time in 1975, and the TNM staging systems published for the first time in 1980 by Owen (Owen, 1980).

The WHO grading provides guidelines for tumor classification including diagnostic criteria, pathological features, and associated molecular alterations (Hendrick, 1998). The TNM

classification, on the other hand, provides a clinical staging of the tumor by evaluating the primary tumor extension (T), by the condition of the regional lymph nodes (N), and by the presence or absence of distant metastases (M) (Owen, 1980). Subsequently, several revisions have been carried out on specific tumors (Vail, 2019) (e.g. an update of mast cell tumor staging was published in the '*European consensus document on mast cell tumours in dogs and cats*' in 2012 (Blackwood, 2012)). Nowadays, new molecular technologies should be simultaneously applied to reach a more precise characterization of the tumors (Roccabianca, 2018).

Chapter 4. Mast cell tumor

Canine mast cell tumor (MCT) is one of the most common skin neoplasms in dogs with a prevalence of 7%–21% (Welle et al., 2008; Grüntzig et al., 2015). It arises from an uncontrolled proliferation of neoplastic mast cells in the cutaneous and subcutaneous tissues (Gross et al., 2005; Welle et al., 2008). It has no gender predilection and the incidents are between 7.5 and 9 years old, even if sometimes it can occur also in younger subjects (Dobson and Scase, 2007; Welle et al., 2008; O'Connell and Thomson, 2013). Some breeds such as Shar-Peis, Boxers, American Staffordshire Terriers, Labrador Retrievers, French Bulldogs, and Golden Retrievers have a higher risk to develop the tumor (Śmiech et al., 2019). Some features including breed, tumor anatomical site, volume, location, growth rate, and presence of ulcerations must be considered as prognostic factors (Welle et al., 2008; Garrett, 2014). The MCT grading is based on Patnaik (grade 1, 2 and 3) and Kiupel (high and low grade) systems which allow understanding the tumor malignancy by the observation of cells atypia (Patnaik et al., 1984; Kiupel et al., 2011; Kiupel and Camus, 2019). The tumor staging is based on evaluation of the draining lymph node with cytology or histology, which is critical to determining the appropriate therapy; an additional cytological screening is applied to the liver and spleen of dogs with MCT considered as high risk, to assess the presence of metastasis (Garrett, 2014; Weishaar et al., 2014). Other prognostic factors to better predict the tumor behavior include DNA aneuploidy, c-kit-staining pattern, presence of c-kit mutations, microvessel density (the concentration of small blood vessel in the tumor), Ki-67 expression (nuclear protein linked with cellular proliferation), and evaluation of the mitotic index (Garrett, 2014). Mutation in the KIT proto-oncogene often occurs in dogs with MCT, leading to an alteration of the protein structure and function (Tamlin et al., 2020). Some kind of KIT mutations is associated with a more aggressive and lethal form as the mutation promotes the ligand-independent KIT activation, leading to an uncontrolled mast cell proliferation and tumor development. The most common mutations associated with the KIT gene, including

duplication, inter tandem duplication and point mutation, are localized in the exons 8, 9, and 11. Other mutations occur in other exons, but with less frequency and do not promote the receptor independent activation (London et al., 1999; Ma et al., 1999; Letard et al., 2008; Giantin et al., 2012; Takeuchi et al., 2013).

The therapeutical approaches include tumor mass excision by surgery, radiotherapy, chemotherapy, and drug administration, such as tyrosine kinase inhibitors (TKIs).

Surgery is the strategy of election to remove the tumor mass, but if it is not applicable, radiotherapy is exploited to reduce the tumor mass or as post-surgical treatment. Chemotherapy is applied on dogs with high-grade or non-surgically resectable tumors to prevent the dissemination of metastasis, to reduce the tumor burden and improve the chance of surgical excision, or to treat the residual microscopic disease (Davies et al., 2004; Mullins et al., 2006; Stanclift and Gilson, 2008; Blackwood et al., 2012). The TKIs drugs inactivate the tyrosine kinase receptor by blocking the ATP binding site, and in combination with conventional chemotherapy showed promising results for patients unresponsive to existing drugs (Blackwood et al., 2012; Tamlin et al., 2020). Recently, a new approach for the treatment of the MCT using the oncolytic Sendai virus was explored (Ilyinskaya et al., 2018).

4.1 Molecular changes in mast cell tumor

To identify new biomarkers to better predict biological behaviors and prognosis of the mast cell tumor, molecular approaches have been applied. Pulz and colleagues discriminated between two MCT's molecular subtypes (high-risk and low-risk) by a genome-wide gene- expression analysis on the primary tumor mass, identifying 71 genes differentially expressed between the tumor subtypes. The functional analysis revealed that two genes correlated with the high-risk MCTs were associated with cell proliferation and extracellular matrix-related terms (Pulz et al., 2019). Genes involved in the loss of cell polarity, the reduction of cell-cell and cell-extracellular matrix adhesion, and the

increase of cell deformability and motility, altogether correlated with the most aggressive form of MCT, were also reported (Blacklock et al., 2018).

4.2 miRNA and mast cell tumor

The role of miRNAs in tumor progression is already well known. MiRNAs are modulators at the post-transcriptional level influencing the activities of the cells by binding the target mRNA. The dysregulation of some miRNAs has been reported in canine mast cell tumors. MiR-9 is up-regulated in the high-grade canine MCTs and MCT malignant cell lines and is associated with aggressive biologic behavior (Fenger et al., 2014). In another study, the potential as biomarkers of two miRNAs, miR-214 and -126, dysregulated in 6 human tumors, was assessed in plasma of several canine's neoplasms revealing that the level of miR-126 was higher in some non-epithelial tumors including the MCT (Heishima et al., 2017).

4.3 Canine tumors and microbiota

The changes in the composition of the microbial population during pato-physiological states were studied in association with tumors in dogs. The fecal microbiota was characterized in dogs affected by multicentric lymphoma demonstrating that 28 bacterial groups were differentially abundant in the tumor compared to the control group; qPCR analysis validated that Faecalibacterium spp., Fusobacterium spp. and Turicibacter spp. were significantly lower in the feces of dogs with lymphoma. On the other hand, the abundance of Streptococcus spp. was higher in tumor-affected dogs (Gavazza et al., 2018). The fecal and mucosa-associated microbiota was investigated in dogs with colorectal epithelial tumors as well, showing that the fecal microbiota of dogs with tumors was characterized by a higher amount of Enterobacteriaceae, *Bacteroides*, *Helicobacter*, *Porphyromonas*, *Peptostreptococcus* and *Streptococcus*, and lower abundance of *Ruminococcaceae*, *Slackia*, *Clostridium XI* and *Faecalibacterium*. The mucosal bacterial didn't show any difference between the tumor and healthy groups (Herstad et al., 2018).

4.4 Exosomes and their role in tumor and metastasis

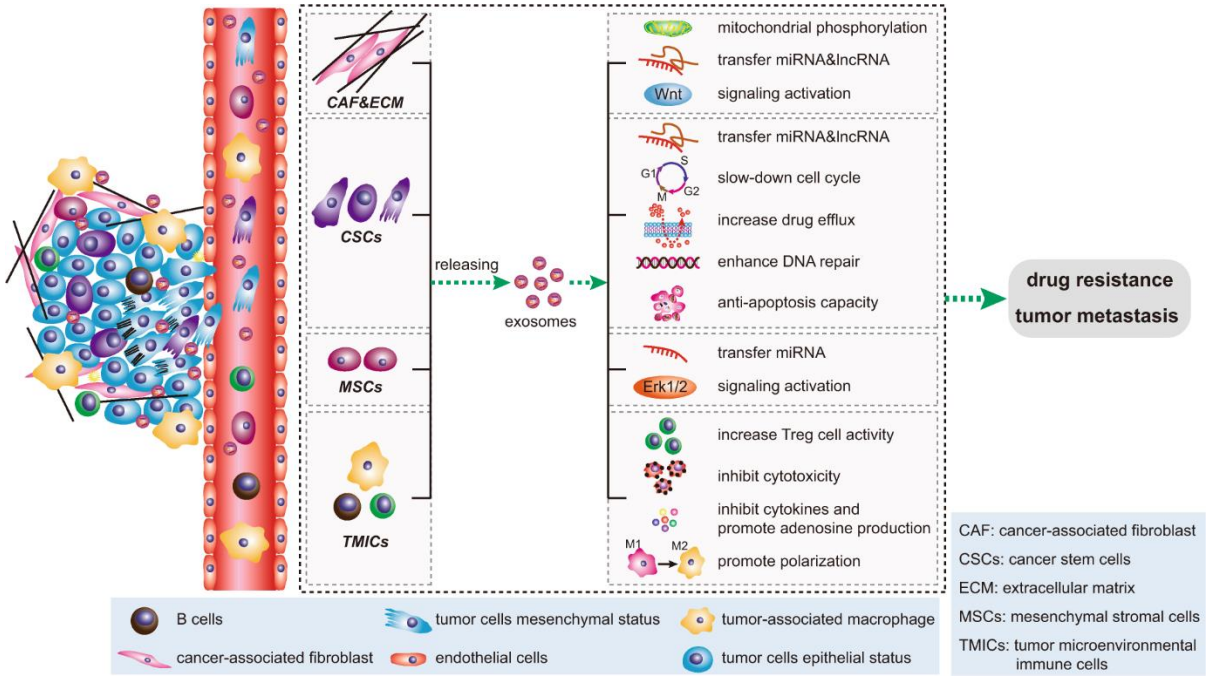

Figure 10 Role of exosome in tumor microenvironment
From (Dai et al., 2020)

Exosomes are extracellular vesicles of 30-120 nm secreted by all cell types in physiological and pathological conditions (Yuana et al., 2013; Théry et al., 2018). They carrier biomolecules such as DNA, RNA, miRNA, proteins, and lipids and are involved in the cell to cell communication (Maia et al., 2018). The tumor cells use exosomes to communicate with other cancer cells, to reprogram a recipient cell towards a tumor-promoting phenotype, and to modify the cells which constitute the tumor microenvironment to support cancer development and metastasis (Figure 10) (Tominaga et al., 2015; Whiteside, 2016; Lobb et al., 2017; Cufaro et al., 2019; Kogure et al., 2019; Lucchetti et al., 2020; Xavier et al., 2020a). The exosome originates from multivesicular bodies, may spread far from the parental cell, and is surrounded by a phospholipid bilayer to protect their cargo and prevent its degradation (Boukouris and Mathivanan, 2015). The similarities between the tumor-derived exosomes and the cell of origin highlight the potential of these vesicles in early diagnosis, prognosis, cancer staging, and follow-up as their cargoes may be defined biomarkers (Soung et al., 2017; Huang

and Deng, 2019). Thus, exosomes are reliable candidates for liquid biopsies (Roy et al., 2019; Vasconcelos et al., 2019).

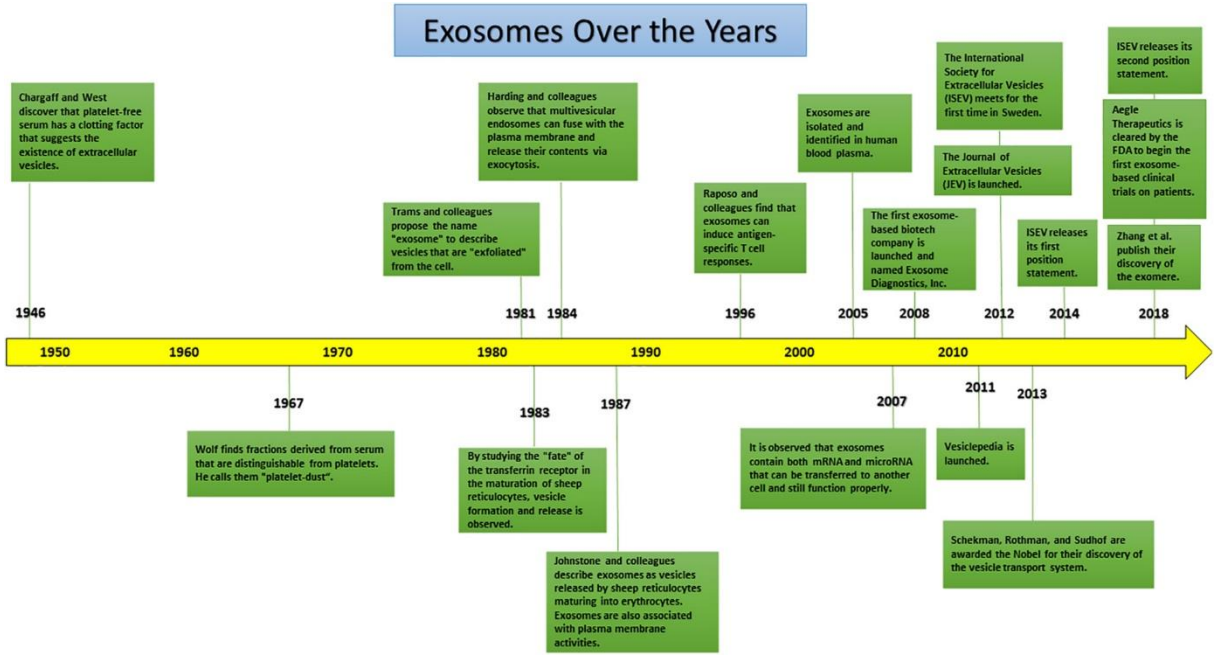

Figure 11 Exosome discovery timeline from 1946 to 2018
From (Srivastava et al., 2020)

The discovery of the extracellular vesicles date backs to 1946 when Chargraff and West supposed their existence in the serum. Then, a series of discoveries lead to the awareness of the presence of these molecular carriers and their important role in the organism, up to their value in clinic application (Figure 11).

Exosome cargo has been characterized in some canine tumors. The proteome associated with circulating exosomes of dogs affected by osteosarcoma was assessed to identify candidate biomarkers (Brady et al., 2018). The miRNome of exosomes isolated from the normal canine mammary epithelial cell and canine mammary carcinoma malignant cells was profiled, highlighting several differences. The gene ontology analysis suggested that these miRNAs could play a role in oncogenic networks (Fish et al., 2018). The proteomic and miRNomic profiles were also assessed in exosomes derived from canine lymphoid cell lines by sequencing analysis (Asada et al., 2019). Although the characterization of exosomes in veterinary oncology is still at the beginning, it seems

to have a great potential in improving the knowledge on tumor behavior and disclosing molecules for prognosis, diagnosis, and patient follow-up.

4.4.1 Different approaches for exosomes purification

Different methods can be applied for the exosome isolation, which depends on the downstream analyses.

The standardization of isolation and purification protocols for EVs is still to be defined, to reduce the pre-analytical and analytical variability (Figure 12) (Gandham et al., 2020).

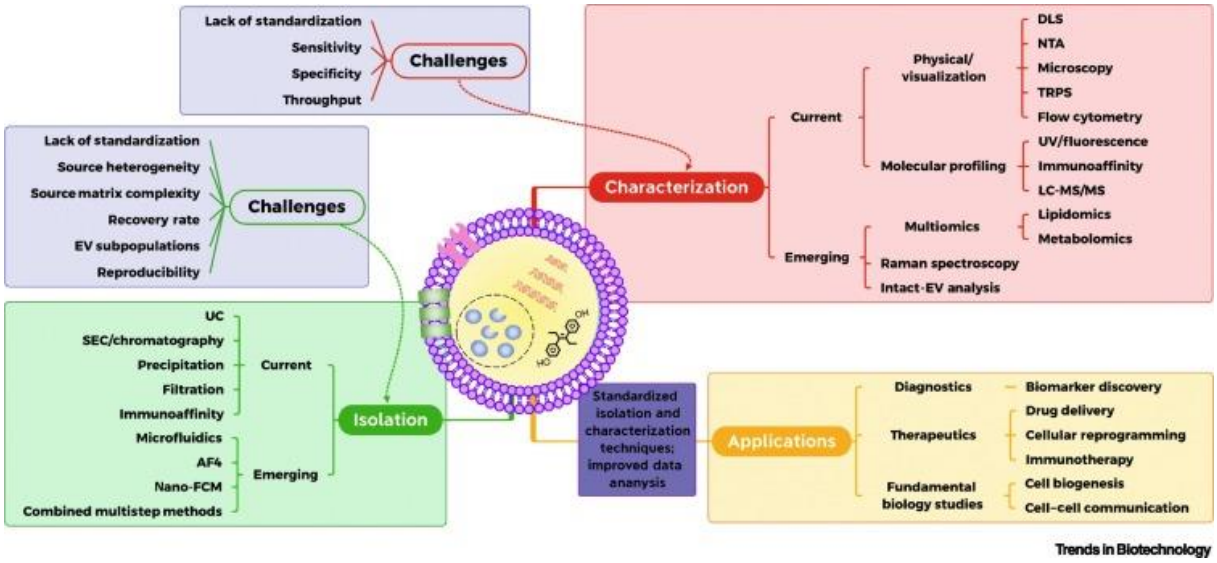

Figure 12 Isolation methods and challenges in extracellular vesicles research

AF4: asymmetric flow field-flow fractionation; DLS: dynamic light scattering; LC: liquid chromatography; MS: mass spectrometry; nano-FCM: nano-flow cytometry; NTA: nanoparticle tracking analysis; TRPS: tunable resistive pulse sensing; UC: ultracentrifugation

From (Gandham et al., 2020)

Different factors can affect the amount, purity, and heterogeneity of the EVs, such as sample collection, storage, and handling (Gandham et al., 2020). For the purification of the EVs from blood, one of the most abundant sources of EVs (Revenfeld et al., 2014; Baranyai et al., 2015; Wu et al., 2017), it is necessary to standardize as much as possible the procedure in terms of needle used (small needle can cause the released of EVs from platelets and red blood cells) (Coumans et al., 2017), time of the collection (Danielson et al., 2016) and type of anticoagulant (Wisgrill et al., 2016). Plasma is a better matrix for EVs isolation than serum, which contains more platelet-derived-vesicles (Palviainen et al., 2020). The centrifugation procedure to obtain plasma is a critical step in the

sample preparation (Gandham et al., 2020). Sample storage is another key point, freeze-thaw cycles should be minimized and a temperature of -80°C contributes to the preservation of the EVs and their content (Jeyaram and Jay, 2017; Kusuma et al., 2018).

Different methods for the EVs isolation have been explored, including ultracentrifugation, separation using density gradients, size exclusion chromatography (SEC), filtration with a specific membrane, immunoaffinity, flow-cytometry, precipitation using polymers, asymmetric flow field-flow fractionation (AF4), or exploit surface chemistry properties applying microfluidic approaches (Gandham et al., 2020). The ultracentrifugation is considered the 'gold standard' for EVs isolation (Van Deun et al., 2017), even if the process of pelleting the EVs can lead to co-precipitation of microparticles, lipoproteins, and protein complexes causing damages to the EV membranes or aggregation. Moreover, the low throughput and the need for specialized equipment may represent additional issues (Liga et al., 2015; Linares et al., 2015; Coumans et al., 2017). SEC, which isolates the EVs based on the hydrodynamic volume, is robust and does not require expensive equipment (Böing et al., 2014). SEC is a valid method for proteomic downstream analysis (Lane et al., 2019), promoting the isolation of active and morphologically intact EVs (Hong et al., 2016; Ludwig et al., 2019a) within a narrower size range and with a lower content of plasma proteins (Stranska et al., 2018; Ludwig et al., 2019b). Some limitations include the low resolution, the dilution of the sample, the contamination of EVs enriched fraction with serum components or lipoproteins (Sódar et al., 2016; Pietrowska et al., 2019; Yang et al., 2020). Takov and colleagues proved that SEC isolated EVs showed a higher EV concertation, markers signal, EV protein and particle/protein ratio compare with the ultracentrifugation, even if non-EV proteins were still present (Takov et al., 2018).

EVs isolation by filtration is dependent on the kind of filter and often needs a preliminary ultrafiltration step (Lobb et al., 2015). Due to the extrusion effects, the structural integrity of the

EVs may be altered. Moreover, the filtration approach may lead to a low recovery rate and the presence of contaminants (Taylor and Shah, 2015).

The EVs precipitation using a polymer precipitation-based-kit is another approach to obtain a yield comparable with the ultracentrifugation approach, even if the level of the protein contamination is very high (Helwa et al., 2017). The immunoaffinity approach has been explored to isolate specific subpopulations taking advantage of the antibody's ability to bind specific proteins on EVs (Sharma et al., 2018). Some disadvantages are the costs, aspecific binding, competitive inhibition, and cross-reactivity (Konoshenko et al., 2018; Gandham et al., 2020).

The most recent emerging techniques are trying to isolate EVs based on different vesicle properties. The microfluidic approach is based on physical, mechanical and/or surface chemistry properties (Guo et al., 2018); Sitar and coworkers developed a laminar flow-based method (Sitar et al., 2015). The flow-cytometry approach is applied for fidelity sorting (Kormelink et al., 2016). Recently, the possibility to combine different purification methods (Vaswani et al., 2017) to obtain a higher recovery rate of EVs morphologically intact and active and with a higher degree of purity and heterogeneity has been explored.

Chapter 5. Canine oral malignant melanoma

Tumors derived from a malignant proliferation of melanocytes are quite commons in dogs. Melanomas can occur in haired skin, nail bed, footpad, eye, gastrointestinal tract, central nervous system, and mucocutaneous junction, but the oral ones are the most aggressive and malignant (Prouteau and André, 2019). Among all the oral lesions, the malignant tumors account for 32.06%, of which the most common was the high-grade melanoma (Bonfanti et al., 2015; Mikiewicz et al., 2019). Gingiva, buccal/labial mucosa, tongue, and hard palate are the most affected sites (Bergman, 2007). Oral malignant melanoma (OMM) arises from a neoplastic proliferation of melanocytes; OMM is considered a malignant tumor with a high degree of local invasiveness and high metastatic propensity especially to the regional lymph nodes (58–74%), lungs (14–67%) and tonsils (65%) (Ramos-Vara et al., 2000; Bowlt Blacklock et al., 2019). UVB light does not promote the onset of canine OMM, as in humans, but is associated with consanguinity, trauma, chemical exposure, hormones, and genetic susceptibility (Modiano et al., 1999). OMM has a high growth rate and is often ulcerated (Nishiya et al., 2016). The prognosis is based on tumor size (WHO staging system) with four stages: stage I < 2 cm-diameter (survival time of 17-18 months), stage II from 2 to < 4 cm-diameter (survival time of 5-6 months), stage III > 4 cm-diameter tumors and/or lymph node metastasis (survival time of 3 months), and stage IV characterized by distant metastasis (survival time of fewer than 3 months). In addition to the WHO classification system, other cytological and histological examinations are applied on lymph nodes, and clinic-pathological indicators - degree of pigmentation, presence of necrosis, ulceration or inflammation, rate of cell proliferation and p53 and Ki67 (mitotic index) expression levels - are analyzed for the prognosis. The treatment of the tumor using surgery or radiotherapy may be successful (Bergman, 2007; Withrow et al., 2012), but the treatment of the disseminated forms using cytotoxic drugs or applying the chemotherapy

doesn’t lead to a real extension of the survival time and the response can be described as modest (Rassnick et al., 2001; Boria et al., 2004).

5.1 Molecular changes in melanoma

In addition to the routine examination, it is fundamental to understand the genetic and epigenetic modifications that lead to tumor onset and progression. Although canine melanoma onset is not linked with the UVB light exposure, it showed several similarities with the human form at the molecular level. Mutation of the receptor tyrosine kinase (Rivera et al., 2008; Murakami et al., 2011; Newman et al., 2012) and activation of pathways such as AKT mTOR (Kent et al., 2009; Turri-Zanoni et al., 2013) are some of the similarities between the species that promote the application of some human therapeutical approaches in dogs, including the plasmid DNA vaccine expressing human tyrosinase (Atherton et al., 2016). Therefore, the characterization of molecular modifications of melanoma may lead to a better understanding of the tumor behavior, supporting a more precise prognosis and the development of new drugs and therapeutical approaches. Transcriptomic analysis of canine OMM was performed to find out metastasis-associated targets. Twelve genes were dysregulated (>1.5 fold) between metastatic and non-metastatic OMMs. Among them, CXCL12 was down-regulated, and APOBEC3A was up-regulated in metastatic OMMs (Bowlt Blacklock et al., 2019). The proteome of canine OMM was assessed. A different protein profile was found in the early-stage compare with the late-stage of OMM and a unique pick marker suitable for early detection of the disease was picked up (Pisamai et al., 2018). The proteomic profile of saliva of OMM-affected dogs was carried out identifying three proteins (SENP7, TLR4, and NF-κB) as candidate salivary biomarkers of canine oral tumors (Ploypetch et al., 2019). Genomic mutation, dysregulation in gene and protein expressions, and metabolites can be studied to disclose tumor biology. The metabolomic profile was evaluated in the plasma of dogs with OMM. Differential expression of twelve plasmatic metabolites was identified in melanoma affected- compare to

healthy dogs: citric acid, isocitric acid, glycerol, lactic acid, threonine, proline, serine, margaric acid, oleic acid, linoleic acid, palmolitoleic acid, and octadecenoic acid (Kawabe et al., 2015). Together these new data will improve the knowledge of cancer and will pave the way for the identification of suitable candidate biomarkers.

5.2 miRNA and melanoma

The role of oncomiRNAs has been investigated in a study on canine oral melanoma through a NGS approach, demonstrating that 8 miRNAs - miR-450b, miR-223, miR-140, miR-542, miR-383, miR-301a, miR-21, and miR-190 - were up-regulated and 7 miRNAs - miR-429, miR-200b, miR-141, miR-375, miR-96, miR-183, and miR-143 - were down-regulated in melanoma compared to the control group. Three miRNAs -miR-450b, miR-301a, and miR-223- showed a significant negative correlation with the expression of their possible targets genes, PAX9, NDRG2, ACVR2A, and BMP4, the down-regulation of which promotes the up-regulation of MMP9 involved in the extracellular matrix degradation and tumor invasion (Rahman et al., 2019). A microarray study revealed that 17 miRNAs were differentially expressed between tumor and healthy controls; in detail, miR-383 and miR-204 were potential oncomiRNAs potentially involved in tumor progression by evading DNA repair and apoptosis (Ushio et al., 2019).

Chapter 6. Aim of the thesis, experimental design and papers

The main goal of this thesis was the characterization of the miRNome and the microbiome of canine mast cell tumor using OMICs approaches, to profile the molecular changes associated with the tumor. Then, a protocol for the plasmatic exosome isolation from MCT-affected dogs, suitable for further proteomic analysis, was set up. Besides, a targeted characterization of melanoma-associated miRNAs was also performed.

The experimental design of my Ph.D. project is reported in Figure 13.

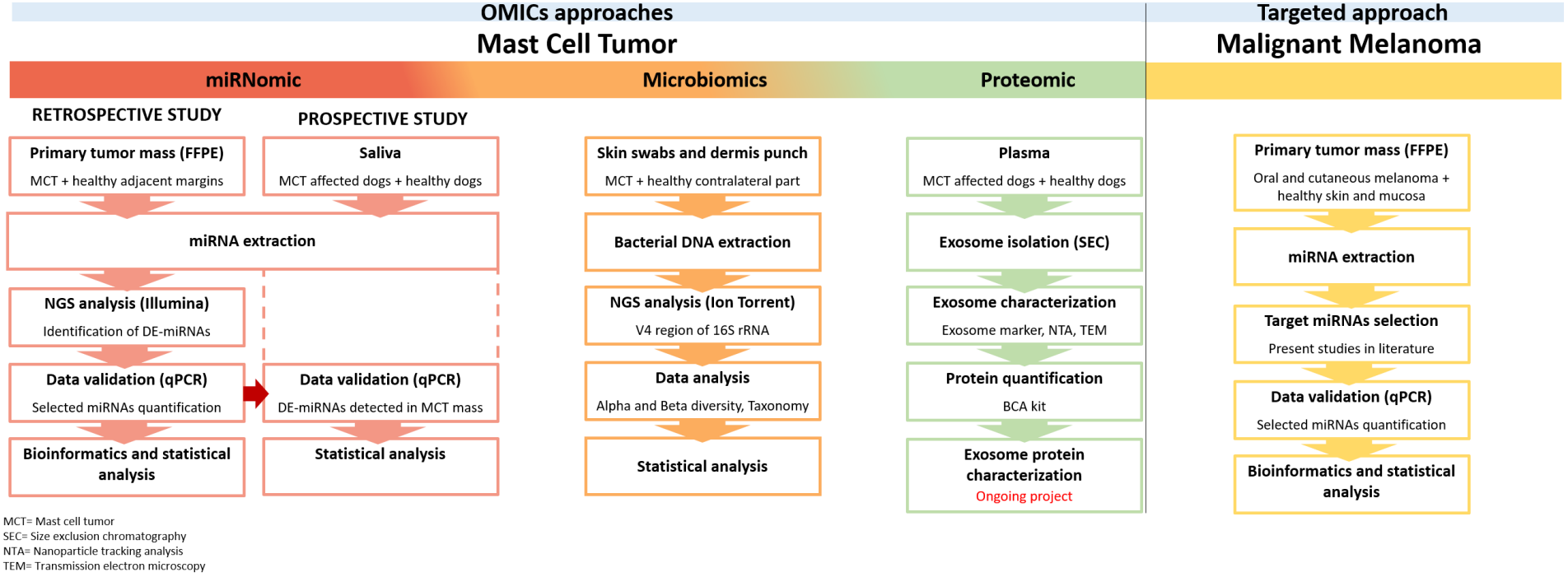

Figure 13 Experimental design of the thesis project.

www.nature.com/scientificreports

scientific reports

Check for updates

OPEN

miRNA profiles of canine cutaneous mast cell tumours with early nodal metastasis and evaluation as potential biomarkers

Valentina Zamarian[1], Roberta Ferrari[1], Damiano Stefanello[1], Fabrizio Ceciliani[1], Valeria Grieco[1], Giulietta Minozzi[1], Lavinia Elena Chiti[1], Maddalena Arigoni[2], Raffaele Calogero[2] & Cristina Lecchi[1]✉

Scientific Reports, 2020, doi: 10.1038/s41598-020-75877-x

miRNA profiles of canine cutaneous mast cell tumours with early nodal metastasis and evaluation as potential biomarkers

Valentina Zamarian[1], Roberta Ferrari[1], Damiano Stefanello[1], Fabrizio Ceciliani[1], Valeria Grieco[1], Giulietta Minozzi[1], Lavinia Elena Chiti[1], Maddalena Arigoni[2], Raffaele Calogero[2], Cristina Lecchi[1*]

(1) Dipartimento di Medicina Veterinaria, Università degli Studi di Milano, Milano, Italy

(2) Molecular Biotechnology Center, Department of Biotechnology and Health Sciences, Università di Torino, 10126, Italy

*Corresponding author: cristina.lecchi@unimi.it

Abstract

Cutaneous mast cell tumours (MCTs) are common skin neoplasms in dogs. MicroRNAs (miRNAs) are post-transcriptional regulators involved in several cellular processes, and they can function as tumour promoters or suppressors. However, the role of miRNAs in canine MCTs has not yet been elucidated. Thus, the current study aimed to characterize miRNA profiles and to assess their value as biomarkers for MCTs. miRNA expression profiles were assessed in formalin-fixed, paraffin-embedded samples by next-generation sequencing (NGS). Ten samples were MCT tissues, and 7 were healthy adjacent tissues. Nine dysregulated miRNAs (DE-miRNAs) were then validated using RT-qPCR in a larger group of MCT samples, allowing the calculation of ROC curves and performance of multiple factor analysis (MFA). Pathway enrichment analysis was performed to investigate miRNA biological functions. The results showed that the expression of 63 miRNAs (18 up- and 45 downregulated) was significantly affected in MCTs. Five DE-miRNAs, namely, miR-21-5p, miR-92a-3p, miR-338, miR-379 and miR-885, were validated by RT-qPCR. The diagnostic accuracy of a panel of 3 DE-miRNAs—miR-21, miR-379 and miR-885—exhibited increased efficiency in discriminating animals with MCTs (AUC= 0.9854) and animals with lymph node metastasis (AUC= 0.8923). Multiple factor analysis revealed clusters based on nodal metastasis. Gene Ontology and KEGG analyses confirmed that the DE-miRNAs were involved in cell proliferation, survival and metastasis pathways.

In conclusion, the present study demonstrated that the miRNA expression profile is changed in the MCT microenvironment, suggesting the involvement of the altered miRNAs in the epigenetic regulation of MCTs and identifying miR-21, miR-379 and miR-885 as promising biomarkers.

Keywords: biomarkers, dog, mast cell tumour, metastasis, microRNA

Introduction

Cutaneous mast cell tumours (MCTs) are a common skin neoplasm in dogs, accounting for up to 21% of all skin tumours[1]. Mast cell tumours originate from uncontrolled proliferation of neoplastic mast cells in cutaneous and subcutaneous tissues and usually occur as single tumours but sometimes as multiple tumours[2]. The clinical phenotype of MCTs ranges from relatively benign to highly malignant tumours that can spread to the local lymph nodes, liver and spleen[3,4]. Their diagnosis and prognosis are usually based on tumour grading as determined by the Patnaik[5] and Kiupel[4,6] systems, and tumour staging, including evaluation of draining lymph nodes[7]. In addition, the proliferation rate (Ki-67), *c-kit* proto-oncogene mutations and KIT expression are significant prognostic factors[7,8]. The pathogenesis and aetiology of MCTs are poorly understood, and the main causes that lead to MCT carcinogenesis remain elusive[9].

Canine MCTs have been recently investigated at the molecular level using next-generation RNA sequencing[10], and two distinct tumour subtypes have been identified with differential expression of 71 genes involved in cell proliferation processes. However, no information about the epigenetic regulation of MCT development, such as regulation mediated by microRNAs, is available.

MicroRNAs (miRNAs) are small non-coding RNAs that are involved in post-transcriptional regulation and thus affect virtually every cellular process. MiRNAs regulate mRNA translation, leading to modulation of protein expression. MiRNA dysregulation occurs during the pathogenesis of several diseases, including cancer, and leads to disruption of pathways that play a role in cancer initiation and progression[11]. MiRNAs can act as oncomiRs, targeting tumour suppressor genes and promoting tumour progression, or as tumour suppressors, although overall miRNA dysregulation is a hallmark of cancer[12–14]. The role of miRNAs in canine MCT is still unknown. The present study aims to close this gap by

assessing the miRNA expression profile of canine MCTs using next-generation sequencing, investigating whether miRNAs are dysregulated in the MCT microenvironment, and identifying links between miRNAs and their target genes and relevant biological processes.

Results

Determination of miRNA profiles and identification of DE-miRNAs in healthy margins *versus* MCTs

After RNA extraction, small RNA libraries were generated, pooled, concentrated and size selected on a non-denaturing acrylamide gel (≈141 bp bands). After elution from the gel, the size-selected libraries were quantified and sequenced on a NextSeq 500 sequencer (Illumina). The resulting number of reads per sample varied from 53,000 to 29,000,000. Eight MCT samples with insufficiently high mapping rates were excluded from further analysis. For two dogs (numbers 8 and 15 in Table 1), the results for the tumours and matched healthy adjacent margins were reported.

A count table was used to identify differentially expressed miRNAs via DESeq2 analysis[15]. The DESeq threshold was set by discarding low-expression miRNAs having an average count of 2 or less. This analysis revealed the expression of 246 and 116 *Canis familiaris* (cfa) miRNAs in healthy margins and MCTs, respectively.

The expression profiles of sequenced samples were used to carry out cluster analysis. Samples were grouped into two clusters: healthy tissues and MCTs (Figure 1A).

To rank the most differentially expressed miRNAs (DE-miRNAs) between healthy and MCT samples, the results of differential expression analysis performed with DESeq2 were further filtered a more stringent cut-off criteria of an adjusted *P*-value of 0.01 and an absolute log2FC of 2.4. This filtering allowed the identification of sixty-three miRNAs whose abundance differed significantly between MCT and healthy

samples, demonstrating that 45 miRNAs were downregulated with a log2FC of between -2.4 and -13.4 and 18 miRNAs were upregulated with a log2FC of between 2.4 and 6.9 (Figure 1B).

Quantification of DE-miRNAs in healthy *versus* MCT samples by RT-qPCR

To validate the NGS results and measure the abundances of DE-miRNAs in MCTs, RT-qPCR was performed on both the sequenced samples and a separate group of 11 MCTs and related healthy adjacent (normal) tissue samples. To validate the sequencing results, 9 DE-miRNAs—miR-370, miR-379, miR-92a, miR-21, miR-26a, miR-342, miR-885, miR-375 and miR-338—were selected based on the fold change and read count values. MiR-122, miR-128 and miR-101 were quantified as controls for normalization. The artificial spike-in cel-miR-39 was used as the internal control. MiRNAs selected for the validation step were detected in almost all samples, except for sample numbers 7, 14, 17 and 18 (Table 1). The results are presented in Figure 2. The RT-qPCR results confirmed that five miRNAs were differentially regulated in healthy adjacent margin tissues *versus* MCTs. In detail, miR-21 (P=0.004, $\log_2FC_{MCT/Healthy}$=2.84) and miR-379 (P= 0.0005, $\log_2FC_{MCT/Healthy}$ = 2.61) were upregulated, while miR-885 (P= 0.008, $\log_2FC_{MCT/Healthy}$ = -2.53), miR-338 (P= 0.025, $\log_2FC_{MCT/Healthy}$ = -0.86) and miR-92a (P= 0.021, $\log_2FC_{MCT/Healthy}$ = -0.78) were downregulated in MCT samples compared to healthy margin samples. Conversely, miR-26a, miR-342, miR-370 and miR-375 did not exhibit statistically significant differences between the groups.

Diagnostic value of DE-miRNAs in dogs with MCT

Receiver operating characteristic (ROC) analysis was used to assess the diagnostic value of DE-miRNAs as biomarkers to further discriminate between MCT and healthy adjacent tissue. To confirm the diagnostic efficacy of each miRNA, the associated area under the curve (AUC) was calculated. Table 2 shows a summary of the diagnostic performance of each DE-miRNA and shows combinations of three

DE-miRNAs. The AUC was fair for miR-92a (AUC= 0.7427) and miR-338 (AUC=0.7339) and excellent for miR-21 (AUC=0.9825), miR-379 (AUC=0.9211) and miR-885 (AUC=0.9181) (Figure 3).

Discriminant analysis was used to further investigate the potential for improving diagnostic performance by analysing multiple DE-miRNAs. Statistical analysis was performed to examine the weighted average relative quantification (RQ) values of the miRNAs with an AUC of > 0.9 (miR-21, miR-379 and miR-885) (Figure 4). The median expression levels were 0.0301 (range, 0.0069 to 0.9334) and 0.99998 (range, 0.3485 to 1) in healthy margin and MCT samples, respectively (Figure 4A). The predicted probability of being able to discriminate a sample as positive based on the logit model [logit = 1 / (1 + exp (-(-4.92611-1.31822 x expression level of miR-885+0.40746 x expression level of miR-379+0.86787 expression level of miR-21)))] was used to construct the ROC curve (Figure 4B). The AUC for the panel of these three DE-miRNAs was 0.9854 (95% CI, 0.9854-0.9854) with a cut-off value of 0.1654, and a sensitivity of 100% and a specificity of 94.4%.

Potential of the miRNA panel for the detection of nodal metastases

Excised lymph nodes were categorized in accordance with the Weishaar classification system for nodal metastases (2014)[7], and the potential of the three-miRNA panel to discriminate patients with and without lymph node involvement was evaluated. Two groups, namely, HN0/1, including non-metastatic and pre-metastatic samples, and HN2, including early metastatic samples, were included for further analysis (Table 1). The weighted average relative quantification (RQ) values of the miRNA panel (miR-21, miR-379 and miR-885) were calculated (Figure 5). The median expression levels were 0.3179 (range, 0.0071 to 0.8858) and 0.9424 (range, 0.3741 to 1) in the HN0/1 and HN2 groups, respectively (Figure 5A). The predicted probability of being able to discriminate a sample as metastatic based on the logit model [logit = 1 / (1 + exp (-(-1.58980-7.91569 x expression level of miR-885 + 0.13130 x expression

level of miR-379 + 0.05084 expression level of miR-21)))] was used to construct the ROC curve (Figure 5B). The AUC for the panel of these three DE-miRNAs was 0.8923 (95% CI, 0.759-1.000) with a cut-off value of 0.5528, a sensitivity of 92.3% and a specificity of 80%. MFA identifies individuals with similar profiles who are close to each other on the factor map. Collectively, the components F1 and F2 explained 68.53% of the total variance in the data (Figure 5C). The first component (F1) explained 42.76% of the variance and separated the HN0/1 group from the HN2 group according to lymph node involvement. The second component (F2) explained 25.77%, discriminating non-metastatic HN0 samples (samples 4 and 10) in the upper right panel from high-grade early metastatic HN2 samples (samples 16 and 9) in the lower-left panel (Supplementary Table S1).

Gene Ontology and pathway enrichment analysis of miRNAs

The MiRWalk 3.0 and DAVID databases were searched to retrieve the candidate target genes of DE-miRNAs and to perform mRNA enrichment analysis, respectively. Of the predicted mRNA targets of downregulated miRNAs, 196 were in the 3'UTR, 45 were in the 5'UTR and 171 were in the CDS. Of the predicted mRNA targets of upregulated miRNAs, 16 were in the 3'UTR, 3 were in the 5'UTR and 11 were in the CDS. The list of candidate target genes is provided in Table 3.

Gene Ontology (GO) analysis was performed using DAVID for three categories: biological process (BP), cellular component (CC) and molecular function (MF). An overview of the top 10 terms significantly enriched with target genes for each of the above GO categories is presented in Figure 6. The enriched GO BP terms mainly included regulation of transcription from RNA polymerase II promoter and protein ubiquitination involved in ubiquitin-dependent protein catabolic process; the CC terms were related to the cytoplasm, nucleus and nucleoplasm, while the MF terms focused on transcription factor activity and sequence-specific DNA binding. KEGG pathway analysis was performed on candidate targets of DE-

miRNAs. Figure 7 shows the top 10 significantly enriched KEGG pathways, with PI3K-Akt signalling pathway, small cell lung cancer, viral carcinogenesis and microRNAs in cancer at the top of the list.

Discussion

The role of miRNAs in canine MCT has not yet been elucidated. The current study aimed to characterize the miRNA profile of canine MCTs using FFPE samples. A multi-step approach was adopted: the pilot part of the study profiled miRNAs in MCTs and healthy adjacent margins via next-generation sequencing. In the second step, the DE-miRNAs were validated by performing RT-qPCR on the samples selected for sequencing and on a separate independent group of FFPE samples. Our results showed that the expression of 63 miRNAs, of which 18 were upregulated and 45 were downregulated, was significantly affected in MCTs. Nine DE-miRNAs were then validated in a larger group by RT-qPCR, demonstrating that five of these DE-miRNAs, namely, miR-21-5p, miR-92a-3p, miR-338, miR-379 and miR-885, were effectively modulated. The diagnostic accuracy of three DE-miRNAs—miR-21, miR-379 and miR-885—was excellent, and the AUC of their combination increased to 0.9854 with 100% sensitivity and 94.4% specificity. Due to their limited nucleotide length, miRNAs have shown higher stability than DNA and mRNA in sample types such as FFPE tissues[16]. However, the preparation of miRNA NGS libraries from FFPE samples is particularly challenging because of the intersample heterogeneity of the RNA quality[17]. In the present investigation, the library preparations were performed in parallel to avoid the batch effect, but mappable miRNA reads were produced from only 2 of 10 tumours. Moreover, mast cells, which release their granules into the tumour mass[9], may also affect library preparation.

Mast cells are crucial players in allergies, immune responses, angiogenesis and the maintenance of tissue function and integrity[18], also promoting tissue repair[19]. Furthermore, mast cells modulate the tumour microenvironment by performing a two-pronged role: they perform a pro-neoplastic role by releasing mitogenic and pro-angiogenic factors such as histamine, IL-10, TNF, FGF2, VEGF, IL-18 and MMP[20], that promote immune suppression, proliferation and angiogenesis; and they perform an anti-neoplastic role by inhibiting cell growth and motility and promoting antitumour inflammatory reactions and apoptosis[21]. Few studies have investigated the dysregulation of miRNAs in MCTs in dogs. Using real-time PCR-based TaqMan Low-Density miRNA Arrays, Fenger and colleagues[22] demonstrated that the expression level of miR-9 was increased in high-grade canine MCTs, promoting an invasive phenotype. Furthermore, circulating miRNA-126 resulted in exacerbation of non-epithelial neoplasms, including MCT[23].

The DE-miRNAs identified herein have been related to neoplasms in humans and, in some cases, in dogs. Of the five miRNAs that were found to be differentially regulated, two, namely, miR-21 and miR-379 were upregulated, whereas three, namely, miR-92a-3p, miR-338, and miR-885, were downregulated. MiR-21, which was found to be upregulated in the present study, has been widely investigated in cancer, and its upregulation has been associated with cell proliferation, invasion, apoptosis and drug resistance[24,25]. MiR-21 is frequently overexpressed in human cancers, including breast cancer, lung cancer, pancreatic cancer, ovarian cancer, glioma, liver neoplasms, gastric cancer, colorectal cancer and kidney cancer[26], and in canine oral melanoma[27], hepatocellular carcinoma[28] and malignant mammary tumours[29]. In humans, overexpression of miR-21 has been related to downregulation of tumour suppressor genes, including *programmed cell death 4* (*PDCD4*), *matrix metalloproteinases* (*MMPs*), *phosphatase and tensin homolog* (*PTEN*), *reversion inducing cysteine-rich*

protein (*RECK*), and *phosphoinositide 3-kinase* (*PI3K*)[26]. MiR-379, which was also upregulated, is an onco-suppressor miRNA. MiR-379 negatively regulates cell proliferation, migration and invasion in several human cancers, including nasopharyngeal carcinoma[30], cervical carcinoma[31], gastric cancer[32] and bladder cancer[33], by targeting *tumor protein D52* (*TPD52*)*, V-crk avian sarcoma virus CT10 oncogene homolog-like* (*CRKL*), *focal adhesion kinase* (*FAK)* and *mouse double minute 2* (MDM2).

Our results demonstrated that miR-92a, miR-338 and miR-885 were downregulated in canine MCTs. MiR-92a belongs to the miR-17-92a cluster, which is dysregulated in many different types of human tumours[34]. The mechanisms by which miR-92a promotes tumorigenesis include augmenting tumour proliferation, inhibiting tumour apoptosis, and enhancing tumour invasion and metastasis[35] by targeting *PTEN* in oesophageal squamous cell cancer[36] and *Dickkopf-related protein 3* (*DKK3*) in osteosarcoma[37]. These features identify miR-92a as an onco-miRNA. However, onco-suppressor activities of the miR-17-92a cluster have also been reported, including anti-proliferative and senescence effects in bladder cancer cells[38] and in prostate[39] and gastric[40] cancers by targeting, among other pathways, the NOTCH/EP4 pathway. Similarly, the role of miR-338 is controversial, as it has been associated with both pro- and antitumour roles. MiR-338 targets oncogenes such as *RAB32* and *EYA2*, and its downregulation in cancer is also linked to overexpression of *epidermal growth factor receptor* (*EGFR*)[41,42] and *MET transcriptional regulator* (*MACC1*)[43]. MiR-338 plays a tumour-promoting role in melanoma that is linked to tumour growth and metastasis[44]. MiR-338 is also involved in hypoxia-induced epithelial-to-mesenchymal transition by targeting *HIF-1α*[45]. MiR-885 is a tumour suppressor miRNA that interferes with cell proliferation and migration by targeting *SOCS* in colorectal cancer[46] and the Wnt/β-catenin pathway in hepatocellular carcinoma[47].

Gene Ontology and KEGG pathway analysis suggested that DE-miRNAs have an impact on transcription activities, cell cycle progression and cell survival and, in general, on several pathways involved in cancer development. This hypothesis is supported by gene expression analysis of canine cutaneous MCTs[10,48]. Gene expression profiling of metastatic and non-metastatic MCTs using an array approach identified differentially expressed genes involved in apoptosis, cell cycle arrest and loss of cell polarity and adhesion[48]. Comparison between these genes and the genes potentially modulated by DE-miRNAs identified in the present study showed that seven genes (*Fos Proto-Oncogene* or *FOS*, *Histone Deacetylase* or *HDAC*, *Striatin* or *STRN*, *Neurofibromin 2* or *NF2*, *Phosphoinositide-3-Kinase Regulatory Subunit 3* or *PIK3R3, Rho Guanine Nucleotide Exchange Factor* or *ARHGEF, C-Type Lectin Domain Containing* or *CLEC*) are potentially modulated by downregulation of miR-92a, miR-338 and miR-885. Conversely, *Sprouty RTK Signaling Antagonist* or *SPRY* can be modulated by upregulation of miR-21 and miR-379. Transcriptome analysis comparing low- and high-risk canine MCTs using next-generation RNA sequencing identified 71 differentially expressed genes associated with cell proliferation and the extracellular matrix[10]. Comparison between these genes and the candidate target genes identified in the present study showed that eight genes belonging to the kelch-like (*KLHL*), collagen (*COL*), matrix metallopeptidase (*MMP*), multi-domain (WW, PDZ, FERM) containing protein (*FRMPD*), C-type lectin domain (*CLEC*) and suppressor of cytokine signaling (*SOCS*) families may be downregulated. Conversely, genes belonging to the *KLHL* and 5-Hydroxytryptamine Receptor (*HTR*) families may be upregulated DE-miRNAs. Previous results obtained via two different strategies, an array-based approach and RNA-seq, support our hypothesis that the dysregulation of miRNAs identified in this study may influence the expression of genes involved in cell proliferation, survival and tumour spread[10].

Although the prognostic role of both the Patnaik[5] and Kiupel[4] grading systems in canine MCTs is widely accepted, histological grading alone cannot accurately predict the risk of local and distant metastases[3–5,9,49]. Nodal metastases have been reported in 20-49% of cutaneous MCTs at first presentation, and identification of lymph node involvement is crucial for accurate tumour staging and prognosis[3,49,50]. Recently, a novel classification system for the evaluation of nodal metastasis in canine MCTs has been proposed and correlated with the clinical outcome, providing evidence that dogs diagnosed with early metastatic/overt metastatic (HN2-HN3) nodes have a shorter life expectancy[7]. In our study, a three-miRNA signature (miR-379-miR-21-miR-885) accurately discriminated between healthy adjacent tissue and MCT tissue (AUC= 0.9854) and identified patients with early nodal metastases (AUC=0.8923). Since the number of enrolled patients did not allow us to perform discriminant analysis of parameters such as survival time and progression-free interval, the present results provide a background to investigate new biomarkers of MCT outcome in different matrices, including blood, to support clinical decision making.

In conclusion, the present study demonstrated that the expression levels of miR-21, miR-379, miR-92a, miR-885 and miR-338 in the tumour microenvironment are changed compared to those in healthy adjacent tissues and differ in dogs with early nodal metastases compared to those without nodal involvement, suggesting that these miRNAs may epigenetically modulate genes involved in MCT progression and metastasis. Our study provides insights into the emerging roles of miRNAs in veterinary oncology, although more efforts are required to establish the role and molecular targets of the investigated DE-miRNAs. Since the sample size influences the clinical sensitivity and specificity of the test, further studies are necessary to confirm the diagnostic value of miRNAs by increasing the number of patients.

Materials and methods

Inclusion criteria and sample collection

Thirty-seven formalin-fixed, paraffin-embedded (FFPE) samples, including 21 MCT samples and 16 healthy adjacent tissue samples (dermal tissue at the excision margins), were selected from the archives of the Department of Veterinary Medicine of the Università degli Studi di Milano. Samples were collected from client-owned dogs that underwent veterinary consultation and surgery during routine oncological management of canine mast cell tumour. All experimental procedures were reviewed and approved by the Ethics Committee of the University of Milano (approval number 118/19). Patients were recruited after the owner provided written informed consent. All experiments were performed following the relevant guidelines and regulations. Samples were trimmed and processed according to currently recommended guidelines[51] (Table 1). Cutaneous MCTs at first presentation without distant metastasis[52] and sentinel/regional lymph nodes were surgically removed and histologically classified[53] and graded[4,5]. In addition, neoplastic involvement of sentinel lymph nodes was categorized as previously described[7,52].

For all samples, after bright field microscopy observation of the haematoxylin-eosin-stained slide, the corresponding paraffin block was penetrated using a biopsy punch with a plunger (Miltex) to collect a portion of the tumour (21 MCTs) or a portion of the healthy dermal connective tissue (16 margins); the latter samples were used as controls. For MCT samples, areas of necrosis, haemorrhage or inflammation were avoided, if present.

miRNA extraction and Next-Generation Sequencing (NGS)

MiRNAs were extracted using an miRNeasy FFPE kit (Qiagen, Cat. No. 217504) following the manufacturer's instructions. The RNA quality and quantity were verified according to MIQE guidelines[54]. The RNA concentration was determined in a Qubit 2.0 fluorometer with a Qubit microRNA Assay Kit (Invitrogen, Cat. No. Q32880). A pilot NGS study was performed on 10 MCTs and 7 healthy adjacent tissue samples (Table 1). Small RNA transcripts were converted into barcoded cDNA libraries. Library preparation was performed as previously reported[55] using an NEBNext Multiplex Small RNA Library Prep Set (Cat. No. NEB#E7560) for Illumina, and sequencing was performed in a NextSeq 500 sequencer (Illumina Inc., USA).

Computational analysis

The output of the NextSeq500 Illumina sequencer was demultiplexed using bcl2fastq Illumina software embedded in the docker4seq package[56]. miRNA expression quantification was performed using the workflow and implementation previously described[57]. In brief, after adapter trimming with cutadapt[58], sequences were mapped using SHRIMP[59] to *Canis familiaris* precursor miRNAs available in miRBase 22.0-March 2018 (http://www.mirbase.org/). Using GenomicsRanges[60], an R script, was used to identify the number of reads on precursor miRNAs mapping to the expected location on mature miRNAs. The detected counts were organized in a table including all analysed samples. For visualization purposes, only CPM (counts per million reads) values were used. Differential expression analysis was conducted using the DESeq2 Bioconductor package[15] implemented in the docker4seq package. Differential expression analysis was performed using the abovementioned count table comparing the tumour and control groups using an adjusted *P*-value of ≤ 0.05 and an absolute log2 fold change (log2FC) of ≥ 1 as the threshold criteria.

miRNA quantification by RT-qPCR

Small RNAs were extracted using an miRNeasy kit for FFPE samples (Qiagen, Cat. No. 217504). The *Caenorhabditis elegans* miRNA cel-miR-39 (25 fmol final concentration) (Qiagen, Cat. No. 219610) was used as a synthetic spike-in control due to its lack of sequence homology to canine miRNAs. RNA extraction was then carried out according to the manufacturer's instructions.

To obtain cDNA, reverse transcription was performed using a TaqMan Advanced miRNA cDNA Synthesis Kit (Cat. No. A28007, Applied Biosystems) following the manufacturer's instructions.

Quantitative real-time PCR (RT-qPCR) was performed to validate the sequencing results following the MIQE guidelines[54]. The selected DE-miRNAs included miR-370-3p (assay ID 478326_mir), miR-379-5p (assay ID 478077_mir), miR-92a-3p (assay ID 477827_mir), miR-21-5p (assay ID rno481342_mir), miR-26a-5p (assay ID mmu481013_mir), miR-342-3p (assay ID 478043_mir), miR-885-5p (assay ID 478207_mir), miR-375-3p (assay ID 481141_mir), and miR-338-3p (assay ID rno480884_mir). The endogenous controls were selected from sequencing data based on microRNA that did not show significant differences, with a log2 fold change equal to zero and the lowest standard error, and included miR-122-5p (assay ID rno480899_mir), miR-128-3p (assay ID mmu480912_mir) and miR-101 (custom probe SO_66039417_6871885).

Quantitation was performed in a scaled down reaction volume (15 μl) in a CFX Connect Real-Time PCR Detection System (Bio-Rad) using 7.5 μl of 2X TaqMan Fast Advanced Master Mix (catalogue number 4444557), 0.75 μl of miRNA-specific TaqMan Advance assay reagent (20X), 1 μl of cDNA and water to make up the remaining volume. The thermal cycling profile was as follows: 50°C for 2 min, 95°C for 3 min and 40 cycles at 95°C for 15 s and 60°C for 40 s. No-RT controls and no-template controls were included. The geometric mean of the reference miRNA abundance was used for normalization. Relative

quantification of target miRNAs was carried out after sample normalization using the geometric mean of the reference miRNA abundance in Bio-Rad CFX Maestro Software using the $2^{-\Delta\Delta Cq}$ method.

miRNA target prioritization

The target genes of DE-miRNAs were retrieved using MiRWalk 3.0[61], which includes 3 miRNA target prediction programs (miRDB[62], miRTarBase[63] and TargetScan[64]). Analysis was performed on the entire gene sequence (including the 5'UTR, CDS, and 3'UTR). The list of target genes predicted by at least two of the three tools was included in further analysis, mRNA functional enrichment analysis was performed using the DAVID bioinformatic resource[65,66], and biological pathways in the KEGG database[67] were examined for enrichment.

Statistical analysis

Statistical analysis was performed using XLStat software for Windows (Addinsoft, New York, USA).

Data were tested for normality using the Shapiro-Wilk test; as the data were not normally distributed, the nonparametric Wilcoxon signed-rank test for paired samples was applied. Quantitative (miRNA quantification and tumour size) and qualitative (lymph node HN classification[7]) variables were used for ordination analysis using the 'Multiple Factor Analysis' (MFA) function. Receiver operating characteristic (ROC) analysis was performed as previously reported to determine the diagnostic accuracy[68]. Statistical significance was accepted at a *P*-value of ≤ 0.05.

Acknowledgements

The funding for this research was provided by Linea 2-2018, awarded by Università degli Studi di Milano, and by Fondo per il Finanziamento delle Attività Base di Ricerca—FFABR-Lecchi, awarded by Ministero dell'Istruzione, dell'Università e della Ricerca.

Author contributions

C.L. and V.Z. designed the study. F.C. and C.L. guided the performance of the experiments. D.S, R.F. and L.E.C. enrolled patients and surgically removed the tumours. V.G. performed histological classification and assessed the grading of tumours. V.Z. and M.A. performed the laboratory experiments. R.C. performed the bioinformatic data analysis. C.L., V.Z. and G.M. performed the statistical analysis. C.L., F.C. and D.S. provided the funding. C.L. and V.Z. wrote the main manuscript. All authors critically read and approved the manuscript.

Competing Interests

The authors declare no competing interests related to this work.

Data availability statement

The data that support the findings of this study are available from the corresponding author upon reasonable request.

References

1. Welle, M. M., Bley, C. R., Howard, J. & Rüfenacht, S. Canine mast cell tumours: A review of the pathogenesis, clinical features, pathology and treatment. *Vet. Dermatol.* **19**, 321–339 (2008).
2. Mullins, M. N. *et al.* Evaluation of prognostic factors associated with outcome in dogs with multiple cutaneous mast cell tumors treated with surgery with and without adjuvant treatment: 54 cases (1998–2004). *J. Am. Vet. Med. Assoc.* **228**, 91–95 (2006).
3. Stefanello, D. *et al.* Comparison of 2- and 3-category histologic grading systems for predicting the presence of metastasis at the time of initial evaluation in dogs with cutaneous mast cell tumors: 386 cases (2009–2014). *J. Am. Vet. Med. Assoc.* **246**, 765–769 (2015).
4. Kiupel, M. *et al.* Proposal of a 2-tier histologic grading system for canine cutaneous mast cell

tumors to more accurately predict biological behavior. *Vet. Pathol.* **48**, 147–155 (2011).

5. Patnaik, A. K., Ehler, W. J. & MacEwen, E. G. Canine Cutaneous Mast Cell Tumor: Morphologic Grading and Survival Time in 83 Dogs. *Vet. Pathol.* **21**, 469–474 (1984).

6. Kiupel, M. & Camus, M. Diagnosis and Prognosis of Canine Cutaneous Mast Cell Tumors. *Vet Clin. North. Am. Small. Anim. Pract.* **49**, 819–836 (2019).

7. Weishaar, K. M., Thamm, D. H., Worley, D. R. & Kamstock, D. A. Correlation of nodal mast cells with clinical outcome in dogs with mast cell tumour and a proposed classification system for the evaluation of node metastasis. *J. Comp. Pathol.* **151**, 329–338 (2014).

8. Sledge, D. G., Webster, J. & Kiupel, M. Canine cutaneous mast cell tumors: A combined clinical and pathologic approach to diagnosis, prognosis, and treatment selection. *Vet. J.* **215**, 43–54 (2016).

9. Blackwood, L. *et al.* European consensus document on mast cell tumours in dogs and cats. *Vet. Comp. Oncol.* **10**, e1–e29 (2012).

10. Pulz, L. H. *et al.* Identification of two molecular subtypes in canine mast cell tumours through gene expression profiling. *PLoS One* **14**, e0217343 (2019).

11. Bracken, C. P., Scott, H. S. & Goodall, G. J. A network-biology perspective of microRNA function and dysfunction in cancer. *Nat. Rev. Genet.* **17**, 719–732 (2016).

12. Di Leva, G., Garofalo, M. & Croce, C.M. miRNA in cancer. *Annu. Rev. Pathol.* **9**, 287–314 (2014).

13. Rupaimoole, R., Calin, G. A., Lopez-Berestein, G. & Sood, A. K. MiRNA deregulation in cancer cells and the tumor microenvironment. *Cancer Discov.* **6**, 235–246 (2016).

14. Lu, J. *et al.* MicroRNA expression profiles classify human cancers. *Nature* **435**, 834–838 (2005).

15. Love, M. I., Huber, W. & Anders, S. Moderated estimation of fold change and dispersion for

RNA-seq data with DESeq2. *Genome Biol.* **15**, 550 (2014).

16. Peiró-Chova, L. *et al.* High stability of microRNAs in tissue samples of compromised quality. *Virchows Arch.* **463**, 765–774 (2013).
17. Jones, W. *et al.* Deleterious effects of formalin-fixation and delays to fixation on RNA and miRNA-Seq profiles. *Sci. Rep.* **9**, 6980 (2019).
18. Maurer, M. *et al.* What is the physiological function of mast cells? *Exp Dermatol* **12**, 886–910 (2003).
19. Noli, C. & Miolo, A. The mast cell in wound healing. *Vet. Dermatol.* **12**, 303–313 (2001).
20. da Silva, E. Z., Jamur, M. C. & Oliver, C. Mast cell function: a new vision of an old cell. *J. Histochem. Cytochem.* **62**, 698–738 (2014).
21. Dyduch, G., Kaczmarczyk, K. & Okoń, K. Mast cells and cancer: enemies or allies? *Pol. J. Pathol.* **63**, 1–7 (2012).
22. Fenger, J. M. *et al.* Overexpression of miR-9 in mast cells is associated with invasive behavior and spontaneous metastasis. *BMC Cancer* **14**, 84 (2014).
23. Heishima, K. *et al.* Circulating microRNA-214 and -126 as potential biomarkers for canine neoplastic disease. *Sci. Rep.* **7**, 2301 (2017).
24. Feng, Y. H. & Tsao, C. J. Emerging role of microRNA-21 in cancer. *Biomed. Rep.* **5**, 395–402 (2016).
25. Grimaldi, A. *et al.* Non-coding RNAs as a new dawn in tumor diagnosis. *Semin. Cell Dev. Biol.* **78**, 37–50 (2018).
26. Javanmardi, S., Aghamaali, M. R., Abolmaali, S. S., Mohammadi, S. & Tamaddon, A. M. miR-21, An Oncogenic Target miRNA for Cancer Therapy: Molecular Mechanisms and Recent

Advancements in Chemo and Radio-resistance. *Curr. Gene Ther.* **16**, 375–389 (2017).

27. Ushio, N. *et al.* Identification of dysregulated microRNAs in canine malignant melanoma. *Oncol. Lett.* **17**, 1080–1088 (2019).

28. Lai, Y. C. *et al.* Aberrant expression of microRNAs and the miR-1/MET pathway in canine hepatocellular carcinoma. *Vet. Comp. Oncol.* **16**, 288–296 (2018).

29. Boggs, R. M., Wright, Z. M., Stickney, M. J., Porter, W. W. & Murphy, K. E. MicroRNA expression in canine mammary cancer. *Mamm. Genome* **19**, 561–9 (2008).

30. Zhao, X. & Chu, J. Microrna-379 suppresses cell proliferation, migration and invasion in nasopharyngeal carcinoma by targeting tumor protein D52. *Exp. Ther. Med.* **16**, 1232–1240 (2018).

31. Shi, X. *et al.* MicroRNA-379 Suppresses Cervical Cancer Cell Proliferation and Invasion by Directly Targeting V-crk Avian Sarcoma Virus CT10 Oncogene Homolog-Like (CRKL). *Oncol. Res.* **26**, 987–996 (2018).

32. Xu, M., Qin, S., Cao, F., Ding, S. & Li, M. MicroRNA-379 inhibits metastasis and epithelial-mesenchymal transition via targeting FAK/AKT signaling in gastric cancer. *Int. J. Oncol.* **51**, 867–876 (2017).

33. Wu, D. *et al.* MicroRNA-379-5p plays a tumor-suppressive role in human bladder cancer growth and metastasis by directly targeting MDM2. *Oncol. Rep.* **37**, 3502–3508 (2017).

34. Li, M. *et al.* miR-92a family and their target genes in tumorigenesis and metastasis. *Exp. Cell Res.* **323**, 1–6 (2014).

35. Zhang, X., Li, Y., Qi, P. & Ma, Z. Biology of MiR-17-92 Cluster and Its Progress in Lung Cancer. *Int. J. Med. Sci.* **15**, 1443–1448 (2018).

36. Li, X., Guo, S., Min, L., Guo, Q. & Zhang, S. miR-92a-3p promotes the proliferation, migration and invasion of esophageal squamous cell cancer by regulating PTEN. *Int. J. Mol. Med.* **44**, 973–981 (2019).

37. Yu, H. *et al.* MiR-92a modulates proliferation, apoptosis, migration, and invasion of osteosarcoma cell lines by targeting Dickkopf-related protein 3. *Biosci. Rep.* **39**, (2019).

38. Tao, J. *et al.* microRNA-18a, a member of the oncogenic miR-17-92 cluster, targets Dicer and suppresses cell proliferation in bladder cancer T24 cells. *Mol. Med. Rep.* **5**, 167–172 (2012).

39. Ottman, R., Levy, J., Grizzle, W. E. & Chakrabarti, R. The other face of miR-17-92a cluster, exhibiting tumor suppressor effects in prostate cancer. *Oncotarget* **7**, 73739–73753 (2016).

40. Shin, V. Y. *et al.* MiR-92 suppresses proliferation and induces apoptosis by targeting EP4/Notch1 axis in gastric cancer. *Oncotarget* **9**, 24209–24220 (2018).

41. Wang, Y. & Qin, H. miR-338-3p targets RAB23 and suppresses tumorigenicity of prostate cancer cells. *Am. J. Cancer Res.* **8**, 2564–2574 (2018).

42. Liang, Y. *et al.* The EGFR/miR-338-3p/EYA2 axis controls breast tumor growth and lung metastasis. *Cell Death Dis.* **8**, e2928 (2017).

43. Zhang, C., Li, H., Wang, J., Zhang, J. & Hou, X. MicroRNA-338-3p suppresses cell proliferation, migration and invasion in human malignant melanoma by targeting MACC1. *Exp. Ther. Med.* **18**, 997–1004 (2019).

44. Long, J., Luo, J. & Yin, X. MiR-338-5p promotes the growth and metastasis of malignant melanoma cells via targeting CD82. *Biomed. Pharmacother.* **102**, 1195–1202 (2018).

45. Shan, Y. *et al.* MicroRNA-338 inhibits migration and proliferation by targeting hypoxia-induced factor 1α in nasopharyngeal carcinoma. *Oncol. Rep.* **34**, 1943–1952 (2015).

46. Su, M., Qin, B., Liu, F., Chen, Y. & Zhang, R. Mir-885-5p upregulation promotes colorectal cancer cell proliferation and migration by targeting suppressor of cytokine signaling. *Oncol. Lett.* **16**, 65–72 (2018).

47. Zhang, Z. *et al.* miR-885-5p suppresses hepatocellular carcinoma metastasis and inhibits Wnt/β-catenin signaling pathway. *Oncotarget* **7**, 75038-75051 (2016).

48. Blacklock, K. B. *et al.* Identification of molecular genetic contributants to canine cutaneous mast cell tumour metastasis by global gene expression analysis. *PLoS One* **13**, e0208026 (2018).

49. Ferrari, R. *et al.* The impact of extirpation of non-palpable/normal-sized regional lymph nodes on staging of canine cutaneous mast cell tumours: A multicentric retrospective study. *Vet. Comp. Oncol.* **16**, 505–510 (2018).

50. Marconato, L. *et al.* Therapeutic impact of regional lymphadenectomy in canine stage II cutaneous mast cell tumours. *Vet. Comp. Oncol.* **16**, 580–589 (2018).

51. Kamstock, D. A. *et al.* Recommended guidelines for submission, trimming, margin evaluation, and reporting of tumor biopsy specimens in veterinary surgical pathology. *Vet. Pathol.* **48**, 19–31 (2011).

52. Stefanello, D. *et al.* Ultrasound-guided cytology of spleen and liver: A prognostic tool in canine cutaneous mast cell tumor. *J. Vet. Intern. Med.* **23**, 1051–1057 (2009).

53. Thompson, J. J. *et al.* Canine subcutaneous mast cell tumors: cellular proliferation and KIT expression as prognostic indices. *Vet. Pathol.* **48**, 169–81 (2011).

54. Bustin, S. A. *et al.* The MIQE guidelines: Minimum information for publication of quantitative real-time PCR experiments. *Clin. Chem.* **55**, 611–622 (2009).

55. Pardini, B. *et al.* microRNA profiles in urine by next-generation sequencing can stratify bladder

cancer subtypes. *Oncotarget* **9**, 20658–20669 (2018).

56. Beccuti, M. *et al.* SeqBox: RNAseq/ChIPseq reproducible analysis on a consumer game computer. *Bioinformatics* **34**, 871–872 (2018).

57. Cordero, F., Beccuti, M., Arigoni, M., Donatelli, S. & Calogero, R. A. Optimizing a Massive Parallel Sequencing workflow for quantitative miRNA expression analysis. *PLoS One* **7**, e31630 (2012).

58. Martin, M. Cutadapt removes adapter sequences from high-throughput sequencing reads. *EMBnet.journal* **17**, 10 (2011).

59. Rumble, S. M. *et al.* SHRiMP: Accurate mapping of short color-space reads. *PLoS Comput. Biol.* **5**, e1000386 (2009).

60. Lawrence, M. *et al.* Software for computing and annotating genomic ranges. *PLoS Comput. Biol.* **9**, e1003118 (2013).

61. Sticht, C., De La Torre, C., Parveen, A. & Gretz, N. Mirwalk: An online resource for prediction of microRNA binding sites. *PLoS One* **13**, e0206239 (2018).

62. Wong, N. & Wang, X. miRDB: An online resource for microRNA target prediction and functional annotations. *Nucleic Acids Res.* **43**, D146–D152 (2015).

63. Hsu, S. D. *et al.* MiRTarBase: A database curates experimentally validated microRNA-target interactions. *Nucleic Acids Res.* **39**, D163–169 (2011).

64. Agarwal, V., Bell, G. W., Nam, J. W. & Bartel, D. P. Predicting effective microRNA target sites in mammalian mRNAs. *Elife* **4**, (2015).

65. Huang, D. W., Sherman, B. T. & Lempicki, R. A. Bioinformatics enrichment tools: Paths toward the comprehensive functional analysis of large gene lists. *Nucleic Acids Res.* **37**, 1–13 (2009).

66. Huang, D. W., Sherman, B. T. & Lempicki, R. A. Systematic and integrative analysis of large gene lists using DAVID bioinformatics resources. *Nat. Protoc.* **4**, 44–57 (2009).

67. Kanehisa, M., Goto, S., Sato, Y., Furumichi, M. & Tanabe, M. KEGG for integration and interpretation of large-scale molecular data sets. *Nucleic Acids Res.* **40**, D109–114 (2012).

68. Lecchi, C. *et al.* Characterization of circulating miRNA signature in water buffaloes (Bubalus bubalis) during *Brucella abortus* infection and evaluation as potential biomarkers for non-invasive diagnosis in vaginal fluid. *Sci. Rep.* **9**, 1945 (2019).

Tables:

	Breed	Sex	Age (years)	Tumor location	Size (cm)	Grade		Lymph node status†
						Patnaik	Kiupel	
1	American Staffordshire Terrier[a,d]	Male	6	Trunk	1	II	Low	HN1
2	Bernese	Female	4	Limb	2.5	II	Low	HN2
3	Boxer	Male	8	Limb	2.2	II	Low	HN2
4	Dachshund	Female	9	Trunk	0.8	II	Low	HN0
5	Dogo[a,b]	Male	6	Limb	2	II	Low	HN2
6	English setter[a,b]	Female	6	Trunk	3	II	Low	HN2
7	English setter[a,c,d]	Female	11	Trunk	5	II	Low	HN3
8	Italian pointer[a,b]	Male	5.5	Trunk	4	II	Low	HN1
9	Jack Russell[a,b]	Male	13	Head	5	II	High	HN2
10	Labrador	Male	1	Head	1	I	Low	HN0
11	Labrador[d]	Male	10	Scrotum	2	II	Low	HN0
12	Labrador	Male	9	Trunk	0.6	II	Low	HN2
13	Labrador	Female	6	Trunk	3.5	II	Low	HN2
14	Mixed breed[a,b,c]	Female	11	Trunk	3	II	Low	HN0
15	Mixed breed[a,b]	Female	6	Trunk	4	II	Low	HN2
16	Mixed breed[a,b]	Male	11	Limb	3	III	High	HN2
17	Mixed breed[a,c,d]	Female	8	Limb	3	III	High	-
18	Mixed breed[c]	Male	12	Neck	7	II	Low	HN3
19	Pug	Male	3.5	Head	1	II	Low	HN2
20	Tosa inu	Male	4	Trunk	3	II	Low	HN2
21	Weimaraner	Male	7	trunk	2	II	Low	HN2

†classification system proposed by Weishaar and colleagues (2014). HN= histological node. NGS= next-generation sequencing.

[a]= MCT samples sequenced using NGS

[b]= healthy margins sequenced using NGS

[c]= samples in which miRNAs selected for the RT-qPCR validation step were not detected

[d]= samples for which healthy margins were not collected

Table 1. Summary of clinical and histopathological data

	miRNA	AUC	95% CI	*P*-value	Cut-off	Sensitivity	1-Specificity
Downregulated	miR-885	0.9181	0.8276-1.000	<0.0001	0.0357	0.8889	0.9474
	miR-92a	0.7427	0.5925-0.8929	=0.0015	0.814	0.7222	0.6842
	miR-338	0.7339	0.5827-0.8851	=0.0024	1.7878	0.6111	0.7895
Upregulated	miR-21	0.9825	0.9825-0.9825	<0.0001	1.6250	0.9444	0.9474
	miR-379	0.9211	0.8328-1.000	<0.0001	11.5688	1.000	0.7895
W-AV*	miR-379+miR-21+miR-885	0.9854	0.9854-0.9854	<0.0001	0.1654	1.000	0.9444
W-AV-HN**	miR-379+miR-21+miR-885	0.8923	0.759-1.000	<0.0001	0.5528	0.9231	0.8000

*W-AV= weighted average relative quantification of miR-379+miR-21+miR-885 in healthy *versus* MCT samples

** W-AV-HN= weighted average relative quantification of miR-379+miR-21+miR-885 in HN0/1 *versus* HN2 samples

Table 2. The area under the curve (AUC), sensitivity and specificity values of DE-miRNAs.

Target genes of downregulated miRNAs	**3'UTR**	*FOS, POF1B, TP63, PTGES2, CCDC113, LPIN1, IL6ST, GTF2A1, HDAC2, MED19, TET2, PBLD, ZBTB7B, KIF1B, PPP1R3D, CNNM4, MED29, PAFAH1B1, RASAL2, ABL2, PAWR, TMCC3, SMARCA5, KLHL3, CDK5R1, TIA1, PDIK1L, FKBP1A, MACROD2, RAB14, ATG9A, SCN1A, FAM168A, NOL4, HEXIM1, C16orf87, SH3PXD2A, TSFM, ARPC1B, MSL2, RIC1, NFIA, GNG12, ZZZ3, DUSP16, SERINC5, LAMC1, IPO9, HNF4G, YRDC, RPH3A, PPM1B, AAK1, LSM14A, CNOT6, SOX6, ZADH2, NOL4L, NFIB, MAP2K4, NEDD4L, TMEM50B, SLC30A7, LIN54, GNAQ, PALM2, SYNDIG1, KIF3B, JPH2, LPP, PCGF3, RGS3, DAB2IP, TSC1, COL5A1, ATXN1, MARCH4, PAX3, TRIP12, EPC2, MAP3K20, SESTD1, ITGAV, TPBGL, LDLRAD4, TECPR2, TRAF3, ACTC1, UBE2Z, OTUD3, LUZP1, MTMR9, RNF157, SLC9A7, TAF1, ATRX, USP28, GRAMD1B, SRPRA, C21orf91, AFF3, KCNC4, ANP32E, SEC31B, CCDC186, PLEKHA1, PITPNM2, LRCH1, AXL, PPP1R37, CDC42BPA, ZBTB18, GRHL1, PHLPP2, ZFHX3, RASSF3, DYRK2, STRN3, STYX, PPP1R9A, SMURF1, PIK3CB, TFDP2, DCX, TMEM255A, MBNL3, PCDH11Y, DESI1, SHOX, PTPRD, DENND4B, KCNN3, NF2, PLXDC2, GPR158, PIK3R3, EVI5, ERGIC2, RAB3C, AGGF1, BTG2, ELK4, ARID1B, FAM20C, SNX13, ATG14, KCNK10, FOXN3, ATXN3, PCMTD1, SGK3, UBE2W, MMP16, CCNE2, MTDH, NIPAL1, CXCL5, G3BP2, WDFY3, TCF21, LIN28A, GAS2L3, EFR3B, KCNK3, YIPF4, SOCS5, SERTAD2, CEP41, CREB3L2, ELOVL6, SETD7, DCLK2, SH3D19, PPARGC1B, CAMK2A, CPEB4, RNF141, EIF4G2, CHST1, ARRDC3, MAN2A1, FNIP1, SLX4, GLYR1, SNN, ATXN7, ZBTB20, SPOCK2, DNAJB12, CCSER2, GID4, PIP5K1C, SCUBE3, CD2AP, TRAM2, PHF3*
	5'UTR	*MYLIP, PCMTD1, RRBP1, ELOVL6, E2F3, GAA, AURKA, ANP32E, CCDC186, PAX9, DYNLT3, DENND4B, WASL, SETD5, FAM135A, XKR7, GAN, CNOT2, RABGAP1L, ZNF287, IDH1, NR4A3, TBC1D19, PLEKHB2, TGIF1, ZNF532, CPEB1, KCNA1, SPHK2, CBFA2T3, COL1A2, TBL1XR1, AIFM1, PTPRD, KLF6, RAB3C, KCNK10, PAPOLA, NAV3, FOSL2, ATL3, SH3D19, SCRG1, WWC1, SNX2*
	CDS	*FOS, DAB2IP, HIPK1, MYLIP, GRAMD1B, MAP2K4, MTF1, PTAR1, RRBP1, NOL4L, TSC1, HIVEP1, ATXN1, IKZF2, TRIP12, SSFA2, VPS4B, TECPR2, GOLGA8A, GOLGA8B, NSF, XYLT2, ELOA, ADAM10, GAA, RBL2, ARFGEF2, SYNJ1, BCL2L11, MCL1, SH3PXD2A, PDZD8, GOLGA3, IPO5, PHLPP2, ITGA5, ANKIB1, FNDC3B, MPP1, RAD21, ZNF17, ZNF776, MYH9, GPBP1L1, CD69, SCAF11, ATP2B4, DSTYK, TULP4, CUX1, CREB3L2, KIAA1109, RBM27, SETD5, TRIM36, TMF1, VPS52, ZBTB34, MBD2, UBR1, NPTN, CNOT2, TTLL7, XPR1, FKBP14, TMCC3, TCHP, PDCD6IP, LCOR, USP7, FRMD3, GNL1, RAB30, WNK4, SS18L1, CELSR2, MYT1L, COX4I1, TSFM, CACNA2D1, PVALB, NFIA, ADGRA2, PPM1B, FBXW7, B4GALT7, RASA1, ZBTB20, SLC35G1, KIAA1024, USF2, TAGAP, STX17, SEL1L3, TBC1D19, ANGPTL2, ADAM23, GIGYF2, LRP1B, SLC4A10, MAP3K20, ZNF385B, ARHGEF17, EPG5, HERC2, RYR3, EPHA8, CSMD1, ATP6V1B2, CHMP7, CPEB1, NRK, FRMPD3, DOK5, TACC2, SBNO1, ITM2B, SPTBN4, HNRNPU, HAS3, WWP2, SCN8A, GDF11, DTX2, PPP1R9A, PIK3CB, PEX5L, VWA5B2, TENM1, CSMD3, EFR3A, PTPRD, TTC28, NOTCH1, P3H3, EPS8, PDZD2, NIPBL, RAB3C, DCAF6, SNX13, PLEKHG3, BSN, ZC2HC1A, RBM47, REST, WDFY3, PTPRK, TCF21, GAS2L3, ADCY3, SRPK2, CTTNBP2, NRF1, NFIX, RHPN2, NPNT, OTUD4, ADAM19, CNTN4, OXSR1, ASB7, CLEC16A, FOXP1, ROBO2, BTLA, FSTL1, MYO18A, C2CD4C, PHF3, COL19A1*

Target genes of upregulated miRNAs	3'UTR	*RECK, NCAPG, PAN3, KLHL42, GID4, CCL1, CD59, SLC20A1, PPP1R3B, NEGR1, THRB, PCDH17, FIGN, HTR2C, FAM126B, ETNK1*
	5'UTR	*KAT6A, ZBTB26, TNRC6B*
	CDS	*EPHA4, ADNP, TNRC6B, ATF7IP, FBXO11, NR2C2, PTPN14, SPRY4, KLF3, CASKIN1, ROBO2*

Table 3. Candidate target genes retrieved from the miRWalk 3.0 database.

Figures:

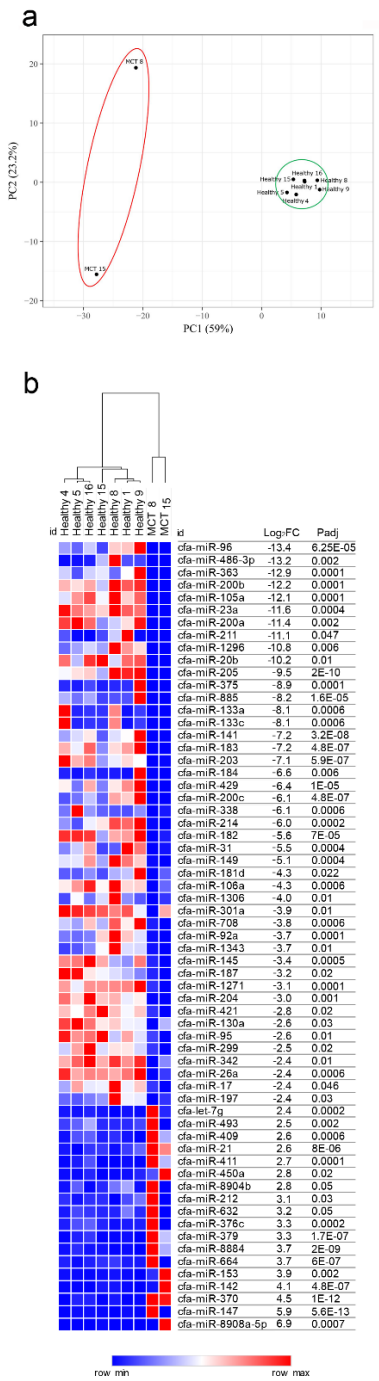

Figure 1. NGS results. (A) Principal component analysis (PCA) of sequenced samples. Two-dimensional PCA was used to determine whether MCTs (red circle) could be differentiated from healthy (green circle) samples. (B) Identification of DE-miRNAs between MCTs and healthy samples. Heat map and table displaying the fold change and Padj of DE-miRNAs.

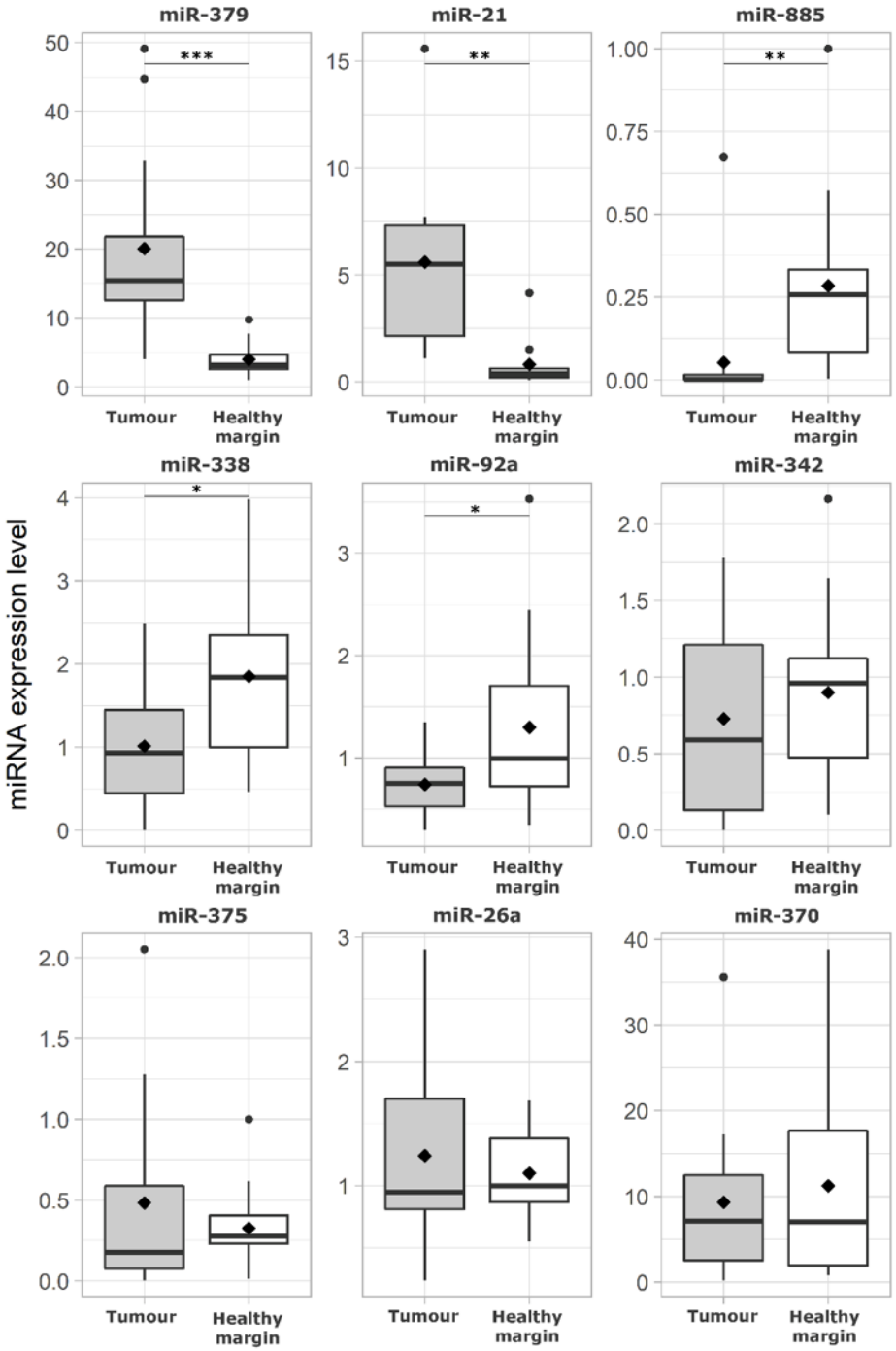

Figure 2. Box plots of DE-miRNAs in MCTs compared with healthy margins. Significance was accepted at *P*<0.05 (*), *P*< 0.01 (**) and *P*< 0.001 (***). The black lines inside the boxes denote the medians. The whiskers indicate variability outside the upper and lower quartiles.

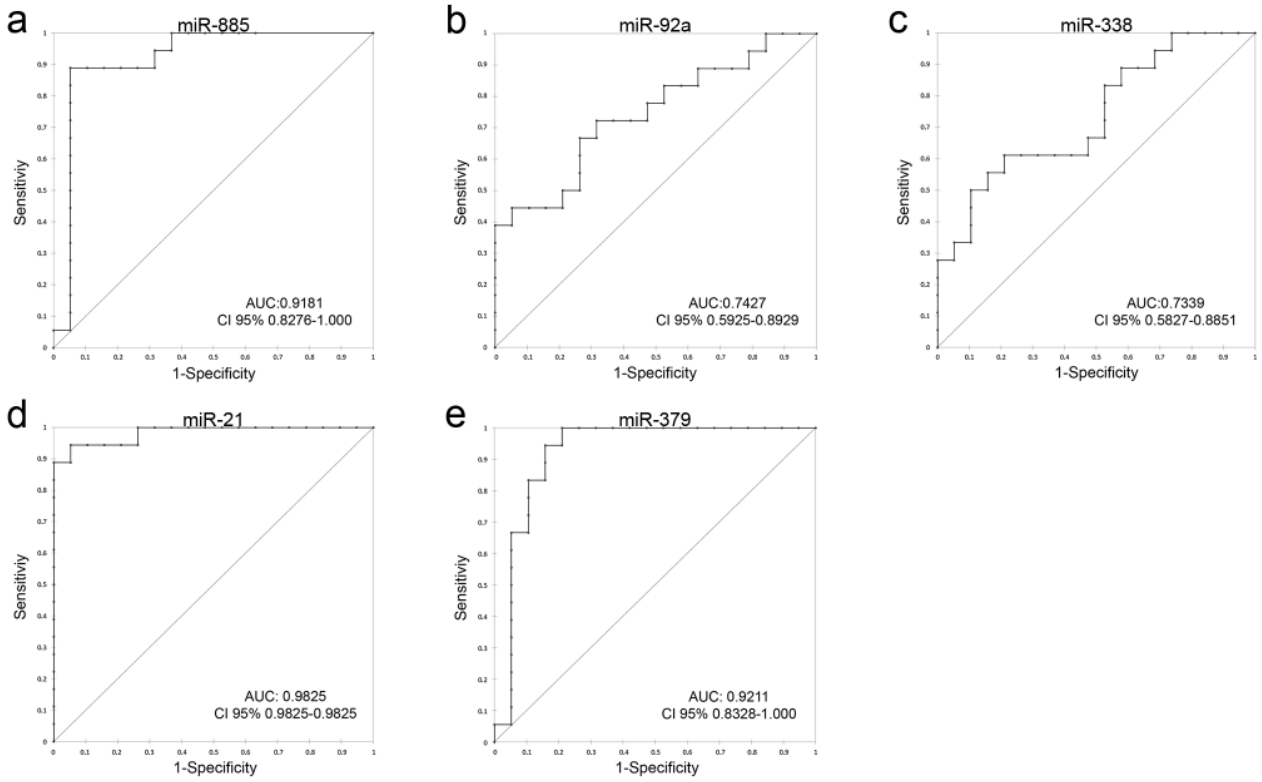

Figure 3. Receiver operating characteristic (ROC) curve analysis of DE-miRNAs. (A) AUC of miR-885; (B) AUC of miR-92a; (C) AUC of miR-338; (D) AUC of miR-21; (E) AUC of miR-379. AUC, area under the curve; CI, confidence interval.

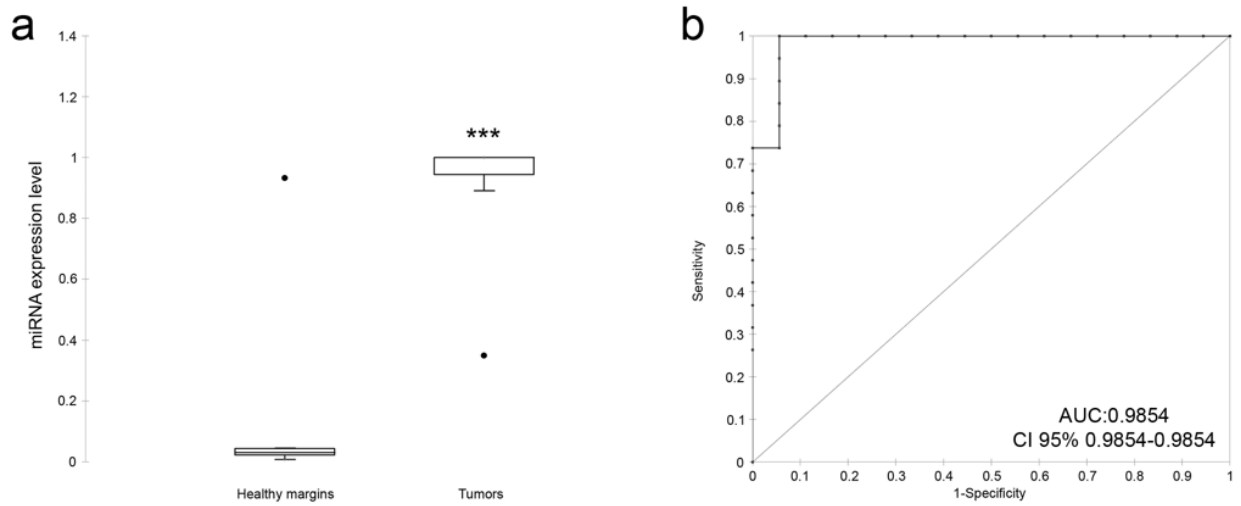

Figure 4. The average expression of the DE-miRNAs with AUC>0.9, including miR-379, miR-21 and miR-885. (A) The weighted average relative quantification (RQ) values of DE-miRNAs in healthy *versus* MCT samples (A) and ROC curve analysis performed using the logit model, for healthy *versus* MCT samples (B). AUC, area under the curve; CI, confidence interval. The black lines denote the medians. ** *P*< 0.001; *** *P*< 0.0001.

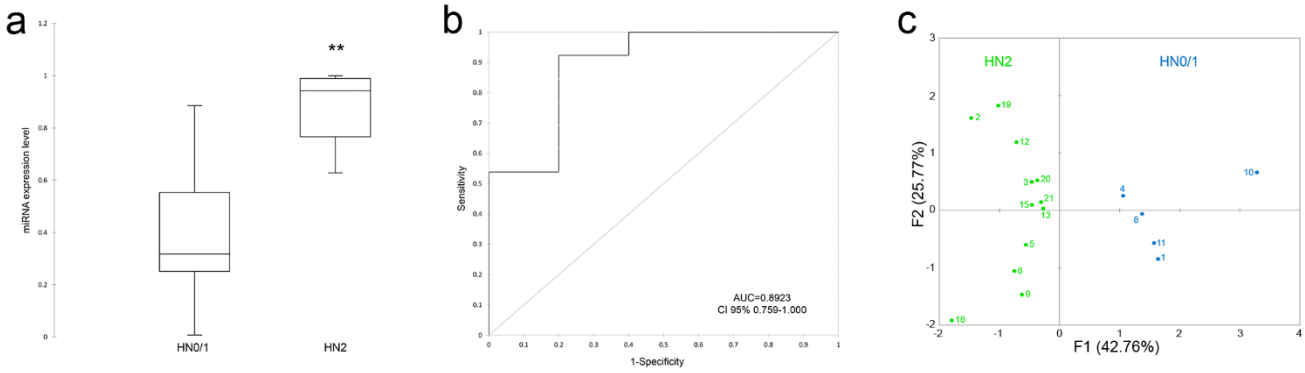

Figure 5. The average expression of the DE-miRNAs with AUC>0.9, including miR-379, miR-21 and miR-885. (A) The weighted average relative quantification (RQ) values of DE-miRNAs in HN0/1 *versus* HN2 samples; (B) ROC curve analysis performed using the logit model for HN0/1 *versus* HN2 samples; (C) Individual map for Multiple Factor Analysis (MFA): each sample name represents the barycentre of the two positions according to the dataset coloured according to lymph node

involvement: HN0/1 (blue) and HN2 (green). AUC, area under the curve; CI, confidence interval. The black lines denote the medians. ** *P*< 0.001; *** *P*< 0.0001.

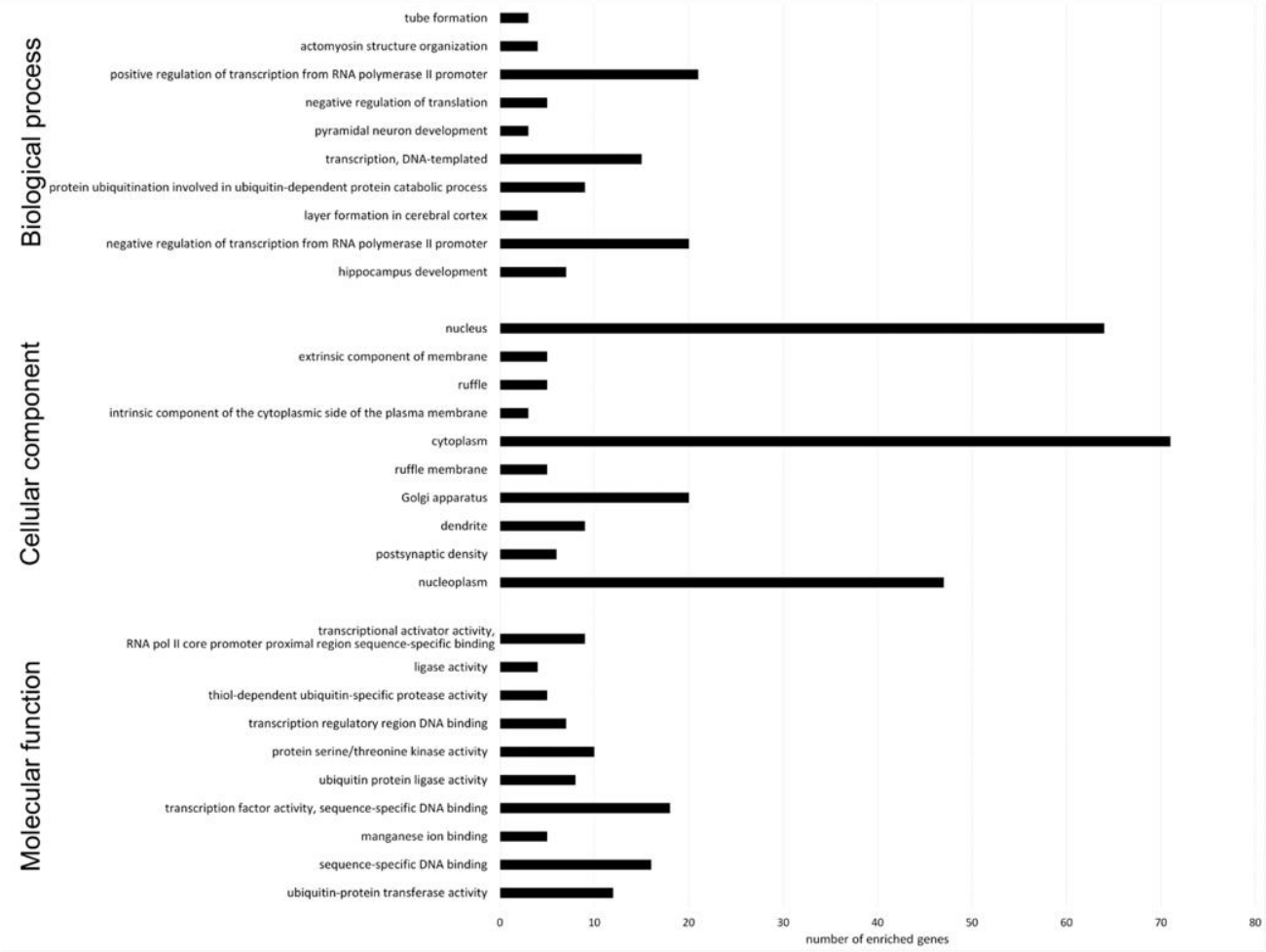

Figure 6. Gene Ontology (GO) enrichment analysis of terms potentially regulated by DE-miRNAs. The target genes were annotated by DAVID in three categories: biological process, cellular component and molecular function. The top 10 significantly enriched terms are shown.

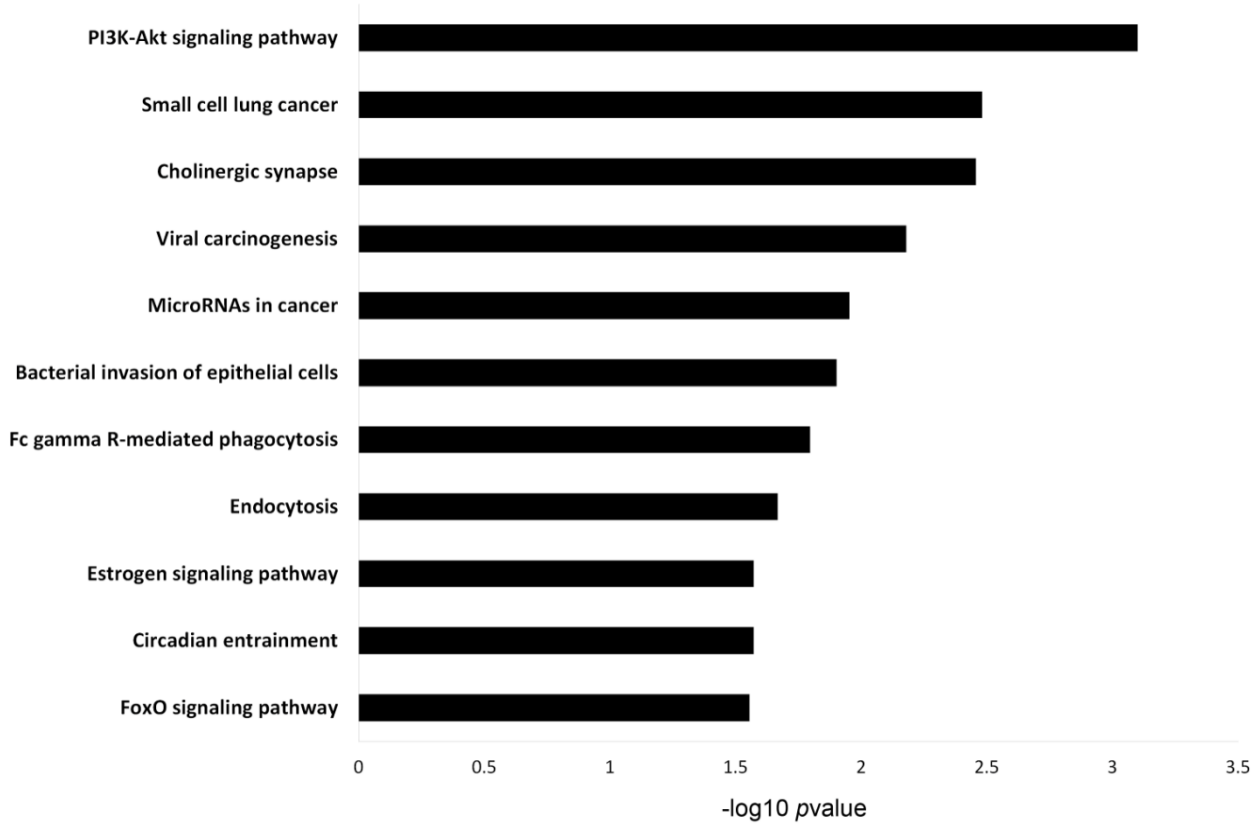

Figure 7. Pathway enrichment analysis for genes potentially regulated by DE-miRNAs. Genes regulated by DE-miRNAs were retrieved and analysed for enrichment in KEGG pathways using DAVID. The *P*-value was -log10 transformed. The top 10 enriched KEGG pathways are reported.

Supplementary Materials:

Supplementary table S1.

https://www.ncbi.nlm.nih.gov/pmc/articles/PMC7609711/bin/41598_2020_75877_MOESM1_ESM.xlsx

Salivary miR-885 as potential minimally invasive biomarker to detect mast cell tumor in dogs

Valentina Zamarian[1], Damiano Stefanello[1], Roberta Ferrari[1], Lavinia Elena Chiti[1], Valeria Grieco[1], Fabrizio Ceciliani[1], Cristina Lecchi[1*]

(1) Dipartimento di Medicina Veterinaria, Università degli Studi di Milano, Milano, Italy

* Corresponding author: Cristina Lecchi.

Address: via Celoria 10, Milan 20133 – Italy

Telephone number: +390250334532

Email: cristina.lecchi@unimi.it

Abstract

MicroRNAs (miRNAs) are a class of non-coding RNA molecules of 20-22 nucleotides playing a crucial role in tumor modulation targeting mRNA. A panel of three miRNAs - miR-21, miR-379 and miR-885 - has been previously identified in canine mast cell tumor (MCT) as markers of lymph node involvement in terms of histological absence (non-metastatic: HN0; pre-metastatic: HN1) and presence (early-metastatic: HN2; overt-metastatic: HN3) of metastasis. This study aimed at validating the diagnostic potential of this panel in the saliva of MCT-affected dogs by quantitative PCR. Forty-seven saliva samples were analyzed, among which 36 were collected from MCT-affected dogs (12 classified as HN0-1 and 24 as HN2-3) and 11 from healthy dogs.

The results showed that the expressions of miR-21 (p=0.034) and miR-885 (p=0.002) were modulated by MCT when compared with the healthy group. MiR-21 (p= 0.029) was up-regulated in HN2-3 compared with the healthy group. MiR-885 was up-regulated in HN0-1 (p< 0,0001) and in HN2-3 (p= 0.027) when compared with the healthy samples and down-regulated in the HN2-3 group compared with HN0-1 (p= 0.011). MiR-379 was not detected in saliva. The diagnostic potential of the two miRNAs in discriminating MCT-affected dogs between the healthy group (AUC=0.8369) and the tumor classes (AUC=0.7833) was proved by ROC curve analysis. The multi-functional analysis (MFA) showed that miR-885 recognized the lymph node involvement, discriminating HN0-1, HN2-3 and healthy groups. Overall, miR-885 was identified as a promising tool, representing a novel approach to detect MCT-associated epigenetic alterations in a minimally invasive manner repeatable over time.

Keywords: mast cell tumor, dog, saliva, miRNA, biomarkers.

Introduction

MicroRNA (miRNAs) are small non-coding RNA acting as molecular orchestrators, in almost all cellular pathways, targeting the mRNA to block or destroy its translation[9]. MiRNAs are present in all biological fluids, and their regulation depends on the pathophysiological condition[15]. miRNA expression changes during cancer[29]. The identification of miRNAs involved in tumor progression (oncomiRNAs) and tumor suppression (tumor suppressor miRNAs) has been investigated[10] in both humans and animals[22]. The need for minimally invasive and repeatable over time biomarkers for early diagnosis and monitoring of the tumor recurrence has driven the research towards the use of alternative biological matrices, like saliva[16,25,33]. Tumor associated-miRNAs dysregulated in both primary tumor mass and plasma are differentially expressed in the saliva of patients with head and neck cancer[23] and oral squamous cell carcinoma[12], respectively. The relevance of saliva as an important source for biomarker identification was also assessed in tumors arising distantly from the oral cavity[21,24]. Several studies in human oncology compared the expression profile of miRNAs in different matrices[20], while, at the best of authors' knowledge, no investigations are reported in canine oncology.

Canine mast cell tumor (MCT) is one of the most frequent skin neoplasms in dogs with a prevalence from 7 to 21%[31], and its variable biological behavior makes challenging the diagnosis and complex the prognosis[2]. The standard diagnostic approach includes the evaluation of the tumor staging and the histological grading, using both Patnaik[17] and Kiupel[8] grading systems. In the last decade, the literature has shown a growing interest in the early detection of lymph node metastasis to accurately stage the disease and suggest appropriate treatment options[6,30,32]. Previous studies detected some MCT-associated miRNAs in plasma and primary tumor mass[5,7,34]. We profiled the miRNome of MCT primary tumor in formalin-fixed paraffin-embedded samples identifying three dysregulated miRNAs - miR-21, miR-379 and miR-885- able to distinguish the lymph node

involvement and discriminate between non-metastatic (HN0-1) and metastatic (HN2-3) tumors[34]. The present study aimed to demonstrate the potential of saliva as minimally invasive reliable biological fluid for detection and quantification of tumor-associated miRNAs suitable for diagnosis and lymph node staging of canine MCT.

Material and methods

Samples collection

Forthy-seven saliva samples were collected from 36 MCT-affected dogs and 11 healthy dogs, using a sterile dryswab™ (Medical Wire & Equipment, UK). Owners signed a written consent to the procedure. In the MCT group we included dogs with a cytological diagnosis of MCT that were preoperatively staged negative for distant metastases and underwent surgical excision of MCT and regional or sentinel lymph node(s). For all dogs, oncological staging consisted of abdominal ultrasound with cytological examination on fine-needle aspirates of the spleen and liver[26] and CBC with peripheral blood smear evaluation was performed. On the day of surgery, after general anaesthesia induction, a sample of saliva was collected by rubbing the sterile swab in the maxillary vestibular area. Dogs were then moved to the operating theater and wide-margins surgical resection of the MCT and regional (n=4) or sentinel (n=32) node extirpation was performed. All excised nodes were non-palpable/normal-sized. The excised MCT and lymph node(s) were submitted for histopathology, fixed in 10% buffered formalin and routinely trimmed and processed. Histopathological evaluation of submitted specimen included: tumor classification (cutaneous or subcutaneous), tumor gradings[8,17], surgical margins (infiltrated or non-infiltrated), and lymph node classification as reported by Weishaar and colleagues (2014). The 36 MCTs samples were grouped in 12 with non-metastatic/pre-metastatic lymph nodes (HN0-1) and 24 with early-metastatic/overt-metastatic lymph nodes (HN2-3). In the healthy group, we included dogs without MCT nor other

oncological or systemic diseases that presented to the University Veterinary Teaching Hospital of University of Milan for routine annual clinical examination or vaccination. The saliva was collected by rubbing the maxillary vestibular area with a sterile swab, with the dog awake. Data regarding the studied population are shown in Supplementary Table S1. The saliva samples were stored at -80°C until use.

MiRNA extraction, retrotranscription and quantitative PCR

Small RNAs were extracted using the miRNeasy Serum/Plasma Kit (Qiagen, Cat. No. 217184). Briefly, the saliva swab was immersed in 2 mL of Qiazol (Qiagen), vortexed, incubated 5 min at room temperature and centrifuged at 14100 x g for 5 min. Then 3.75 µl (25 fmol final concentration) of the *Caenorhabditis elegans* miRNA cel-miR-39 (Qiagen, Cat. No. 219610) was added as synthetic spike-in control due to the lack of sequence homology to canine miRNAs. The extraction was then carried on following the manufacturing procedure, and miRNAs were eluted in 18µl of RNase free water. The reverse transcription was performed using the TaqMan Advanced miRNA cDNA Synthesis Kit (Applied Biosystems, Cat. No. A28007) following the manufacturer's instruction.

The quantitative PCR (qPCR) reaction was performed following the MIQE guidelines[3]. Target miRNAs were selected following what previously reported[34] to validate their diagnostic potential in saliva. The selected probe assays (Life Technologies) included cel-miR-39-3p (assay ID 478293_mir), miR-21-5p (assay ID rno481342_mir), miR-379-5p (assay ID 478077_mir) and miR-885-5p (assay ID 478207_mir). The qPCR was performed on CFX Connect Real-Time PCR Detection System (Biorad). The reaction included 7.5 µl of 2X TaqMan Fast Advanced Master Mix (Cat. No. 4444557), 0.75 µl of miRNA specific TaqMan Advance assay (20X), 1 µl of cDNA and water to reach the final volume (15µl). The thermal profile was 50°C for 2 min, 95 °C for 3 min and 40 cycles of 95°C for 15s and 60 °C for 40s. Cel-miR-39 expression was used for data normalization. The relative expression was

calculated using Bio-Rad CFX Maestro™ Software. MiRNAs expression are presented in terms of fold change normalized to cel-miR-39 expression using the $2^{-\Delta\Delta Cq}$ formula.

Statistical analysis

The statistical analysis was performed on XLStat software for Windows (Addinsoft, New York, USA). The data were tested for normality using the Shapiro-Wilk test, and as the data were not normally distributed the Kruskal-Wallis for multiple pairwise comparisons was applied, as a non-parametric test. A principal component analysis (PCA) was performed to detect any correlation between groups. A receiver operating characteristic (ROC) and a multi-functional analysis (MFA) were performed using miRNAs relative expression and lymph node classification (NH) as variables. Statistical significance was accepted at *p*-value≤ 0.05.

Results

miR-21 and miR-885 were differentially expressed between tumor and healthy samples and discriminate lymph nodal involvement

The qPCR was carried out on all 47 enrolled samples. Two out of three selected miRNAs, miR-21 and miR-885, were quantified in all samples, while miR-379 was not detected in saliva. MiR-21 and miR-885 showed a dysregulation in tumor samples (Figure 1a and b). In detail, miR-21 (p=0.034, $\log2FC_{Tumor/Healthy}$=2.0) (Figure 1a) and miR-885 (p=0.002, $\log2FC_{Tumor/Healthy}$=1.61) (Figure 1b) were up-regulated in MCT compared with the healthy group.

Considering tumor classes based on the lymph nodal involvement, miR-21 (p= 0.029, $\log2FC_{HN2-3/Healthy}$=1.75) was up-regulated in HN2-3 class compared with the healthy group (Figure 1c). MiR-885 was up-regulated in both tumor classes, HN0-1 and HN2-3, compared to the healthy samples (p< 0,0001, $\log2FC_{HN0-1/Healthy}$=2.49; p=0.027, $\log2FC_{HN2-3/Healthy}$=0.98, respectively) and was down-

regulated in the early-metastatic/overt-metastatic (HN2-3) group when compared with non-metastatic/pre-metastatic (HN0-1) (p= 0.011, $log2FC_{HN2\text{-}3/HN0\text{-}1}$=-1.51) (Figure 1d).

Salivary miRNAs distinguish the lymph node involvement

A PCA analysis was performed to detect any differences between healthy and tumor groups based on miRNAs expression levels (Figure 2). Data with a higher correlation had a lower degree of separation (< 45°). Comparing MCT and healthy samples, mir-21 and miR-885 were correlated within the same group and discriminated tumor from healthy samples, as the degree between the data points were higher than 45° Figure 2a. Considering tumor classes (HN0-1 and HN2-3) and healthy samples (Figure 2b), miR-21 and miR-885 are positively correlated with each other within the same group of healthy and HN0-1 samples, while no correlation was identified in HN2-3 class. Healthy, HN0-1 and HN2-3 groups are not correlated, highlighting the significant differences given by the miR-21 and miR-885 expression level. MiR-885 discriminates the HN0-1 to HN2-3 MCT groups as the X and the Y-axis separate the data points better than the miR-21, in which the HN classes were separated only by the X-axis.

To prove the reliability of the quantified miRNAs in discriminating the MCT-affected dogs from the healthy subjects and in predicting the lymph node involvement, ROC analysis was performed. The area under the curve (AUC) was calculated to estimate the diagnostic potential of the DE-miRNAs. Figure 3 shows all the AUC values calculated by comparing healthy, tumor, HN1-0 and HN2-3 groups for miR-21 and miR-885. The AUC of tumors *versus* healthy samples was fair for miR-21 (AUC=0.7146; 95% CI 0.5565-0.8728) and good for miR-885 (AUC=0.8182; 95% CI 0.7055-0.9308). The AUC of HN0-1 class *versus* healthy samples was poor for miR-21 (AUC=0.6894; 95% CI 0.4826-0.8962) and excellent for miR-885 (AUC=0.9636; 95% CI 0.9636-0.9636). The AUC of HN2-3 class *versus* healthy group was fair for both miR-21 (AUC=0.7273; 95% CI 0.5598-0.8947) and miR-885 (AUC=0.7576; 95% CI 0.6098-0.9054). The AUC of HN0-1 *versus* HN2-3 was bad for miR-21

(AUC=0.4410; 95% CI 0.2244-0.6576) and good for miR-885 (AUC=0.8042; 95% CI 0.6555-0.9528). To improve the diagnostic potential of the test, a statistical analysis considering the weighted average relative quantification (RQ) values of miR-21 and miR-885 was performed (Figure 3). The predicted probability to be able to discriminate MCT-affected dogs from healthy subjects based on the logit model [logit = 1 / (1 + exp(-(-1.13220+3.08391 x expression level of miR-885+0.10992 x expression level of miR-21)))] was good with an AUC value of 0.8369 (95% CI 0.7266-0.9472). The probability to be able to discriminate healthy from the HN0-1 class based on the logit model [logit = 1 / (1 + exp(-(-5.68147+7.59331 x expression level of miR-885+0.02111 x expression level of miR-21)))] was excellent with an AUC value of 0.9636 (95% CI 0.9636-0.9636). The predicted probability to be able to discriminate healthy from HN2-3 class based on the logit model [logit = 1 / (1 + exp(-(-1.07874+2.50026 x expression level of miR-885+0.13449 x expression level of miR-21)))] was fair with an AUC value of 0.7689 (95% CI 0.6192-0.9187). The probability to be able to discriminate HN0-1 from HN2-3 class based on the logit model [logit = 1 / (1 + exp(-(2.67322-1.30733 x expression level of miR-885-0.02818 x expression level of miR-21)))] was fair with an AUC value of 0.7833 (95% CI 0.6145-0.9522). All the data on the AUC, the sensitivity and the specificity of the miRNAs are reported in the Supplementary Table S2.

As miR-885 provides a higher diagnostic potential in discriminating between non-metastatic/pre-metastatic (HN0-1) and the early-metastatic/overt-metastatic (HN2-3) group, a MFA analysis was performed (Figure 4). The group of healthy samples was included as a control. The component F1 explains 49.65% of the variance and discriminates the HN0-1 from the HN2-3 and healthy groups. The component F2 explains 33.33% of the variance and discriminates the HN2-3 from HN0-1 and healthy groups. The components F1 and F2 together describe 82.99% of the variability of the data.

Discussion

In the current study, the potential of saliva as a reliable minimally invasive matrix for the quantification of MCT-associated miRNAs in dogs has been investigated for the first time. Three MCT-associated miRNAs, namely miR-21, miR-379 and miR-885, previously reported discriminating between MCT-affected and healthy dogs in formalin-fixed paraffin-embedded primary tumor mass[34], have been quantified in saliva samples of healthy and MCT affected dogs to investigate their potential as a biomarker in a minimally invasive, repeatable over time matrix. The three miRNAs were quantified using a qPCR approach, and the results showed that miR-21 and miR-885 were modulated in the presence of the MCT, while miR-379 was not detected in saliva. Despite the standard prognostication of MCT based on grading, using Patnaik[17] and Kiupel[8] systems, the tumors with a low histological grading, suggestive of less aggressive behavior, could spread to the local lymph nodes, develop further metastasis or de novo masses and promote fatal outcome due to MCT-associated disease[6,8,27,30]. Therefore, the ability to discriminate the non-metastatic/pre-metastatic (HN0-1 class) from the early-metastatic/overt-metastatic (HN2-3 class) lymph nodes may provide a step forward in obtaining a more accurate prognosis. Few studies had investigated the epigenetic changes correlated with the MCT using transcriptomic[18] and miRNomic[34] approaches. Fenger and colleagues characterized the role of miR-9, overexpressed in high-grade canine MCT[5]. MiRNA-126 was found up-regulated in some epithelial and non-epithelial neoplasms, like MCT [7] and miR-21, miR-379 and miR-885 were able to predict the spread to lymph nodes in MCT affected dogs[34]. The up-regulation of miR-21 was observed in the saliva of several human cancer, suggesting its role as an oncomiRNA[20] since it promotes the tumor progression[4]. The present study confirmed that miR-21 is up-regulated in the saliva of MCT affected dogs as well, as compared with healthy dogs. The comparison between healthy, HN0-1 and the HN2-3 tumor classes showed that the expression level of miR-21 increased with tumor progression.

On the other hand, the role of miR-885 as oncomiRNA[28] or tumour-suppressor[13] is still debated, and likely dependent on the tumor type. In the present study, miR-885 was up-regulated in the saliva of MCT affected dogs compared to the healthy group. Specifically, the miR-885 expression was higher in the HN0-1 tumors than in the HN2-3 class and the healthy group. However, the result might be affected by the different number of samples collected from HN0-1 group (12 samples) and HN2-3group (24 samples). Moreover, we speculate that miR-885 might play a role as metastasis regulator, affecting genes involved in metastasis spread, as previously hypothesized[1,11].

In this study, the relevance of saliva as a suitable matrix to detect miRNAs able to discriminate the lymph node involvement in MCT affected dogs was suggested. MiRNAs in saliva are already considered as potential candidates for cancer detection in human oncology[20]; if confirmed in further studies in a broader cohort, the finding of the present study may be a reliable support for excluding early nodal metastases and avoid unnecessary lymphadenectomy in the HN0-HN1 group. The PCA analysis highlighted that miR-21 and miR-885 could discriminate MCT affected dogs from healthy ones and identified the lymph node involvement (HN0-1 and HN2-3 classes). Healthy and HN0-1 groups were more similar to each other than HN2-3 group, as they are both on the right part of the plot. This finding implies that the expression level of the two miRNAs considerably changes in metastatic tumors (HN2-3). MiR-885 better discriminates between HN0-1 and HN2-3 lymph nodes than miR-21, highlighting its diagnostic potential. Several studies in human medicine demonstrated the potential of salivary miRNAs in the identification and follow up of cancer patients[19,24] and in discriminating the metastatic from less aggressive tumors[14].

The ROC curve analysis pointed out that miRNA with the higher diagnostic potential in discriminating the MCT from the healthy group and in detecting the non-metastatic/pre-metastatic (HN0-1) from the early-metastatic/overt-metastatic (HN2-3) lymph nodes was miR-885. The weighted average relative quantification (RQ) values of the two miRNAs didn't significantly increase the reliability of

the diagnostic test, highlighting that miR-885 had a considerable impact on the discriminating power. The MFA analysis supported the reliability of miR-885 as a salivary biomarker because healthy, HN0-1 and HN2-3 clustered in three separated groups.

Although this study provided new and important insights in the potential of the saliva as an alternative minimally invasive matrix for the detection of MCT-associated miRNAs, further experiments involving a higher number of patients are required to validate the miRNAs' potential use in veterinary clinical oncology.

Declaration of conflicting interests

The author(s) declared no potential conflicts of interest with respect to the research, authorship, and/or publication of this article.

Funding

The funding for this research was provided by Linea 2-2018, awarded by Università degli Studi di Milano.

Bibliography

1. Afanasyeva EA, Mestdagh P, Kumps C, et al. MicroRNA miR-885-5p targets CDK2 and MCM5, activates p53 and inhibits proliferation and survival. *Cell Death Differ*. 2011;18:974–984.
2. Blackwood L, Murphy S, Buracco P, et al. European consensus document on mast cell tumours in dogs and cats. *Vet Comp Oncol*. 2012;10:e1–e29.
3. Bustin SA, Benes V, Garson JA, et al. The MIQE guidelines: Minimum information for publication of quantitative real-time PCR experiments. *Clin Chem*. 2009;55:611–622.
4. Feng Y-H, Tsao C-J. Emerging role of microRNA-21 in cancer. *Biomed Reports*. 2016;5:395–402.
5. Fenger JM, Bear MD, Volinia S, et al. Overexpression of miR-9 in mast cells is associated with invasive behavior and spontaneous metastasis. *BMC Cancer*. 2014;14:84.
6. Ferrari R, Marconato L, Buracco P, et al. The impact of extirpation of non-palpable/normal-sized regional lymph nodes on staging of canine cutaneous mast cell tumours: A multicentric retrospective study. *Vet Comp Oncol*. 2018;16:505–510.
7. Heishima K, Ichikawa Y, Yoshida K, et al. Circulating microRNA-214 and -126 as potential biomarkers for canine neoplastic disease. *Sci Rep*. 2017;7:2301.
8. Kiupel M, Webster JD, Bailey KL, et al. Proposal of a 2-tier histologic grading system for canine cutaneous mast cell tumors to more accurately predict biological behavior. *Vet Pathol*. 2011;48:147–155.
9. Lai EC. Micro RNAs are complementary to 3' UTR sequence motifs that mediate negative post-transcriptional regulation. *Nat Genet*. 2002;30:363–364.
10. Di Leva G, Garofalo M, Croce CM. miRNA in cancer. *Annu Rev Pathol*. 2014;9:287–314.
11. Li C, Wang X, Song Q. MicroRNA 885-5p Inhibits Hepatocellular Carcinoma Metastasis by

Repressing AEG1. *Onco Targets Ther*. 2020;13:981–988

12. Liu C-J, Lin S-C, Yang C-C, Cheng H-W, Chang K-W. Exploiting salivary miR-31 as a clinical biomarker of oral squamous cell carcinoma. *Head Neck*. 2012;34:219–224.
13. Liu Y, Bao Z, Tian W, Huang G. MiR-885-5p suppresses osteosarcoma proliferation, migratioand invasion through regulation of β-catenin. *Oncol Lett*. 2019;17:1996–2004.
14. Matse JH, Yoshizawa J, Wang X, et al. Discovery and prevalidation of salivary extracellular microRNA biomarkers panel for the noninvasive detection of benign and malignant parotid gland tumors. *Clin Cancer Res*. 2013;19:3032–3038.
15. Ortiz-Quintero B. Cell-free microRNAs in blood and other body fluids, as cancer biomarkers. *Cell Prolif*. 2016;49:281–303.
16. Park NJ, Zhou H, Elashoff D, et al. Salivary microRNA: Discovery, characterization, and clinical utility for oral cancer detection. *Clin Cancer Res*. 2009;15:5473–5477.
17. Patnaik AK, Ehler WJ, MacEwen EG. Canine Cutaneous Mast Cell Tumor: Morphologic Grading and Survival Time in 83 Dogs. *Vet Pathol*. 1984;21:469–474.
18. Pulz LH, Barra CN, Alexandre PA, et al. Identification of two molecular subtypes in canine mast cell tumours through gene expression profiling. *PLoS One*. 2019;14:e0217343.
19. Rapado-González Ó, Majem B, Álvarez-Castro A, et al. A Novel Saliva-Based miRNA Signature for Colorectal Cancer Diagnosis. *J Clin Med*. 2019;8:2029.
20. Rapado-González Ó, Majem B, Muinelo-Romay L, et al. Human salivary microRNAs in Cancer. *J Cancer*. 2018;9:638–649.
21. Rapado-González Ó, Majem B, Muinelo-Romay L, López-López R, Suarez-Cunqueiro MM. Cancer salivary biomarkers for tumours distant to the oral cavity. *Int J Mol Sci*. 2016;17:1531.
22. Sahabi K, Selvarajah GT, Abdullah R, Cheah YK, Tan GC. Comparative aspects of microRNA

expression in canine and human cancers. *J Vet Sci*. 2018;19:162–171.

23. Salazar C, Nagadia R, Pandit P, et al. A novel saliva-based microRNA biomarker panel to detect head and neck cancers. *Cell Oncol (Dordr)*. 2014;37:331–338.

24. Sazanov AA, Kiselyova EV, Zakharenko AA, Romanov MN, Zaraysky MI. Plasma and saliva miR-21 expression in colorectal cancer patients. *J Appl Genet*. 2017;58:231–237

25. Setti G, Pezzi ME, Viani MV, et al. Salivary microRNA for diagnosis of cancer and systemic diseases: A systematic review. *Int J Mol Sci.* 2020;21:907.

26. Stefanello D, Valenti P, Faverzani S, et al. Ultrasound-guided cytology of spleen and liver: A prognostic tool in canine cutaneous mast cell tumor. *J Vet Intern Med*. 2009;23:1051–1057.

27. Stefanello D, Buracco P, Sabattini S, et al. Comparison of 2- and 3-category histologic grading systems for predicting the presence of metastasis at the time of initial evaluation in dogs with cutaneous mast cell tumors: 386 cases (2009–2014). *J Am Vet Med Assoc*. 2015;246:765–769.

28. Su M, Qin B, Liu F, Chen Y, Zhang R. Mir-885-5p upregulation promotes colorectal cancer cell proliferation and migration by targeting suppressor of cytokine signaling. *Oncol Lett*. 2018;16:65–72.

29. Syeda ZA, Langden SSS, Munkhzul C, Lee M, Song SJ. Regulatory mechanism of microrna expression in cancer. *Int J Mol Sci.* 2020;21:1723.

30. Weishaar KM, Thamm DH, Worley DR, Kamstock DA. Correlation of nodal mast cells with clinical outcome in dogs with mast cell tumour and a proposed classification system for the evaluation of node metastasis. *J Comp Pathol*. 2014;151:329–338.

31. Welle MM, Bley CR, Howard J, Rüfenacht S. Canine mast cell tumours: A review of the pathogenesis, clinical features, pathology and treatment. *Vet Dermatol*. 2008;19:321–339.

32. Worley DR. Incorporation of sentinel lymph node mapping in dogs with mast cell tumours:

20 consecutive procedures. *Vet Comp Oncol*. 2014;12:215–226.

33. Yoshizawa JM, Wong DTW. Salivary MicroRNAs and Oral Cancer Detection. *Methods Mol Biol*. 2013;936:313–324.

34. Zamarian V, Ferrari R, Stefanello D, Ceciliani F, Grieco V, Minozzi G, Chiti LE, Arigoni M, Calogero R, Lecchi C. miRNA profiles of canine cutaneous mast cell tumors with early nodal metastasis and evaluation as potential biomarkers. *Sci Rep*. 2020;10.1038/s41598-020-75877-x.

Figures:

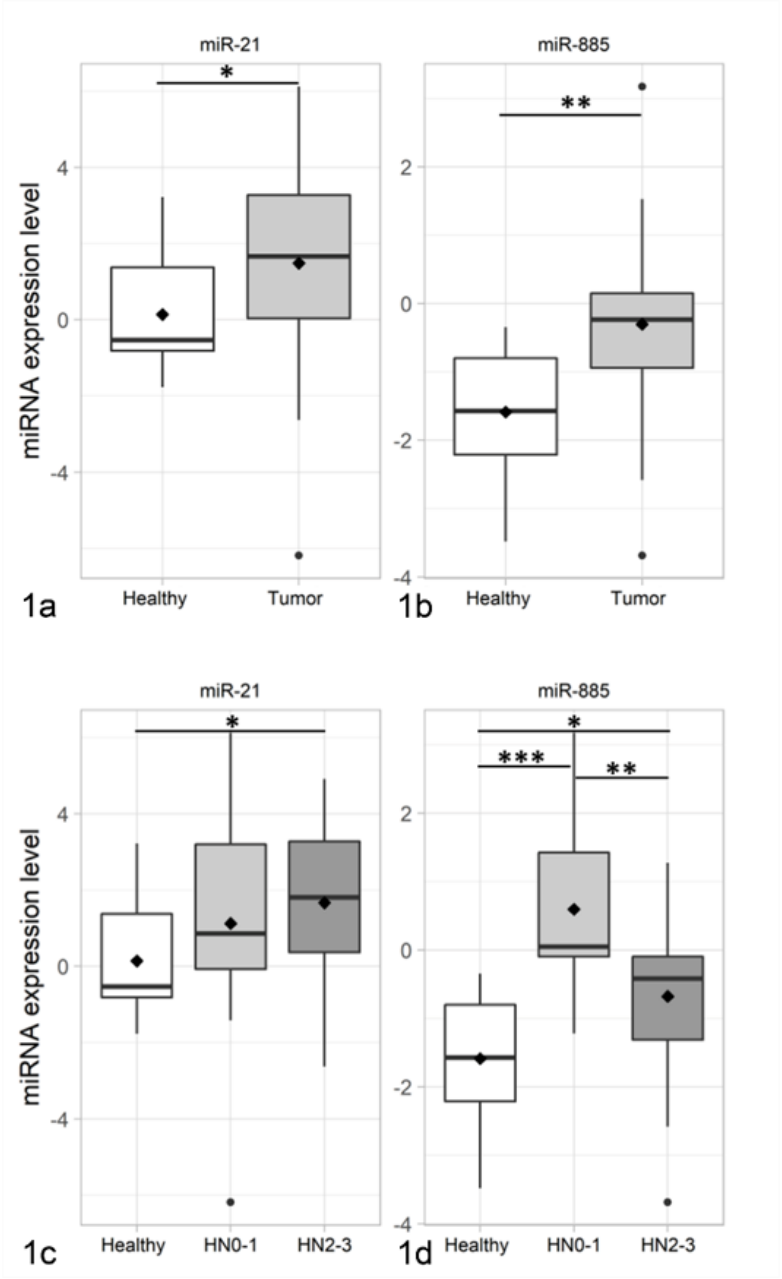

Figure 1. Box Plot of miR-21 (A, C) and miR-885 (B, D) expression level in healthy compared with the tumor groups and in healthy samples compared with the tumor classes (non-metastatic/pre-metastatic HN0-1 and the early metastatic/metastatic HN2-3). Blackline inside the boxes marks the median and the rhombus marks the mean. Whiskers indicate variability outside the upper and lower quartiles. Significance was declared at P<0.05 (*), P< 0.01 (**) and P< 0.001 (***).

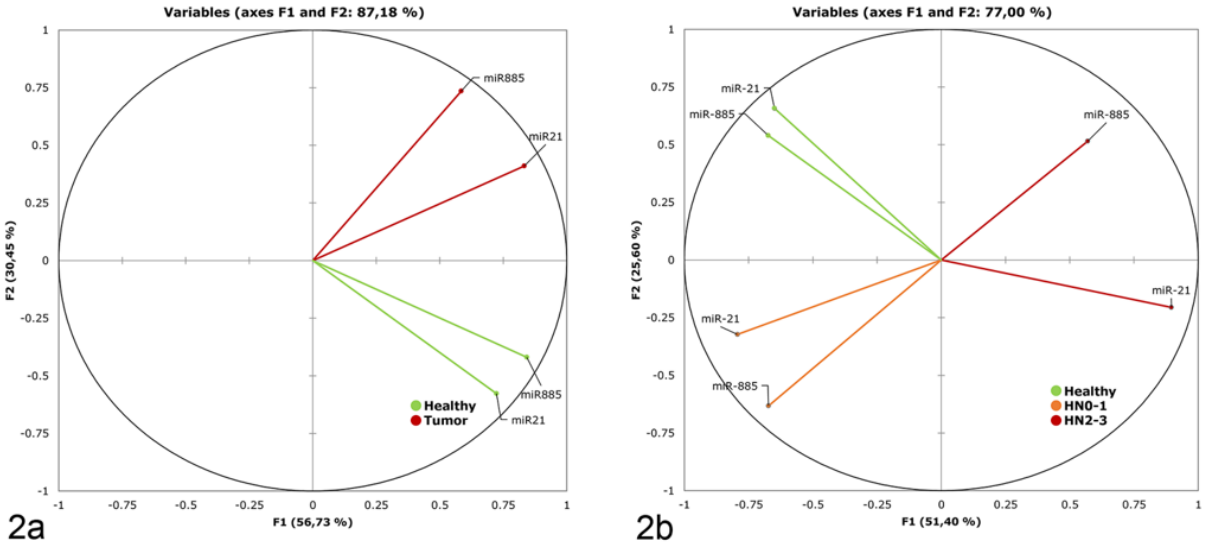

Figure 2. Principal component analysis (PCA) of miR-21 and miR-885 in healthy and MCT affected dogs. The circles show the correlation between (A) healthy and tumor samples and (B) between healthy and non-metastatic/pre-metastatic (HN0-1 class) and the early metastatic/metastatic (HN2-3 class) tumors. Data with a higher correlation had a lower degree of separation (< 45°). Data points on the opposite side of the centerline or orthogonal are respectively negatively correlated and non-correlated.

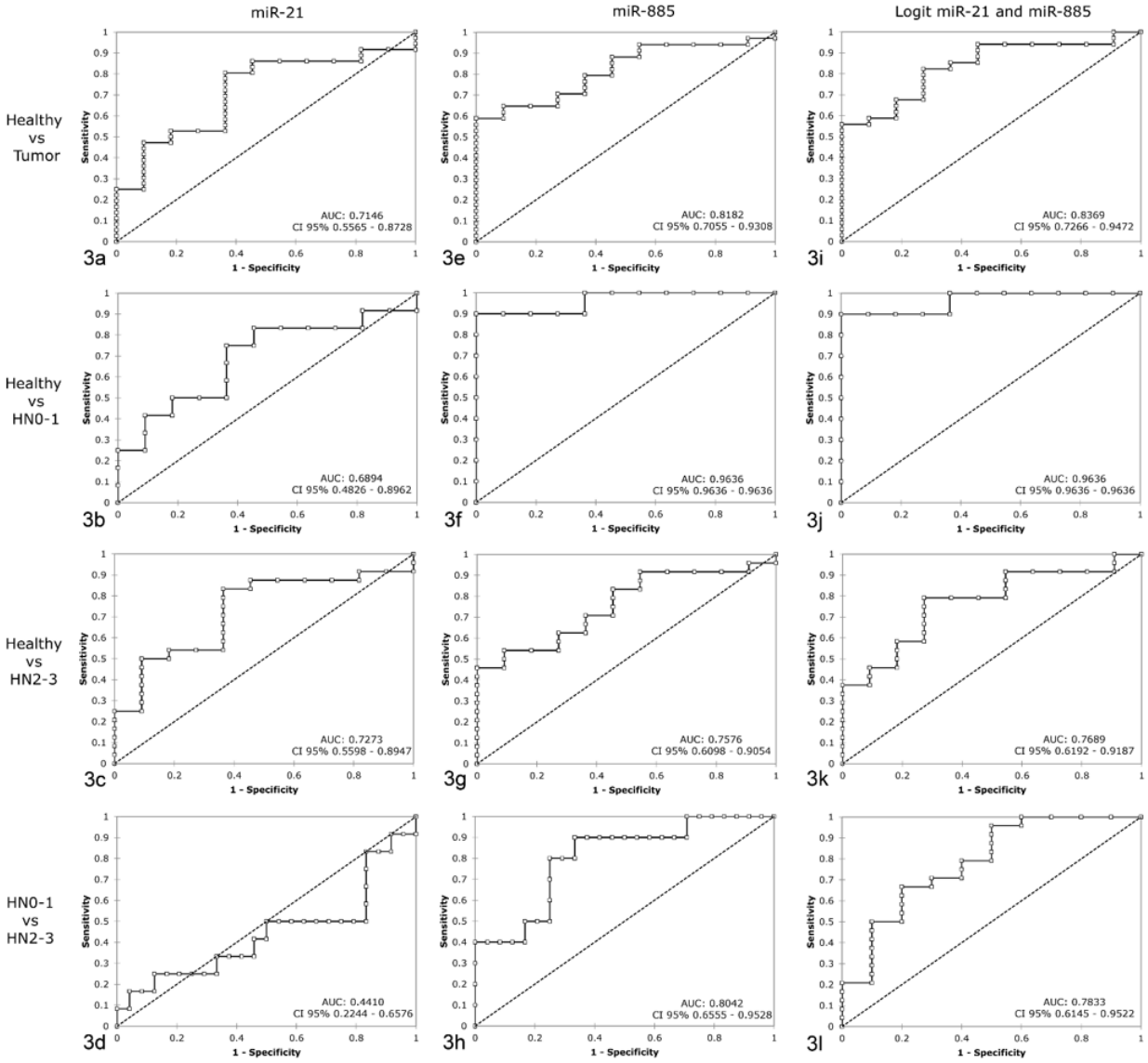

Figure 3. Receiver-operator characteristic (ROC) curve analysis of DE-miRNA and the weighted average relative quantification (RQ) values of the two miRNAs (Logit). AUC= area under the curve. CI= confidence interval.

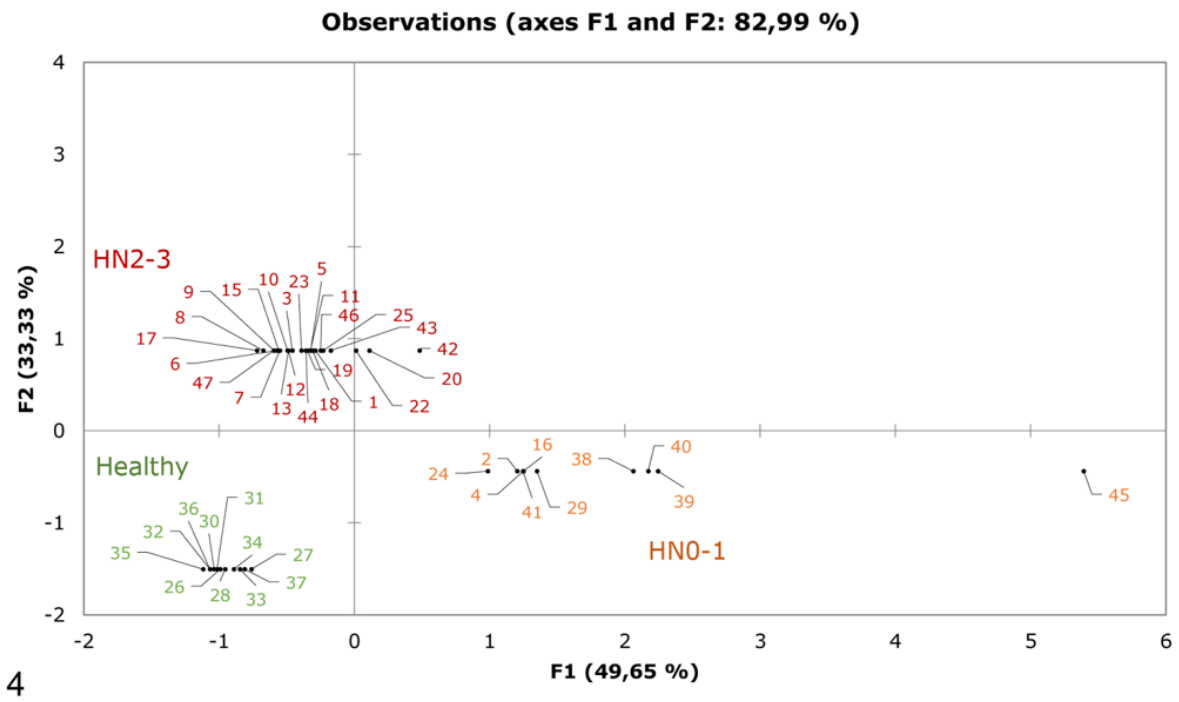

Figure 4. Multi-functional analysis (MFA) using miR-885 expression values in healthy, non-metastatic/pre-metastatic (HN0-1 class) and the early metastatic/metastatic (HN2-3 class) samples. Each sample is plotted in the graphic based on the miRNA expression level. Healthy samples (green), HN0-1 class (orange) and HN2-3 class (red).

Supplementary materials:

ID	Breed	Gender	Age (years)	Tumor location	Site	Grade		Lymph node*
						Patnaik	Kiupel	
26	Mixed breed	Female	3	-	-	-	-	Healthy
27	Mixed breed	Female	2	-	-	-	-	Healthy
28	Mixed breed	Male	2	-	-	-	-	Healthy
30	Mixed breed	Female	8	-	-	-	-	Healthy
36	Mixed breed	Female	7	-	-	-	-	Healthy
34	Mixed breed	Male	1	-	-	-	-	Healthy
31	Hound	Male	3	-	-	-	-	Healthy
32	Saluki	Male	8	-	-	-	-	Healthy
33	Spinone	Female	6	-	-	-	-	Healthy
35	Labrador	Female	7	-	-	-	-	Healthy
37	Norfolk Terrier	Male	4	-	-	-	-	Healthy
2	Mixed breed	Male	6	Knee	Subcutaneous	-	-	HN0-1
21	Boxer	Male	9	Neck	Subcutaneous	-	-	HN0-1
39	Cocker Spaniel	Female	8	Breast	Subcutaneous	-	-	HN0-1
4	Labrador	Male	10	Scrotum	Cutaneous	II	Low	HN0-1
14	Labrador	Male	1	Head	Cutaneous	I	Low	HN0-1
16	Dachshund	Female	9	Tail	Cutaneous	II	Low	HN0-1
38	Golden Retriever	Female	4	Hock	Cutaneous	II	Low	HN0-1
41	Pug	Male	7	Shoulder	Cutaneous	II	Low	HN0-1
40	American Staffordshire	Female	13	Limb	Cutaneous	II	Low	HN0-1
24	Mixed breed	Male	5	Trunk	Cutaneous	II	Low	HN0-1
29	Mixed breed	Female	10	Shoulder	Cutaneous	II	Low	HN0-1
45	Mixed breed	Female	9	Limb	Cutaneous	II	Low	HN0-1
1	English setter	Female	9	Neck	Subcutaneous	-	-	HN2-3
19	English setter	Male	7	Limb	Subcutaneous	-	-	HN2-3
20	Golden Retriever	Female	4	Hock	Subcutaneous	-	-	HN2-3

22	English setter	Female	10	Limb	Subcutaneous	-	-	HN2-3
23	Pit-bull	Female	5	Limb	Subcutaneous	-	-	HN2-3
7	Mixed breed	Female	14	Breast/Limb	Subcutaneous	-	-	HN2-3
25	Mixed breed	Male	12	Limb	Subcutaneous	-	-	HN2-3
44	Mixed breed	Male	9	Limb	Subcutaneous	-	-	HN2-3
42	Weimaraner	Male	9	Limb	Subcutaneous	-	-	HN2-3
3	Cocker Spaniel	Female	10	Knee	Cutaneous	II	Low	HN2-3
8	Swiss mountain dog	Female	4	Limb	Cutaneous	II	Low	HN2-3
9	Labrador	Male	9	Trunk	Cutaneous	II	Low	HN2-3
13	Labrador	Female	6	Breast	Cutaneous	II	Low	HN2-3
17	Labrador	Male	7	Foreskin	Cutaneous	II	Low	HN2-3
15	Golden Retriever	Female	11	Limb	Cutaneous	I	Low	HN2-3
5	Golden Retriever	Female	7	Shoulder	Cutaneous	II	Low	HN2-3
10	Boxer	Male	8	Limb	Cutaneous	II	Low	HN2-3
11	Pug	Male	3.5	Head/Shoulder	Cutaneous	I/II	Low	HN2-3
12	Weimaraner	Male	7	Limb	Cutaneous	II	Low	HN2-3
43	Fox Terrier	Female	9	Neck	Cutaneous	II	Low	HN2-3
46	English setter	Male	8	Trunk	Cutaneous	II	Low	HN2-3
6	Mixed breed	Male	12	Neck	Cutaneous	II	Low	HN2-3
18	Mixed breed	Female	7	Breast	Cutaneous	II	Low	HN2-3
47	Mixed breed	Male	8	Foreskin	Cutaneous	II	Low	HN2-3

*classification system proposed by Weishaar and colleagues (2014). HN= histological node

Supplemental Table S1. Summary of samples enrolled in the study

Comparison	miRNA	AUC	95% CI	Cut-off	Sensitivity (%)	Specificity (%)
Healthy vs Tumor	miR-21	0.7146	0.5565-0.8728	0.9884	80.6	63.6
	miR-885	0.8182	0.7055-0.9308	0.8028	58.8	100
	Logit (miR-21 + miR885)	0.8369	0.7266-0.9472	0.8606	55.9	100
Healthy vs HN0-1	miR-21	0.6894	0.4826-0.8962	0.9884	75.0	63.6
	miR-885	0.9636	0.9636-0.9636	0.8524	90.0	100
	Logit (miR-21 + miR885)	0.9636	0.9636-0.9636	0.6897	90.0	100
Healthy vs HN2-3	miR-21	0.7273	0.5598-0.8947	1.0871	83.3	63.6
	miR-885	0.7576	0.6098-0.9054	0.8028	45.8	100
	Logit (miR-21 + miR885)	0.7689	0.6192-0.9187	0.6343	79.2	72.7
HN0-1 vs HN2-3	miR-21	0.4410	0.2244-0.6576	16.0307	25.0	87.5
	miR-885	0.8042	0.6555-0.9528	0.8524	90.0	66.7
	Logit (miR-21 + miR885)	0.7833	0.6145-0.9522	0.8087	66.7	80.0

HN= histological node. Classification system proposed by Weishaar and colleagues (2014).
CI= confidence interval

Supplemental Table S2. The area under the curve (AUC), the sensitivity and the specificity of the DE-miRNA

www.nature.com/scientificreports

SCIENTIFIC REPORTS
nature research

OPEN

Characterization of skin surface and dermal microbiota in dogs with mast cell tumor

Valentina Zamarian[1,6], Carlotta Catozzi[1,6], Anna Cuscó[2], Damiano Stefanello[1], Roberta Ferrari[1], Fabrizio Ceciliani[1], Olga Francino[3], Armand Sánchez[3], Valeria Grieco[1], Davide Zani[1], Andrea Talenti[4], Paola Crepaldi[5] & Cristina Lecchi[1]✉

Scientific Reports, 2020, doi: 10.1038/s41598-020-69572-0

Characterization of skin surface and dermal microbiota in dogs with mast cell tumor

Valentina Zamarian[1#], Carlotta Catozzi[1#], Anna Cuscó[2], Damiano Stefanello[1], Roberta Ferrari[1], Fabrizio Ceciliani[1], Olga Francino[3], Armand Sánchez[3], Valeria Grieco[1], Davide Zani[1], Andrea Talenti[4], Paola Crepaldi[5], Cristina Lecchi[1*]

(1) Dipartimento di Medicina Veterinaria, Università degli Studi di Milano, Milano, Italy

(2) Vetgenomics. Ed Eureka. PRUAB. Campus UAB, Barcelona, Spain

(3) Molecular Genetics Veterinary Service (SVGM), Veterinary School, Universitat Autònoma de Barcelona, Barcelona, Spain

(4) The Roslin Institute, University of Edinburgh, Easter Bush Campus, Midlothian, EH25 9RG, United Kingdom

(5) Department of Agricultural and Environment Science, Università degli Studi di Milano, Milano, Italy.

#Equal contribution

*Corresponding author: cristina.lecchi@unimi.it

Abstract

The skin microbiota interacts with the host immune response to maintain the homeostasis. Changes in the skin microbiota are linked to the onset and the progression of several diseases, including tumors. We characterized the skin surface and dermal microbiota of 11 dogs affected by spontaneous mast cell tumor (MCT), using skin contralateral sites as intra-animal healthy controls. The microbial profile differed between healthy and tumor skin surfaces and dermis, demonstrating that the change in microbiota composition is related to the presence of MCT. The number of observed taxa between MCT and healthy skin surfaces was detected, showing a decrease in number and heterogeneity of taxa over the skin surface of MCT, at both inter- and intra-individual level. Preliminary data on bacterial population of MCT dermis, obtained only on three dogs, demonstrated an intra-individual reduction of taxa number when compared to the skin surface. Taxonomy reveals an increase of *Firmicutes* phylum and *Corynebacteriaceae* family in MCT skin surface when compared to the healthy contralateral. In conclusion, we demonstrate that microbial population of skin surface and dermis is related to mast cell tumor. Our study provides the basis for future investigations aiming to better define the interaction between mast cell tumors, microbiota and host immune response.

Key words: mast cell tumor, skin microbiota, dermal microbiota, dog, biodiversity.

Introduction

The epidermis, or skin surface, provides the external layer to the three parts of the skin, the inner layer being the dermis and hypodermis. The epidermis is regarded as a microenvironment containing a rich eukaryotic and prokaryotic population, currently defined as the microbiota[1,2], which plays a role as protective and immunological barrier[3].

Culture-independent determination of the microbial profile of dog skin surface has been recently determined, showing that microbiota largely differs between body sites[4]. The skin microbiota is modulated by extrinsic (e.g. diet, environment) and intrinsic (e.g. genetics) factors[5], and is not only limited to skin surface but also extends to the dermis[6]. Remarkably, bacteria detected within the human healthy dermis and subcutaneous adipose tissue showed a different microbial population profile as compared to the skin surface[7]. Four major phyla – namely *Actinobacteria*, *Firmicutes*, *Proteobacteria*, *Bacteroidetes* – and four major families – namely *Corynebacteriaceae*, *Propionibacteriaceae*, *Staphylococcaceae*, *Micrococcaceae* – dominate both canine[2] and human epidermal surfaces[1].

Given the limited number of studies, the definition of canine skin “healthy microbiota” is still debated. Changes in microbiota composition are associated with the development of skin disorders in both humans and dogs[8,9] , as previously reported dermatitis[10] in dogs.

The defensive capability of skin is supported by healthy and balanced microbiota through the interaction with the residing immune cells in the cutis[9,11,12]. Due to their localization within the skin, mast cells are in close contact with the bacterial population[13]. The activities of mast cells may be amplified when changes in microbiota composition occur[14]. The relationship between mast cells and skin surface microbiota[15] has been poorly investigated, so far.

Canine Mast Cell Tumor (MCT) arises from an uncontrolled proliferation of neoplastic mast cells in cutaneous and subcutaneous tissues and is one of the most common skin neoplasms in dogs, with

a prevalence of 21%[16]. The alterations of the microbiota of epidermal surface and its relationship with tumors have been investigated in humans and in experimental animals[17,18]. The onset of MCT and the presence of a high number of mast cells, the degranulation of which triggers a release of histamine, heparin and proteases, collectively defined as Darier's signs[19], could lead to changes in microbiota at both skin surface and dermis level. This hypothesis is supported by a study performed on P815, a mouse mastocytoma tumor model, showing that butyrate, an intestinal microbial metabolite, was able to modulate mast cells[20].

To the best of our knowledge, no investigation has been carried out to characterize the skin surface microbiota of dogs affected by MCT. The presence of bacteria in the dermis of dogs remains unexplored as well. The present investigation aimed to profile the skin surface and dermis microbiota of owned-client dogs affected by spontaneous mast cell tumors in order to elucidate if and how the microbial community can change as associated with the neoplasm.

Results

Sequencing results

After sequencing, a total of 17 samples (8 skin swabs, 6 tumor dermal biopsies and 3 healthy tissue biopsies) showed a low reads count that led to their exclusion from subsequent analyses. The sequencing data of the remaining 19 samples from 9 dogs, including 14 skin swabs and 5 tumor dermal biopsies, produced a total of 1,906,333 reads and 5,869 features were obtained with an average of 54,399 (a minimum of 4,542 and a maximum of 459,808 sequences) after filtering. Detailed sequencing data for each sample are available in Supplementary Table S1 online.

Skin surface microbiota

Taxonomy results at phylum and family level are shown in Figure 1 a and b, respectively. An abundance of 2% was arbitrarily selected as the cut-off for the analysis. All taxa found at phylum

and family level are provided in Supplementary Table S2 online. At the phylum level, the most representative taxa on dog skin surface were *Actinobacteria*, *Bacteroidetes*, *Firmicutes*, *Fusobacteria* and *Proteobacteria*. *Firmicutes* showed an increase in their abundance in MCT as compared to healthy skin samples (mean of 30% ± 4.8% and 21% ± 9.7% in tumor and healthy, respectively; p= 0.030). The most abundant families were *Corynebacteriaceae*, *Staphylococcaceae*, *Moraxellaceae*, *Mycoplasmataceae*. A statistically significant increase of *Corynebacteriaceae* was found on the tumor skin surface as compared to healthy contralateral (mean of 6.5% ±3.4% and 2.4% ± 0.7% for tumor and healthy, respectively; p= 0.050).

The alpha diversity was investigated to study the species richness (number of OTU) and their relative abundance (Shannon index), whereas the beta diversity was calculated to assess the microbiota structure using qualitative (unweighted UniFrac) and quantitative (weighted UniFrac) approaches without taking into account the phylogeny (Bray-Curtis).

The expected mean percentage of observed taxa was 63.06% (confidence interval 59% – 67%) and 36.94% (confidence interval 33% – 40%) for healthy and tumor skin surface, respectively. Within alpha diversity analysis, the observed species decreased over the tumor skin surface (p<0.001) at the Chi-square test (Supplementary Table S3 online). In 3 out of 5 samples, a significant reduction (p= 0.02) of observed taxa on the tumor skin surface respectively to the healthy skin contralateral was observed. Two animals showed a remarkably different pattern; dog D2 presented the same number of observed species in the MCT and the contralateral sample, whereas in dog D7 the number of observed species increased in MCT. Considering all samples, the mean and standard deviation of observed taxa among groups were 599 ±324 and 351 ±324 for healthy and tumor samples, respectively. Taking into account the microorganisms' abundance, the groups did not show any variation in the Shannon index.

Comparing the beta diversity of microbial structure in tumor and healthy skin surface, the dissimilarity was calculated by three distance matrices, namely unweighted UniFrac, weighted UniFrac and Bray-Curtis. Regarding the intra-group variation, a change in distances between healthy (mean of 0.37 ±0.13) and tumor skin surface (mean of 0.26 ±0.02) groups was observed in weighted UniFrac matrix (p= 0.02). Healthy skin samples present more divergent diversities than the more homogeneous diversities of MCT samples (Figure 2).

Comparing the intra-animal distances, statistically significant changes in the microbiota structure were found for unweighted UniFrac (healthy vs tumor skin distance mean of 0.69 ±0.08, p< 0.001), weighted UniFrac (healthy vs tumor skin distance mean of 0.29 ±0.11, p= 0.004) and Bray-Curtis (healthy vs tumor skin distance mean of 0.78 ±0.079, p< 0.001) distance methods (Supplementary Table S4 online).

The multi-dimensional scaling (MDS) analysis based on all distances present between skin samples of unweighted and weighted UniFrac distances is reported in Figure 3 a and b, respectively. A shift of the healthy and tumor skin surfaces paired samples towards the same direction in the second dimension of the plot in both matrices, highlighting a clear separation between tumor and healthy skin surface groups by the y-axis, is visible. As previously described in alpha diversity, dog D7 presented an opposite behavior also in beta diversity. MDS analysis was also shown using Bray-Curtis distances (Supplementary Figure S1 online).

The contribution of the taxa with a relative abundance ≥2% that mostly drove the shift from healthy to the tumor skin surface is presented in Figure 4.

Preliminary characterization of the microbiota composition of tumor dermis and comparison with its associated skin surface

After quality control step, the preliminary characterization of the microbiota composition of the tumor dermis was carried out on 5 tumor biopsies. An abundance of 2% was arbitrarily selected as

the cut-off for the analysis. Results are presented in Figure 1 a and b for phylum and families, respectively. The most representative phyla of dermal microbiota were similar to those of skin surface. At family level, *Corynebacteriaceae*, *Staphylococcaceae*, *Moraxellaceae, Peptostreptococcaceae*, *Porphyromonadaceae* and *Nocardiaceae* were the most abundant.

Alpha and beta diversities between tumor dermis and the associated epidermal surface were also analyzed. A very preliminary statistical analysis was performed on alpha and beta diversity comparing the microbiota composition of the tumor dermis with overlying skin microbiota in 3 paired samples. Intra-animal chi-square test showed a difference in observed taxa between dermis and skin surface. The expected percentage of observed ASVs estimated by the test was 63.33% and 36.67% in skin surfaces and dermis, respectively (tumor skin swab CI: 58% – 67%; tumor dermis CI: 31% – 41%). A decrease in the number of ASVs detected in the dermis was found as compared to the corresponding skin surface (p<0.001). The number of observed OTUs is presented in Supplementary Table S3 online. No difference was detected between dermis and skin surface microbiota using a quantitative test or analyzing the microbiota structure through the Shannon index. Intra-animal beta diversity analysis showed differences between tumor dermis and skin surfaces in unweighted (dermis vs tumor skin distance mean of 0.66 ±0.09, p=0.006), weighted (dermis vs tumor skin distance mean of 0.35 ±0.14, p= 0.047) UniFrac and Bray-Curtis (dermis vs tumor skin distance mean of 0.80 ±0.05, p= 0.001) matrices (Supplementary Table S4 online). No variation was found comparing dermis and skin intra- groups (data not shown). The contribution of the main taxa which drove the shift between tumor skin surface and dermis is shown in figure 4 and it is represented through the MDS plot of unweighted, weighted and the Bray-Curtis matrices, shown in Supplementary Figure S1 online.

Core microbiota in skin surface and dermis of MCT affected dogs

The core microbiota, defined as the bacterial taxa shared by all the analyzed samples, was identified in the tumor skin surface, contralateral healthy skin surfaces and in tumor dermis (Figure 5). The core microbiota of tumor skin surface is composed of 12 ASVs, 6 of this shared with contralateral healthy skin surfaces and tumor dermis, belonged to 6 main families, namely *Corynebacteriaceae*, *Micrococcaceae*, *Propinibacteriaceae*, *Staphylococcaceae*, *Streptococaceae* and *Pseudomonadales*. Ten ASVs are present only in the tumor, 3 only on the tumor skin surface (*Moraxellaceae*, *Clostridiaceae*, *Pasteurellaceae* - families) and 6 only in the tumor dermis (*Nocardiaceae*, *Shewanellaceae*, *Enterobacteriaceae*, *Comamonadaceae*, *Corynebacteriaceae* - families). One ASVs is shared by tumor skin and dermis belonged to *Moraxallaceae* family.

Discussion

In the present study, the microbial population present over the skin surface and within the dermis of dogs affected by spontaneous mast cell tumor was investigated for the first time by determining the microbiota after amplification and sequencing of the V4 region of 16S rRNA[21]. The significant changes detected in the microbiota community provided the evidence that it is possible to discriminate between healthy and mast cell tumor site, even if with the limited number of samples included in this study.

Our results revealed that the number of observed OTUs decreased on the tumor skin surface compared to the healthy contralateral, suggesting a lost in the heterogeneity of microbial community on the skin surface over the tumor area.

Core microbiota of the healthy contralateral skin surface included more bacterial types (27 ASVs) than those of tumor skin surface or dermis (12 and 16 ASVs, respectively), confirming that a decrease in microbial diversity characterizes the tumor site, as already observed during an unhealthy status[22,23].

We found that it is possible to discriminate the intra-patient tumor skin surface from healthy contralateral, as determined by beta diversity analysis using the weighted UniFrac matrix.

Several studies were carried out to investigate the relationship between microbiota and the development of skin disorders, including tumor and dermatitis. In the present study, an increase of *Firmicutes* phylum was observed, while investigation on human oral and pancreatic cancer[24] reported a reduction of this phylum, highlighting that different cancers exert different selective pressures on the microbial population. Our results reported also an increase of *Corynebacteriaceae* family on the tumor skin surface compared to the healthy contralateral. Studies on dermatitis described a decrease in microbiota diversity[10] with an increase of *Corynebacteriaceae* [25], suggesting that a compromised skin barrier[26] and local immune response[11] are associated with changes in microbiota composition. All MCT samples included in this study featured an increase of *Corynebacteriaceae*, except dog 7, which had an opposite profile. Given the background that this was the only patient with ulcerations, we speculate that the development of a huge inflammatory reaction over the skin may potentially hamper the analyses and probably explain the inconsistent results, as previously described[27].

Differences detected on the skin surface of MCT affected dogs suggest that tumor could interfere with the microbial population. The clonal proliferation of neoplastic mast cells[19,28] and the presence of other immune cells[29] infiltrating the tumor play a role in the host-microbiota interaction[30]. No data are available about the relationship between mast cells and surface microbiota. Skin microbiome can influence mast cell migration, localization and maturation in the skin[31]. A study on mouse skin microbiota supported its ability to recruit mast cells, promoting their maturation in dermis via stem cell factor production[32]. Furthermore, the activation of mast cells can be boosted by molecules produced by bacteria, such as δ-toxin released by *S.aureus* during atopic dermatitis[33,34]. The relationship between mast cells and microbiota is particularly interesting due to

the microbiota capability to activate immune cells within the tumor microenvironment, and the potential exploiting of bacterial derived molecules to boost tumor immune defense[35].

In the second part of the study, we focused on the presence of bacteria in dermis and on the comparison of dermis with the skin surface microbiota. The sequencing data demonstrated that bacteria were detectable in 5 out of 11 tumor dermal biopsies. On the contrary, the bacterial DNA was unquantifiable in the 3 healthy tissue biopsies, due to the low reads number. The limited number of case blocks any speculation about the possible relationship between dermis microbiota and the staging/grading of the MCT cases included in the study. In general, the presence of microbiota in the dermis has been poorly investigated so far, but having detected bacterial DNA in dermal compartment is a relevant finding for future investigation. Bacterial DNA was found in the dermal compartment[6] and more recently human's sebaceous and sweat glands were found to be inhabited by *Propionibacterium spp* and *Corynebacterium spp*, respectively[36].

The comparison of the microbial population of tumor dermis and of tumor skin surface revealed a decrease in the number of OTUs in tumor dermis as well as a difference in intra-patient beta-diversity. Both these findings are corroborated by previously results, which reported that the skin surface is characterized by a greater bacterial abundance and community richness than biopsies.[7]

Conclusions

The relationship between skin microbiota and MCT in dogs has yet to be fully elucidated. The next-generation sequencing approach allowed to demonstrate for the first time that the presence of MCT promotes an alteration of the epidermis microbiota structure and composition when compared to healthy skin; few differences were detected between tumor dermis and the associated epidermal surface microbiota, beside the decrease of ASV. Although the number of clinical case is limited, and the different stages and grades were not included in the statistical analysis, these preliminary findings pave the way to elucidate the relationship between mast cell tumor and composition of

skin microbiota. Further studies on a larger number of patients are needed to support the reported results, which, if confirmed, have the potential to increase the knowledge of MCT pathophysiology and diagnostic.

Materials and methods

Ethics Statement

The samples were collected at the Veterinary Teaching Hospital of the Università degli Studi di Milano from client-owned dogs that underwent veterinary consultation and surgery during the routine oncological management of canine mast cell tumor. All experimental procedures were reviewed and approved by the Ethics Committee of the University of Milano (approval number 118/19). Patients were recruited after written owner consent. All experiments were performed in accordance with the relevant guidelines and regulations.

Studied population and sample collection

The experimental group was composed of 14 client-owned dogs, of which 11 were diagnosed with spontaneous MCT and three were healthy animals. All patients were companion dogs heterogeneous for the breed, age and gender. Detailed information about the enrolled animals is provided in Supplementary Table S5 online. Dogs with MCT were staged[37] in order to exclude metastasis[38] and were admitted to MCT wide margins excision and surgical removal of the sentinel lymph node. Tumors were histologically classified[39] and grading was assessed[40,41]. In addition, the neoplastic involvement of sentinel lymph-node was assessed as previously described[42]. From each MCT affected the dog, skin microbiota was collected using Sterile Dryswab (Medical wire) from the hairless area of the tumor and healthy contralateral site in the surgery room as previously described[4]. The surgical field was then scrubbed with an antiseptic solution of 2% chlorhexidine acetate as standard surgical preparation. To determine the dermis microbiota content, 4 to 5-mm

punch biopsies from the center of the MCT mass, corresponding to dermis, were collected after the tumor excision and preserved in RNAlater solution (Sigma). Biopsies of cutaneous tissue derived from the margin of the surgical incision were collected from 3 healthy dogs that underwent elective sterilization, as healthy controls. Dermal biopsies from contralateral sites from MCT affected animals were not carried out for ethical reasons. Skin swabs and biopsies were then stored at -80°C until DNA extraction.

DNA extraction, library preparation and sequencing

The DNA was extracted from skin swabs and tissue biopsies using DNeasy PowerSoil Kit (Qiagen, catalogue number 12888-100) following the manufacture's general procedures, with some differences. Briefly, the skin swabs were cut directly into the PowerBead Tubes with Solution C1, vortexed and centrifuged at 10,000 x g for 30 sec; the supernatant was used for extraction. Twenty mg of the dermal biopsy were cut, treated with 20µl of Proteinase K (Qiagen) and 60µl of Buffer C1, incubated at 65°C for 30 min and then transferred in the PowerBead Tubes to continue the procedure. Extraction blanks, processed like the other samples, were included for each extraction batch, as a control for contaminants. The DNA obtained from swabs and tissues were eluted in 30µl and 60µl of DNase-RNase free water, respectively, and stored at -20°C until use. DNA quantity and purity were checked using NanoDrop 1000 Spectrophotometer (Thermo Scientific) at wavelengths 230, 260 and 280 nm.

V4 region of 16S rRNA gene was amplified using the following primer pair, the Forward primer - (5'-CCATCTCATCCCTGCGTGTCTCCGAC**TCAG**NNNNNNNNNNNNNNNNNN**GAT**GTGYCAGCMGCCGCGGTAA-3') composed of the adapter linker, the key, the sample-specific barcode and the F515 forward primer and the Reverse primer (5'-CTCTCTATGGGCAGTCGGTGATGGACTACNVGGGTWTCTAAT-3') composed of the adapter linker and the R806 reverse primer. The Thermo Scientific Phusion Hot Start II High-Fidelity DNA polymerase kit (Thermo Fisher Scientific) was used to perform the PCR in

25 µl of the final volume. The mix contained RNAse and DNAse free water, 5x Phusion Buffer HF (5 µl), dNTPs 2mM (2.5 µl), Primer Fw 10µM (1.25 µl), primer Rv 10 µM (1.25 µl) and Phusion High Fidelity Taq polymerase 2 U/µl (0.25 µl), and 5 ng of input DNA for dermal biopsy samples and 2.5 µl for the skin surface samples with an unquantifiable concentration. The thermal profile consisted of an initial denaturation of 30 sec at 98°C, followed by 27 cycles of 15 sec at 98°C, 15 sec at 55°C, 20 sec at 72°C and a final extension of 7 min at 72°C. Quality and quantity of amplification were assessed in all samples, including extraction blanks and non-template controls (NTC), through Agilent Bioanalyzer 2100 and Qubit fluorometer. The nucleic acid concentration of 12 (7 swabs and 5 biopsies) out of 33 samples was lower than 1ng/µl after 27 cycles of PCR. Thus, an additional PCR was applied to these samples using the same condition increasing the number of cycles to 32. Each PCR reaction included an NTC to confirm the absence of contaminants in the reagents. The DNA sequencing was performed using an Ion Torrent Personal Genome Machine (PGM) with the Ion 318 Chip v2 (Thermo Fisher Scientific), following the manufacturer's instructions. A mock community (ZymoBIOMICS Microbial Community DNA Standard, Zymo Research), as a positive control, was also sequenced to assess the quality of the run. In addition, 4 extraction blanks (2 from skin swabs DNA purification and 2 from tissue biopsy DNA purification) and 2 not template controls from the two PCR amplification reactions were sequenced to exclude the presence of contaminants in the reagents. Taxa considered as contaminants were excluded from all the samples analyzed (Supplementary methods).

Quality control and sequence demultiplexing

Raw sequences were submitted to the National Center for Biotechnology Information under Bioproject accession number SUB6027391 – Bioproject number: PRJNA555200. Raw data were imported into Quantitative Insight Into Microbial Ecology 2 software (QIIME 2; https://qiime2.org)[43] for the analysis. Raw sequencing reads were demultiplexed to remove the Rv primer sequence and

to associate each barcode to the correspondent sample. DADA2[44] was used to denoise, dereplicate single-end sequences and remove chimaeras. Reads with a length of 253 bp were taken into account, considering the quality plot result and the V4 length mean of 250 bases. After that, the Amplicon Sequence Variants (ASVs), units of observation composed of unique sequences, were used to classify them and assign taxonomy using SILVA[45] at 99% of Operational Taxonomic Units (OTUs) identity and trimmed to V4 region, as the reference database. The complete workflow is provided in Supplementary Methods online.

Statistical analysis

Statistical analysis was performed using XLStat software for Windows (Addinsoft, New York, USA) on taxonomy and alpha and beta diversities. Data distribution was assessed using the Shapiro-Wilk test. From taxonomy results, the relative abundance of taxa present was determined in all samples. Alpha diversity describes the differences within samples or groups and indicates how many taxa are present by using a qualitative (observed species or observed ASVs) and a quantitative (Shannon index) approach. Beta diversity defines the differences between groups and takes into account how many taxa are shared between samples, generating distance matrices. We analyzed the beta diversity through unweighted and weighted UniFrac methods as a phylogenetic qualitative and quantitative approach, respectively and Bray Curtis analysis that does not consider the microbial community phylogeny. For both alpha and beta diversity, a sequence depth of 4500 was applied.

The statistical analysis was performed on paired samples to assess the microbiota variation within the same individual. To characterize the core microbiota, we analyzed the shared ASVs between groups, considering the cutoff of 80% for the presence of the features within the groups. The difference between observed and expected features for healthy and tumor tissues was calculated by means of Chi-square test. T-test, Wilcoxon-signed- and Mann-Whitney- tests were applied based on the distribution of each dataset. Statistical significance was accepted at $p\text{-}value \leq 0.05$.

For graphical representations, we plotted the shared ASVs using an online Venn tool (http://bioinformatics.psb.ugent.be/webtools/Venn/).

Multi-dimensional scaling (MDS) analysis was generated by means of XLStat software considering the distance matrix calculated on unweighted and weighted UniFrac and Bray-Curtis by QIIME2. The Kruskal's stress (from 0 to 1) was taken into account to evaluate the goodness-of-fit of the test, with values closer to zero corresponding to a better and more reliable data representation. Box- and bar-plots were produced using R software (http://www.R-project.org) by the R package ggplot2 (https://cran.r-project.org/web/packages/ggplot2/, version 3.2.0) as shown in the Supplementary Methods online.

In addition to the previous multi-dimensional scaling, we produced a second MDS plot using the R cmdscale function on the Manhattan distances calculated on the relative abundance matrices for both samples and ASVs (both part of the R built-in stats package, R version 3.5.2). This step was carried out for both phyla and families separately, and for the skin and the dermal biopsy separately, for a total of four different analyses. Eigenvalues for the ASVs have been plotted as bar charts to identify the leading eigenvalues. Finally, a principal component analysis (PCA) using the PCA function in FactoMineR package[46] (https://cran.r-project.org/web/packages/FactoMineR/, version 1.42), allowing for the detection of the percentage of contribution of every ASVs to the different components, was carried out. For this study, only the contribution to the first component was considered. The detailed bioinformatics workflow is available in Supplementary Methods online.

Acknowledgements

The funding for this research was provided by Linea 2017 - DIMEVET – Università degli Studi di Milano.

Author Contributions Statement

C.L., V.Z. and C.C. designed the study. F.C. and A.S. guided the experimental performance. D.S, R.F. and D.Z. enrolled patients and surgically removed the tumors. V.G. histologically classified and assessed grading of tumors. V.Z., C.C., A.C. and O.F. performed the laboratory experiments and bioinformatic data analysis. A.T. and P.C performed statistical analysis. C.L., F.C. and D.S. provided the funding. C.L. V.Z. and C.C wrote the main manuscript. All authors critically read and approved the manuscript.

Competing Interests

The authors declare no competing interests related to this work.

Bibliography

1. Byrd, A. L., Belkaid, Y. & Segre, J. A. The human skin microbiome. *Nat. Rev. Microbiol.* **16**, 143–155 (2018).
2. Rodrigues Hoffmann, A. *et al.* The skin microbiome in healthy and allergic dogs. *PLoS One* **9**, e83197 (2014).
3. Kwiecien, K. *et al.* Architecture of antimicrobial skin defense. *Cytokine Growth Factor Rev.* **S1359-6101**, (2019).
4. Cuscó, A. *et al.* Individual signatures and environmental factors shape skin microbiota in healthy dogs. *Microbiome* **5**, 139 (2017).
5. Baldwin, H. E. *et al.* The Role of Cutaneous Microbiota Harmony in Maintaining a Functional Skin Barrier. *J Drugs Dermatol.* **16**, 12-18 (2017).
6. Nakatsuji, T. *et al.* The microbiome extends to subepidermal compartments of normal skin. *Nat. Commun.* **4**, 1431–1438 (2013).
7. Prast-nielsen, S. D. *et al.* Investigation of the skin microbiome : swabs vs . biopsies. *Br J Dermatol*. **181,** 572-579 (2019).
8. Kong, H. H. & Segre, J. A. Skin microbiome: Looking back to move forward. *J Invest Dermatol.* **132**, 933–939 (2012).
9. Tizard, I. R. & Jones, S. W. The Microbiota Regulates Immunity and Immunologic Diseases in Dogs and Cats. *Vet. Clin. North Am. Small Anim. Pract.* **48**, 307–322 (2018).
10. Bradley, C. W. *et al.* Longitudinal evaluation of the skin microbiome and association with microenvironment and treatment in canine atopic dermatitis. *J Invest Dermatol*. **136**, 1182–1190 (2016).
11. Abdallah, F., Mijouin, L. & Pichon, C. Skin Immune Landscape: Inside and Outside the Organism. *Mediators Inflamm.* **2017**, 5095293 (2017).

12. Tong, P. L. *et al.* The skin immune atlas: Three-dimensional analysis of cutaneous leukocyte subsets by multiphoton microscopy. *J. Invest. Dermatol.* **135**, 84–93 (2015).

13. Kawakami, T. & Kasakura, K. Mast Cell Eavesdropping on Bacterial Communications. *Cell Host Microbe.* **26**, 3–5 (2019).

14. Afrin, L. B. & Khoruts, A. Mast Cell Activation Disease and Microbiotic Interactions. *Clin. Ther.* **37**, 941–953 (2015).

15. Hershko, A. Y. Insights into the mast cell–microbiome connection in the skin. *J. Allergy Clin. Immunol.* **139**, 1137–1139 (2017).

16. Mullins, M. N. *et al.* Evaluation of prognostic factors associated with outcome in dogs with multiple cutaneous mast cell tumors treated with surgery with and without adjuvant treatment: 54 cases (1998–2004). *J. Am. Vet. Med. Assoc.* **228**, 91–95 (2006).

17. Salava, A. *et al.* Skin microbiome in melanomas and melanocytic nevi. *Eur. J. Dermatol.* **26**, 49–55 (2016).

18. Mrázek, J. *et al.* Melanoma-related changes in skin microbiome. *Folia Microbiol. (Praha).* **64**, 435–442 (2019).

19. Welle, M. M., Bley, C. R., Howard, J. & Rüfenacht, S. Canine mast cell tumours: A review of the pathogenesis, clinical features, pathology and treatment. *Vet. Dermatol.* **19**, 321–339 (2008).

20. Zhang, H., Du, M., Yang, Q. & Zhu, M. J. Butyrate suppresses murine mast cell proliferation and cytokine production through inhibiting histone deacetylase. *J. Nutr. Biochem.* **27**, 299–306 (2016).

21. Kuczynski, J. *et al.* Experimental and analytical tools for studying the human microbiome. *Nat. Rev. Genet.* **13**, 47–58 (2011).

22. Sanford, J. A. & Gallo, R. L. Functions of the skin microbiota in health and disease. *Semin.*

Immunol. **25**, 370–7 (2013).

23. Zeeuwen, P. L., Kleerebezem, M., Timmerman, H. M. & Schalkwijk, J. Microbiome and skin diseases. *Curr. Opin. Allergy Clin. Immunol.* **13**, 514–520 (2013).

24. Chen, J., Domingue, J. C. & Sears, C. L. Microbiota dysbiosis in select human cancers: Evidence of association and causality. *Semin Immunol.* **32**, 25–34 (2017).

25. Pierezan, F. *et al.* The skin microbiome in allergen-induced canine atopic dermatitis. *Vet. Dermatol.* **27**, 332-e82 (2016).

26. Prescott, S. L. *et al.* The skin microbiome: Impact of modern environments on skin ecology, barrier integrity, and systemic immune programming. *World Allergy Organ J.* **10**, 29 (2017).

27. Van Leuvenhaege, C. *et al.* Bacterial diversity in Buruli ulcer skin lesions: Challenges in the clinical microbiome analysis of a skin disease. *PLoS One* **12**, e0181994 (2017).

28. Valent, P. *et al.* Diagnostic criteria and classification of mastocytosis: a consensus proposal. *Leuk. Res.* **25**, 603–25 (2001).

29. Kovalszki, A. & Weller, P. F. Eosinophilia in mast cell disease. *Immunol Allergy Clin North Am.* **34**, 357–364 (2014).

30. Mezouar, S. *et al.* Microbiome and the immune system: From a healthy steady-state to allergy associated disruption. *Human Microbiome Journal* **10**, 11–20 (2018).

31. Naik, S. *et al.* Compartmentalized control of skin immunity by resident commensals. *Science.* **337**, 1115–1119 (2012).

32. Wang, Z. *et al.* Skin microbiome promotes mast cell maturation by triggering stem cell factor production in keratinocytes. *J. Allergy Clin. Immunol.* **139**, 1205-1216.e6 (2017).

33. Nakamura, Y. *et al.* Staphylococcus δ-toxin induces allergic skin disease by activating mast cells. *Nature* **503**, 397–401 (2013).

34. Fazakerley, J. *et al.* Staphylococcal colonization of mucosal and lesional skin sites in atopic

and healthy dogs. *Vet. Dermatol.* **20**, 179–184 (2009).

35. Kaesler, S. *et al.* Targeting tumor-resident mast cells for effective anti-melanoma immune responses. *JCI insight* **4**, (2019).

36. Barnard, E. & Li, H. Shaping of cutaneous function by encounters with commensals. *J. Physiol.* **595**, 437–450 (2017).

37. Owen, L.N. TNM Classification of tumours in domestic animals. *World Heal. Organ.* 1–52 (1980).

38. Stefanello, D. *et al.* Ultrasound-guided cytology of spleen and liver: A prognostic tool in canine cutaneous mast cell tumor. *J. Vet. Intern. Med.* **23**, 1051–1057 (2009).

39. Thompson, J. J. *et al.* Canine subcutaneous mast cell tumors: cellular proliferation and KIT expression as prognostic indices. *Vet. Pathol.* **48**, 169–81 (2011).

40. Patnaik, A. K., Ehler, W. J. & MacEwen, E. G. Canine Cutaneous Mast Cell Tumor: Morphologic Grading and Survival Time in 83 Dogs. *Vet. Pathol.* **21**, 469–474 (1984).

41. Kiupel, M. *et al.* Proposal of a 2-tier histologic grading system for canine cutaneous mast cell tumors to more accurately predict biological behavior. *Vet. Pathol.* **48**, 147–155 (2011).

42. Weishaar, K. M., Thamm, D. H., Worley, D. R. & Kamstock, D. A. Correlation of nodal mast cells with clinical outcome in dogs with mast cell tumour and a proposed classification system for the evaluation of node metastasis. *J. Comp. Pathol.* **151**, 329–338 (2014).

43. Caporaso, J. G. *et al.* QIIME allows analysis of high-throughput community sequencing data. *Nature Methods* **7**, 335–336 (2010).

44. Callahan, B. J. *et al.* DADA2 paper supplementary information: High resolution sample inference from amplicon data. *Nat. Methods.* **13**, 581-3 (2016).

45. Yilmaz, P. *et al.* The SILVA and 'all-species Living Tree Project (LTP)' taxonomic frameworks. *Nucleic Acids Res.* **42**, D643–D648 (2014).

46. Lê, S., Josse, J. & Husson, F. FactoMineR: An R package for multivariate analysis. *J. Stat. Softw.* **25**, 1–18 (2008).

Figures:

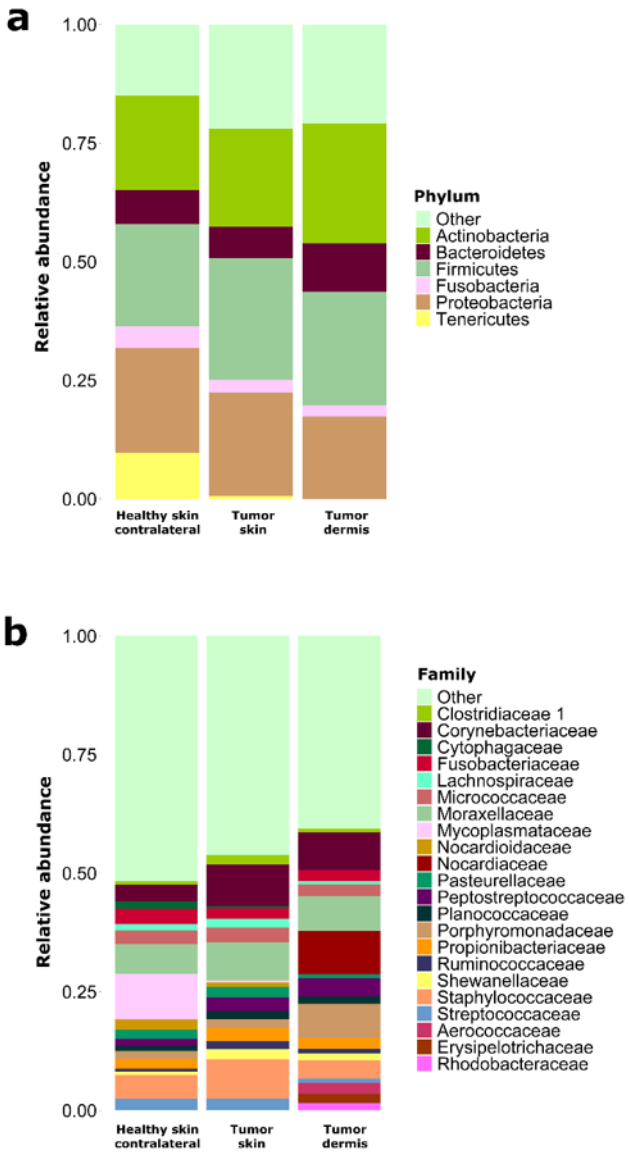

Figure 1. Skin surface and dermis taxonomy profile of MCT affected dogs. Taxonomy of seven healthy skin surfaces and seven tumor skin surfaces and five dermis is shown at phylum (a) and family (b) level, respectively.

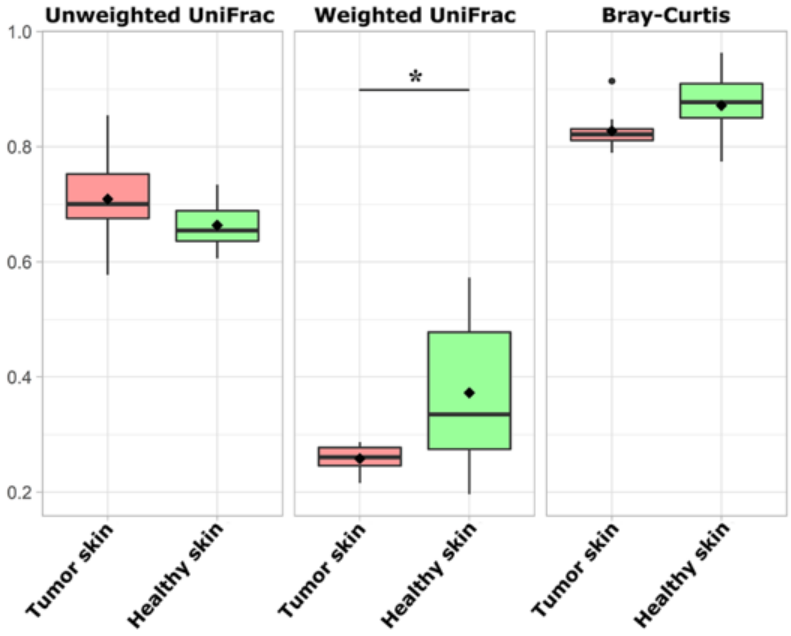

Figure 2. Boxplots of unweighted, weighted UniFrac and Bray-Curtis distances between tumor skin and healthy skin surface groups. Weighted UniFrac matrix shows an intra-group variation in distances between healthy and tumor skin surface (p= 0.02).

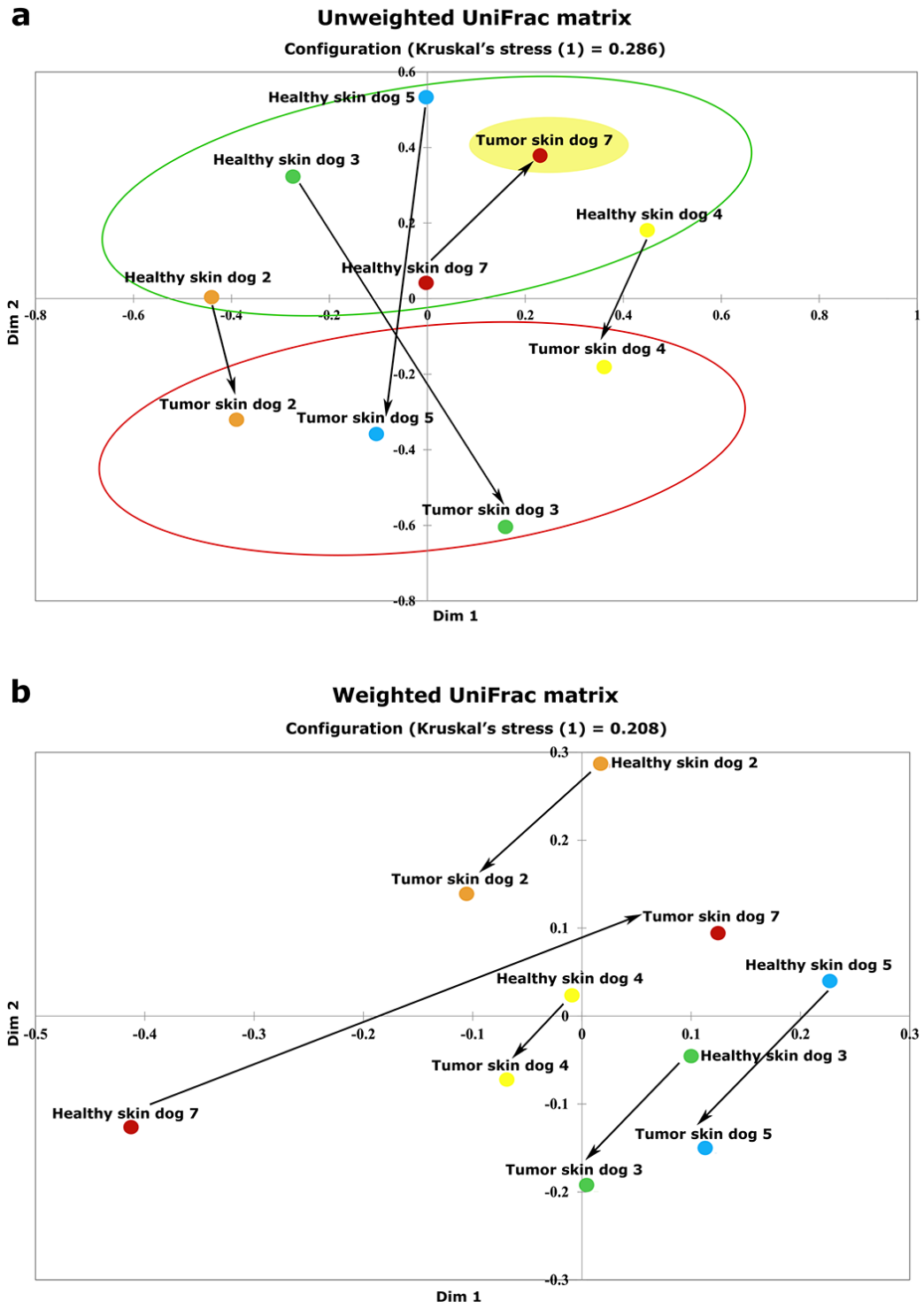

Figure 3. Multidimensional scaling plots of unweighted (a) and weighted (b) UniFrac distances comparing healthy (green circle) and tumor skin (red circle) surfaces. The arrows highlight the intra-animal shift from healthy and tumor skin surfaces.

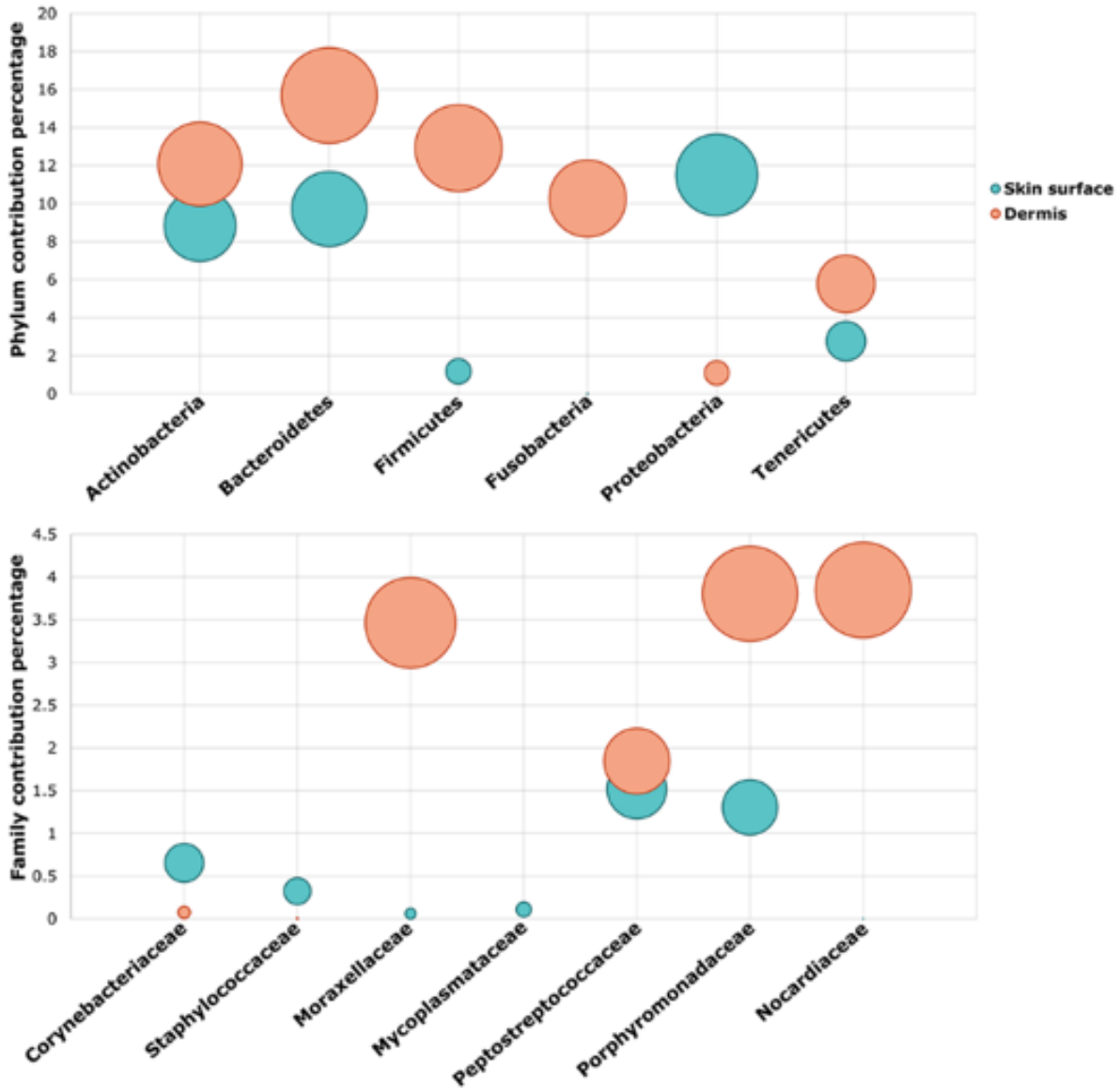

Figure 4. Balloon plot showing the contribution of the taxa (with a relative abundance ≥2%) which explain the shift from healthy to the tumor skin surface at phylum and family level.

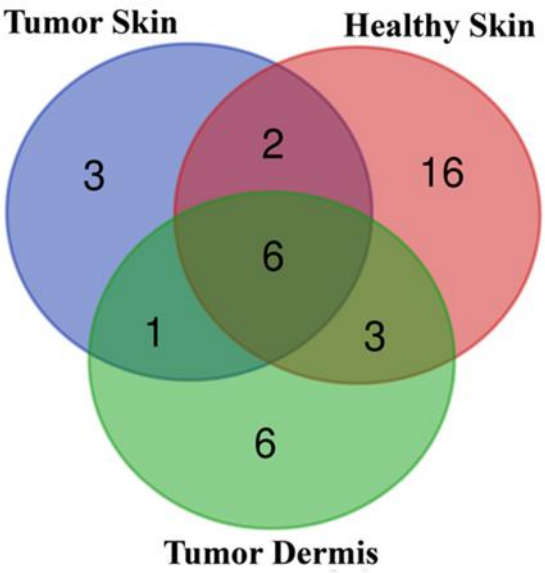

Figure 5. Venn diagram of ASVs, shared by tumor, healthy skin surface and tumor dermis which define core microbiota.

Supplementary materials:

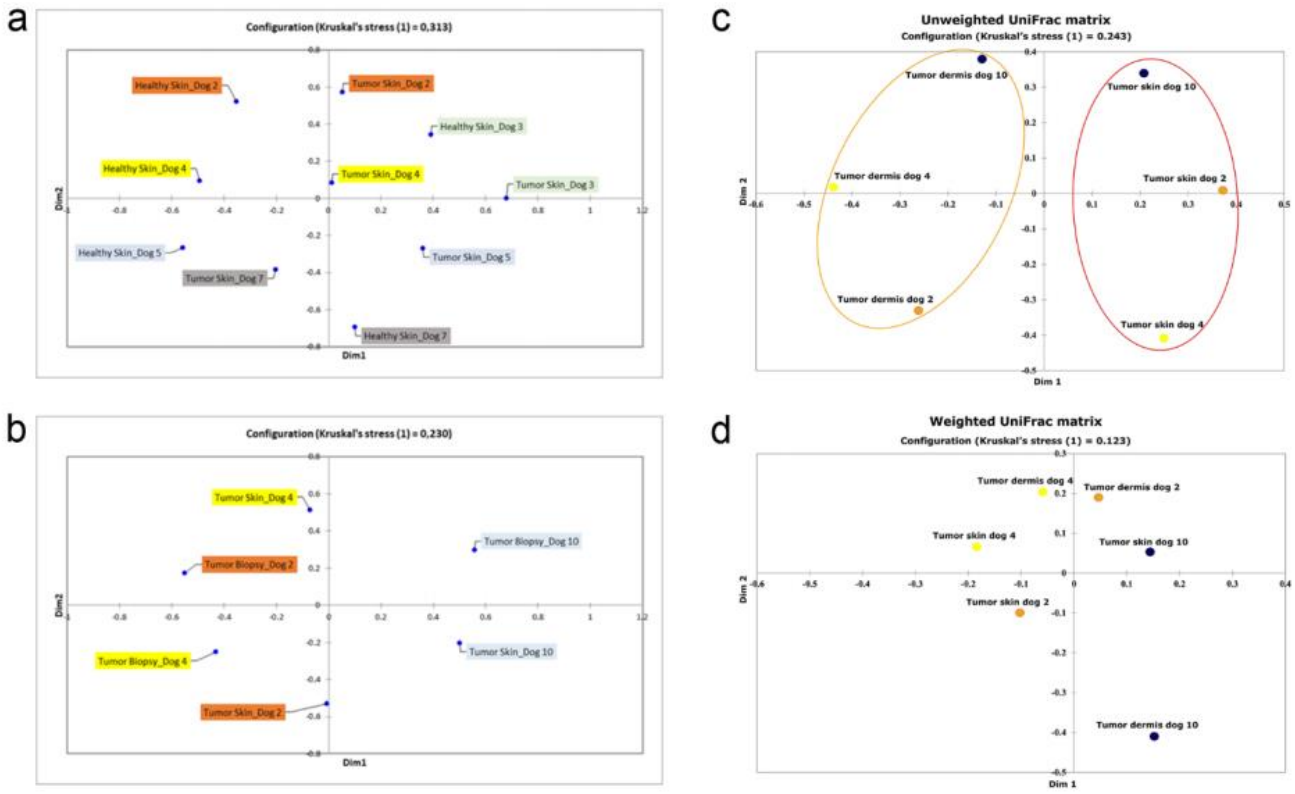

Supplementary Figure S1. Multidimensional scaling plots (a) of Bray-Curtis distances of the tumor and healthy skin surface and (b) of tumor skin surface and tumor dermis biopsy samples using Bray-Curtis matrix; (c) of unweighted and (d) weighted UniFrac distances comparing tumor dermis biopsy (orange circles) and the associated tumor skin surface (red cirles).

Supplementary Methods. Bioinformatics workflow of sequencing and statistical analysis. https://www.ncbi.nlm.nih.gov/pmc/articles/PMC7387470/bin/41598_2020_69572_MOESM2_ESM.pdf

Supplementary Table S1. The number of reads of each sample before and after filtering and chloroplasts removal**.**

https://www.ncbi.nlm.nih.gov/pmc/articles/PMC7387470/bin/41598_2020_69572_MOESM3_ESM.xlsx

Supplementary Table S2. Complete taxonomy at phylum, family and genus level of sequenced samples.

https://www.ncbi.nlm.nih.gov/pmc/articles/PMC7387470/bin/41598_2020_69572_MOESM4_ESM.xlsx

Sequencing sample ID	*Patient*	*Status*	*Observed OTU*
M003	Dog 2	Tumor skin surface	198
M004	Dog 2	Healthy skin controlateral	183
M007	Dog 3	Tumor skin surface	95
M008	Dog 3	Healthy skin controlateral	599
M009	Dog 4	Tumor skin surface	367
M010	Dog 4	Healthy skin controlateral	901
M017	Dog 5	Tumor skin surface	191
M018	Dog 5	Healthy skin controlateral	930
M020	Dog 6	Healthy skin controlateral	1029
M021	Dog 7	Tumor skin surface	904
M022	Dog 7	Healthy skin controlateral	383
M025	Dog 9	Tumor skin surface	178
M027	Dog 10	Tumor skin surface	155
M030	Dog 11	Healthy skin controlateral	102
M031	Dog 1	Tumor dermis biopsy	96
M032	Dog 2	Tumor dermis biopsy	95
M035	Dog 4	Tumor dermis biopsy	108
M043	Dog 10	Tumor dermis biopsy	218
M045	Dog 11	Tumor dermis biopsy	101

Supplementary table S3. The number of observed OTUs detected in tumor and heathy skin surface

Supplementary table S4. Beta diversity distances of uweighted, weighted UniFrac and Bray-Curtis matrices intra-groups (tumor and healthy skin surface and tumor dermis) and intra-individuals.

https://www.ncbi.nlm.nih.gov/pmc/articles/PMC7387470/bin/41598_2020_69572_MOESM6_ESM.xlsx

Animal	*Sex*	*Age (years)*	*Breed*	*Tumor*	*Onset site*	*Patnaik*	*Kiupel*
Dog 1	F	10	Cocker	+	Cutaneous	II	Low
Dog 2	M	10	Labrador	+	Cutaneous	II	Low
Dog 3	M	12	Mixed breed	+	Cutaneous	II	Low
Dog 4	F	4	Swiss Mountain dog	+	Cutaneous	II	Low
Dog 5	M	7	Weimaraner	+	Cutaneous	II	Low
Dog 6	F	6	Labrador	+	Cutaneous	II	Low
Dog 6	M	1	Labrador	+	Cutaneous	I	Low
Dog 8	F	9	Setter	+	Subcutaneous	II	N/A
Dog 9	M	6	Mixed breed	+	Subcutaneous	II	N/A
Dog 10	M	10	Shar-pei	+	Subcutaneous	II	N/A
Dog 11	F	14	Mixed breed	+	Subcutaneous	II	N/A
Dog 12	F	3	Mixed breed	-			
Dog 13	F	2	Mixed breed	-			
Dog 14	M	2	Mixed breed	-			

Supplementary Table S5. Data of dogs enrolled in the study. F= female; M= male; += MCT- affected dog; -= healthy dog; N/A= not applicable.

Set up of a method for purification, quantification and characterization of exosomes from plasma of dogs with mast cell tumor

Valentina Zamarian[1], Damiano Stefanello[1], Roberta Ferrari[1], Samantha Milanesi[2,3], Fabrizio Ceciliani[1], Cristina Lecchi[1]

(1) Dipartimento di Medicina Veterinaria, Università degli Studi di Milano, Milano, Italy

(2) IRCCS Humanitas Clinical and Research Center, Via Manzoni 56, 20089 Rozzano, MI, Italy

(3) Department of Medical Biotechnologies and Translational Medicine, Università degli Studi di Milano, Via Fratelli Cervi, 20090 Segrate, Italy

*Corresponding author: cristina.lecchi@unimi.it

Abstract

Cells communicate with each other by a carrier system called extracellular vesicles (EVs). Exosomes are a class of EVs (30-120 nm), which are born from the endosomal compartment playing a key role in tumor progression and metastasis. Exosome delivers several molecules, including DNA, long and small RNA, and proteins, and its cargo is composed of uniquely sorted material carrying it from the cytosol of parent cell to the target cell throughout the body.

Cancer cells use exosomes to communicate with other tumor cells or with cells of the microenvironment to promote the tumorigenic process and to predispose distant metastatic niches. The study of the exosome cargo is a valid approach to disclose the tumor communication strategy, to discover new candidate biomarkers. The isolation method of exosomes with reliable quality and substantial concentration is still a major challenge for the feasibility of downstream analyses, including proteomics. The present study aims at developing a suitable protocol for the isolation of exosomes from plasma of mast cell tumor(MCT)-affected dogs to be able to carry out proteomic analysis.

The size exclusion chromatography (SEC) approach was applied to isolate exosomes from plasma of MCT-affected dogs (6 metastatic and 4 non-metastatic tumors) and 4 healthy individuals. The presence, concertation, and size of isolated exosomes were assessed by Western blot, Nanoparticle tracking analysis (NTA), and transmission electron microscopy (TEM). Total protein concertation was quantified as well.

Results showed that exosomes expressed the specific exosomal marker CD9, and that the concentration was min 1.37E+10 (±1.15E+07 SE) and max 3.98E+10 (±2.28E+07 SE) particles/ml in the non-metastatic and min 8.95E+09 (±1.18E+07 SE) and max 5.95E+10 (±2.47E+07 SE) particles/ml in the metastatic tumors; in the healthy samples the concertation was min 2.07E+10 (±4.42E+06 SE) and max 6.13E+10 (±1.12E+07 SE) particles/ml. The size of isolated vesicles was in the exosome

expected size range, 99.6nm, 101.7nm, and 124nm in non-metastatic, metastatic, and healthy samples, respectively. The protein concertation mean was 381.6 µg/ml; the blue Coomassie staining demonstrated that SEC depleted plasmatic proteins with high efficiency.

In conclusion, the present work demonstrated that a relatively pure population of exosomes can be isolated from plasma of MCT-affected dogs using the SEC approach.

Keywords: Mast cell tumor, exosomes, SEC, dog

Introduction

Extracellular vesicles (EVs) are particles released by all cell types in normal and pathological conditions[1,2]. EVs are present in different body fluids, including plasma[3], urine[4], milk[5], and saliva[6]. EVs are classified into three main subtypes identified by the biogenesis pathway: exosomes (30–120 nm), microvesicles (100–1000 nm), and apoptotic bodies (800 to 5000 nm). The exosome originates from the multivesicular bodies coming from the endolysosomal system. The microvesicles are directly released by shedding of the plasma membrane and the apoptotic bodies from outward blebbing and decomposition of apoptotic cells[7,8]. Unlike apoptotic bodies, exosomes and microvesicles are characterized by a phospholipid bilayer, which promotes stability and resistance to degradation and spread far from parental cells[15]; they are involved in cell-to-cell communication by carrying small and long RNAs, proteins, lipids, metabolites, and DNA fragments, which can induce phenotypic reprogramming of recipient cells[8–10].

Cancer cells communicate with each other and with surrounding cells (like immune cells, fibroblast, and endothelial cells) through EVs[11,12], playing a crucial role in all steps of tumor progression and especially in the metastatic process[13]. Tumor EVs can reprogram a recipient cell inducing a tumor-promoting phenotype and modifying the microenvironment cells to support tumor growth, survival, invasion, metastasis, and also to sustain angiogenesis, resistance to cell death, evasion from the immune response, reprogramming of cellular metabolism, and the drug resistance[8,14]. The similarities between tumor-derived EVs and parental tumor cells prove the potential of these vesicles as targets for liquid biopsies[16,17] as they are carriers of biomarkers that could be used for early diagnosis, prognosis, cancers staging and monitoring, and patient follow up[18,19].

Canine mats cell tumor (MCT) with a prevalence from 7% to 21% is one of the most frequent skin neoplasms in dogs[20]. It has a variable biological behavior which makes challenging the diagnosis and complex the prognosis[21]. Several studies have been performed in veterinary oncology to investigate

the exosome cargo and their role in tumors[22–25], but only one study investigated the concentration of EVs in the blood of MCT-affected dogs with different histological grade[26]. To date, several approaches for exosome isolation have been developed, but no data on the isolation of plasmatic exosomes for proteomic analysis on MCT-affected dogs has been reported so far.

Exosomes contain specifics markers for their characterization, such as tetraspanins (CD9, CD63, and CD81) and TSG101[27,28]. Different methods can be applied for the exosome isolation and the choice is driven by the downstream analysis, since a sample with high purity should be required, as in proteomics[29]. The size exclusion chromatography (SEC) is one of the applied methods for exosome isolation for proteome profiling as it allows the co-purification of a low amount of plasma proteins[30–33]. The purpose of the present study was to assess the feasibility of SEC to isolate plasma exosomes from MCT-affected dogs with a good degree of purity and depleted from the most abundant plasmatic proteins for further proteomic analyses.

Material and methods

Sample collection

Fourteen plasma samples were collected from healthy (N= 4) and MCT-affected (N= 10) dogs (Table 1), after written owner consent, from client-owned dogs during the veterinary consultation and surgery for the routine oncological management of canine mast cell tumor.

In detail, blood samples were collected into Monovette EDTA tubes (Sarstedt Company, Nümbrecht, Germany) and centrifuged at 800 × g for 15 min. Plasma was stored at -80 °C until use.

MCTs were histologically classified[34] and graded[35,36] and then grouped base on lymph node involvement in two classes, non-metastatic/pre-metastatic (HN0-1 class) and early-metastatic/overt-metastatic (HN2-3 class) as previously described[37,38].

Isolation of extracellular vesicle from plasma

Extracellular vesicles (EVs) were purified from 0.5 ml of plasma by size exclusion chromatography (SEC) using the qEV original - 35nm columns (IZON). The column allowed the purification of EVs with a size from 35 to 350 nm. The sample was pre-purified from the cell debris by a series of centrifugations at 1000, 2000, 3000 x g for 15 min at 4°C. After each centrifugation step, the supernatant was transferred in a new tube for the next step and the pre-purified plasma was loaded into the qEV column and the EVs isolation was performed following the manufacturer's procedure with some adjustments. Briefly, after sample loading, the first 3.5 ml were discarded (void volume) and the next three fractions (0.5 ml each) containing the EVs were collected and pooled together. The column equilibration and the fractions' elution were carried out using an Ammonium Bicarbonate buffer 20mM pH 7.5 sterile filtered (0.2 µm).

Nanoparticle tracking analysis (NTA)

Size and concentration of EVs purified from plasma of dogs affected by MCT was assessed immediately after isolation in all the samples using the NanoSight NS300 (Malvern Panalytical). The purified exosomes were diluted 50 or 100 times using fresh filtered PBS (0.22µm) before loading. Particles were visualized and analyzed by the NTA 3.3 Dev Build 3.3.301 software. The instrument set up were to operate at 22°C, syringe pump speed 30 AU, and for each sample were recorded 5 videos of 60 sec each; results were the mean of the 5 measurements.

Protein quantification, Blue Coomassie staining, and Western blot analysis

The protein concentration was assessed in all the samples using the Pierce™ BCA Protein Assay kit (Thermo Fisher Scientific, Cat. No. 23225) following the manufacturer's procedure. Blue Coomassie staining was performed to evaluate the depletion of plasmatic proteins, especially albumin, in the collected fraction before sample pooling. Four micrograms of total protein of each fraction and 1 µl of whole plasma were loaded on a 12% SDS-polyacrylamide gel and stained with Blue Coomassie.

The bands were visualized after a destining step with a solution of 30% methanol and 10% acetic acid.

Western blot analysis was performed to assess the presence of exosomes in the purified samples by the detection of the exosome marker (CD9). Samples were run in a 12% SDS-polyacrylamide gel electrophoresis. The sample mix included 4 µg or 16 µg of total proteins, for samples and positive control respectively, 5 µl of loading buffer 4x, 2 µl of β-mercaptoetanolo (stock solution: 1.114 g/ml) and water in a final volume of 20 µl. The positive control consisted of proteins extracted from canine whole blood. The proteins into the gel were transferred on a nitrocellulose membrane using Trans-Blot Turbo Midi 0.2 µm Nitrocellulose Transfer Packs (Biorad, Cat. No. 1704159) on the Trans-Blot Turbo Transfer System (Biorad). After that, the membrane was washed for 10 min in PBS 1X and then blocked for 1 h in PBS 1X and ROTI®Block 1X (Carlroth, Cat. No. A151.1). The primary antibodies (anti-CD9: Biorad, MCA469GT, 1:1500) were diluted in PBS 1X and ROTI®Block 1X and incubated with the membrane over night at 4°C. After three washes with 0.1% of Tween 20 in PBS 1X the membrane was incubated with the secondary antibody (polyclonal anti-mouse HRP conjugated: Dako, P0260) for 1 h at room temperature in a final concertation of 1:2000. The immunodetection of the reactive bands was performed after a 5 min incubation with the Immobilion Western chemiluminescent HRP substrate (Millipore, Cat. No. WBKLS0050).

Transmission electron microscopy (TEM)

To assess the morphology, exosomes were visualized using negative staining by TEM. Few microliters of samples were absorbed on glow-discharged carbon-coated formvar copper grids contrasted with 2% uranyl acetate, air-dried, and observed in an FEI Talos 120kV transmission electron microscope (FEI Company, Netherlands). Images of exosomes were acquired by a 4k×4K Ceta CMOS camera.

Statistical analysis

XLStat software for Windows (Addinsoft, New York, USA) was used to perform the statistical analysis. The non-parametric Kruskal-Wallis test for multiple pairwise comparisons was applied as data were not normally distributed by the Shapiro-Wilk test. Statistical significance was accepted at *p*-value≤ 0.05.

Results

Concentration and size of plasma-derived EVs

The concentration and size of the EVs were assessed in all samples collected during the isolation procedure (Figure 1), data are reported in Table 2.

In non-metastatic/pre-metastatic (HN0-1) MCT samples the EVs concertation was min 1.37E+10 (±1.15E+07 SE) and max 3.98E+10 (±2.28E+07 SE) particles/ml, in early-metastatic/overt-metastatic (HN2-3) MCT the concentration was min 8.95E+09 (±1.18E+07 SE) and max 5.95E+10 (±2.47E+07 SE) particles/ml, and in healthy samples the concertation was min 2.07E+10 (±4.42E+06 SE) and max 6.13E+10 (±1.12E+07 SE) particles/ml. Most of EVs were in the expected exosomal range, with a size mean of 99.6nm (min= 66.6nm; MAX= 124.5nm) in non-metastatic/pre-metastatic (HN0-1) MCTs, 101.7nm (min= 90nm; MAX= 108.3nm) in early-metastatic/overt-metastatic (HN2-3) and 124nm (min= 110.4nm; MAX= 143.8nm) in healthy samples. No significant differences were detected between healthy, HN0-1 and HN2-3 classes in terms of vesicles concertation and size.

Identification of exosomes

The protein concentration means were assessed and were reported in Supplementary Table 1. Comparing the protein profiles of fractions obtained by SEC isolation and whole plasma using blue Coomassie staining, the result highlighted that SEC depleted the most abundant plasmatic proteins (Figure 2a). The EVs marker protein CD9 was evaluated by immunoblot analysis; the bands with the expected MW were visualized in all tested samples and the positive control (Figure 2b).

Transmission electron microscopy showed that exosomes derived from the plasma of MCT-affected dogs exhibited the expected round vesicular membranes 30–150 nm in diameter and the ultrastructure of exosome-like vesicles[39] (figure 2c).

Discussion

A protocol for the isolation, quantification, and characterization of plasmatic exosomes of dogs with mast cell tumors, depleted from the most abundant plasmatic proteins and suitable for a proteomic characterization, was assessed. The exosome isolation was performed using a size exclusion chromatography approach starting from a small amount of plasma (0.5 mL). The results showed that the vast majority of the EVs had the exosome expected size with a mean of 107.4 nm and the yield was good (2.92E+10 particle/ml). Exosomes are carriers of biological markers suitable for the tumor characterization and monitoring the response to therapy, and are continuously release and cumulate in biological fluids[16,40], they acquired fame as important targets for liquid biopsy. Exosome enrichment is a challenging task and many collection methods are currently available. SEC allows the isolation of active and morphologically intact exosomes from plasma of cancer patients[32,41], necessary features for further proteomic profiling[42]. Unlike ultracentrifugation, SEC is not the classical method for exosome isolation and allows the purification of a good yield of exosomes without damage to the vesicle structure starting from a very small biofluid volume. SEC is fast, easy to perform, reproducible, and does not require specialized equipment; thus, it represents a feasible method for clinical monitoring of exosomal biomarkers[32,43,44].

Enough yield of proteins for characterizing the protein cargo of exosomes, which should be around 0.5-2 µg[45,46], has been obtained using SEC. The isolation method is a crucial choice for further downstream analyses and SEC proved to be a valid alternative for a proteomic approach[47], allowing the isolation of EVs within the expected size and with a small content of plasma proteins[30,48].

However, some issues associated with contamination of EVs enriched fraction with serum components or lipoproteins can still persist[49,50].

Takov and colleagues demonstrated that EV concertation, markers signal, EV protein, and particle/protein ratio were higher using SEC than ultracentrifugation, even if non-EV proteins were still present [51].

In the present study, the exosomal marker CD9[27] was identified in all samples and, to confirm the nature of isolated MVs, TEM microscopy confirmed the presence and the morphology of the exosomes in the collected fractions. The EVs released by mast cells during systemic mastocytosis played a role in the disease influencing different organs[52]. The development of a good and standardized protocol for the isolation of MCT-derived exosomes for further proteomic profiling, which could provide a step forward disclosing the molecular strategy of the tumor to communicate with cells far from the primary mass and prepare metastatic niches.

Bibliography

1. Yuana, Y., Sturk, A. & Nieuwland, R. Extracellular vesicles in physiological and pathological conditions. *Blood Rev.* **27**, 31–39 (2013).

2. Théry, C. *et al.* Minimal information for studies of extracellular vesicles 2018 (MISEV2018): a position statement of the International Society for Extracellular Vesicles and update of the MISEV2014 guidelines. *J. Extracell. Vesicles* **7**, 1535750 (2018).

3. Caby, M., Lankar, D., Vincendeau-Scherrer, C., Raposo, G. & Bonnerot, C. Exosomal-like vesicles are present in human blood plasma. *Int Immunol.* **17**, 879–887 (2005).

4. Gonzales, P. A. *et al.* Isolation and purification of exosomes in urine. *Methods Mol. Biol.* **641**, 89–99 (2010).

5. Admyre, C. *et al.* Exosomes with Immune Modulatory Features Are Present in Human Breast Milk. *J. Immunol.* **179**, 1969–1978 (2007).

6. Palanisamy, V. *et al.* Nanostructural and transcriptomic analyses of human saliva derived exosomes. *PLoS One* **5**, e8577 (2010).

7. Yáñez-Mó, M. *et al.* Biological properties of extracellular vesicles and their physiological functions. *Journal of Extracellular Vesicles* **4**, 27066 (2015).

8. Xavier, C. P. R. *et al.* The Role of Extracellular Vesicles in the Hallmarks of Cancer and Drug Resistance. *Cells* **9**, 1141 (2020).

9. Cufaro, M. C. *et al.* Extracellular Vesicles and Their Potential Use in Monitoring Cancer Progression and Therapy: The Contribution of Proteomics. *J. Oncol.* **2019**, 1639854 (2019).

10. Whiteside, T. L. Exosomes and tumor-mediated immune suppression. *J. Clin. Invest.* **126**, 1216–1223 (2016).

11. Tominaga, N., Katsuda, T. & Ochiya, T. Micromanaging of tumor metastasis by extracellular vesicles. *Seminars in Cell and Developmental Biology* **40**, 52–59 (2015).

12. Kogure, A., Kosaka, N. & Ochiya, T. Cross-talk between cancer cells and their neighbors via miRNA in extracellular vesicles: An emerging player in cancer metastasis. *Journal of*

Biomedical Science **26**, (2019).

13. Lobb, R. J., Lima, L. G. & Möller, A. Exosomes: Key mediators of metastasis and pre-metastatic niche formation. *Seminars in Cell and Developmental Biology* **67**, 3–10 (2017).

14. Lucchetti, D., Tenore, C. R., Colella, F. & Sgambato, A. Extracellular vesicles and cancer: A focus on metabolism, cytokines, and immunity. *Cancers (Basel.)* **12**, 171 (2020).

15. Boukouris, S. & Mathivanan, S. Exosomes in bodily fluids are a highly stable resource of disease biomarkers. *Proteomics - Clinical Applications* **9**, 358–367 (2015).

16. Vasconcelos, M. H., Caires, H. R., Ābols, A., Xavier, C. P. R. & Linē, A. Extracellular vesicles as a novel source of biomarkers in liquid biopsies for monitoring cancer progression and drug resistance. *Drug Resist. Updat.* **47**, 100647 (2019).

17. Roy, S. *et al.* Navigating the landscape of tumor extracellular vesicle heterogeneity. *International Journal of Molecular Sciences* **20**, 1349 (2019).

18. Huang, T. & Deng, C. X. Current progresses of exosomes as cancer diagnostic and prognostic biomarkers. *International Journal of Biological Sciences* **15**, 1–11 (2019).

19. Soung, Y. H., Ford, S., Zhang, V. & Chung, J. Exosomes in cancer diagnostics. *Cancers (Basel.)* **9**, 8 (2017).

20. Welle, M. M., Bley, C. R., Howard, J. & Rüfenacht, S. Canine mast cell tumours: A review of the pathogenesis, clinical features, pathology and treatment. *Vet. Dermatol.* **19**, 321–339 (2008).

21. Blackwood, L. *et al.* European consensus document on mast cell tumours in dogs and cats. *Vet. Comp. Oncol.* **10**, e1-e29 (2012).

22. Żmigrodzka, M. *et al.* Extracellular vesicles in the blood of dogs with cancer—a preliminary study. *Animals* **9**, 575 (2019).

23. Fish, E. J. *et al.* Malignant canine mammary epithelial cells shed exosomes containing differentially expressed microRNA that regulate oncogenic networks. *BMC Cancer* **18**, 832 (2018).

24. Brady, J. V *et al.* A Preliminary Proteomic Investigation of Circulating Exosomes and Discovery of Biomarkers Associated with the Progression of Osteosarcoma in a Clinical Model of Spontaneous Disease. *Transl. Oncol.* **11**, 1137–1146 (2018).

25. Asada, H. *et al.* Comprehensive analysis of miRNA and protein profiles within exosomes derived from canine lymphoid tumour cell lines. *PLoS One* **14**, e0208567 (2019).

26. Šimundić, M. *et al.* Concentration of extracellular vesicles isolated from blood relative to the clinical pathological status of dogs with mast cell tumours. *Vet. Comp. Oncol.* (2019). doi:10.1111/vco.12489

27. Doyle, L. M. & Wang, M. Z. Overview of Extracellular Vesicles, Their Origin, Composition, Purpose, and Methods for Exosome Isolation and Analysis. *Cells* **8**, 727 (2019).

28. Witwer, K. W. *et al.* Standardization of sample collection, isolation and analysis methods in extracellular vesicle research. *J. Extracell. Vesicles* **2**, (2013).

29. Hou, R. *et al.* Advances in exosome isolation methods and their applications in proteomic analysis of biological samples. *Analytical and Bioanalytical Chemistry* **411**, 5351–5361 (2019).

30. Stranska, R. *et al.* Comparison of membrane affinity-based method with size-exclusion chromatography for isolation of exosome-like vesicles from human plasma. *J. Transl. Med.* **16**, 1 (2018).

31. Ramirez, M. I. *et al.* Technical challenges of working with extracellular vesicles. *Nanoscale* **10**, 881–906 (2018).

32. Hong, C. S., Funk, S., Muller, L., Boyiadzis, M. & Whiteside, T. L. Isolation of biologically active and morphologically intact exosomes from plasma of patients with cancer. *J. Extracell. Vesicles* **5**, 29289 (2016).

33. Böing, A. N. *et al.* Single-step isolation of extracellular vesicles by size-exclusion chromatography. *J. Extracell. Vesicles* **3**, (2014).

34. Thompson, J. J. *et al.* Canine subcutaneous mast cell tumors: cellular proliferation and KIT expression as prognostic indices. *Vet. Pathol.* **48**, 169–181 (2011).

35. Kiupel, M. *et al.* Proposal of a 2-tier histologic grading system for canine cutaneous mast cell tumors to more accurately predict biological behavior. *Vet. Pathol.* **48**, 147–155 (2011).

36. Patnaik, A. K., Ehler, W. J. & MacEwen, E. G. Canine Cutaneous Mast Cell Tumor: Morphologic Grading and Survival Time in 83 Dogs. *Vet. Pathol.* **21**, 469–474 (1984).

37. Weishaar, K. M., Thamm, D. H., Worley, D. R. & Kamstock, D. A. Correlation of nodal mast cells with clinical outcome in dogs with mast cell tumour and a proposed classification system for the evaluation of node metastasis. *J. Comp. Pathol.* **151**, 329–338 (2014).

38. Stefanello, D. *et al.* Ultrasound-guided cytology of spleen and liver: a prognostic tool in canine cutaneous mast cell tumor. *J. Vet. Intern. Med.* **23**, 1051–1057 (2009).

39. Wu, Y., Deng, W. & Klinke, D. J. Exosomes: Improved methods to characterize their morphology, RNA content, and surface protein biomarkers. *Analyst* **140**, 6631–6642 (2015).

40. LeBleu, V. S. & Kalluri, R. Exosomes as a Multicomponent Biomarker Platform in Cancer. *Trends in Cancer* (2020). doi:10.1016/j.trecan.2020.03.007

41. Ludwig, N. *et al.* Isolation and Analysis of Tumor-Derived Exosomes. *Curr. Protoc. Immunol.* **127**, (2019).

42. Chandran, V. I. *et al.* Ultrasensitive immunoprofiling of plasma extracellular vesicles identifies syndecan-1 as a potential tool for minimally invasive diagnosis of glioma. *Clin. Cancer Res.* **25**, 3115–3127 (2019).

43. Taylor, D. D. & Shah, S. Methods of isolating extracellular vesicles impact down-stream analyses of their cargoes. *Methods* **87**, 3–10 (2015).

44. Sidhom, K., Obi, P. O. & Saleem, A. A review of exosomal isolation methods: is size exclusion chromatography the best option? (2020). doi:10.20944/preprints202007.0485.v1

45. Smolarz, M., Pietrowska, M., Matysiak, N., Mielańczyk, Ł. & Widłak, P. Proteome profiling of exosomes purified from a small amount of human serum: The problem of co-purified serum components. *Proteomes* **7**, 18 (2019).

46. Kuang, M. *et al.* Proteomic analysis of plasma exosomes to differentiate malignant from

benign pulmonary nodules. *Clin. Proteomics* **16**, 5 (2019).

47. Lane, R. E., Korbie, D., Trau, M. & Hill, M. M. Optimizing Size Exclusion Chromatography for Extracellular Vesicle Enrichment and Proteomic Analysis from Clinically Relevant Samples. *Proteomics* **19**, e1800156 (2019).

48. Ludwig, N., Whiteside, T. L. & Reichert, T. E. Challenges in exosome isolation and analysis in health and disease. *International Journal of Molecular Sciences* **20**, 4684 (2019).

49. Pietrowska, M., Wlosowicz, A., Gawin, M. & Widlak, P. MS-Based Proteomic Analysis of Serum and Plasma: Problem of High Abundant Components and Lights and Shadows of Albumin Removal. *Adv. Exp. Med. Biol.* **1073**, 57–76 (2019).

50. Yang, D. *et al.* Progress, opportunity, and perspective on exosome isolation - Efforts for efficient exosome-based theranostics. *Theranostics* **10**, 3684–3707 (2020).

51. Takov, K., Yellon, D. M. & Davidson, S. M. Comparison of small extracellular vesicles isolated from plasma by ultracentrifugation or size-exclusion chromatography: yield, purity and functional potential. *J. Extracell. Vesicles* **8**, 1560809 (2019).

52. Kim, D. K. *et al.* Mastocytosis-derived extracellular vesicles exhibit a mast cell signature, transfer KIT to stellate cells, and promote their activation. *Proc. Natl. Acad. Sci. U. S. A.* **115**, E10692–E10701 (2018).

Figures:

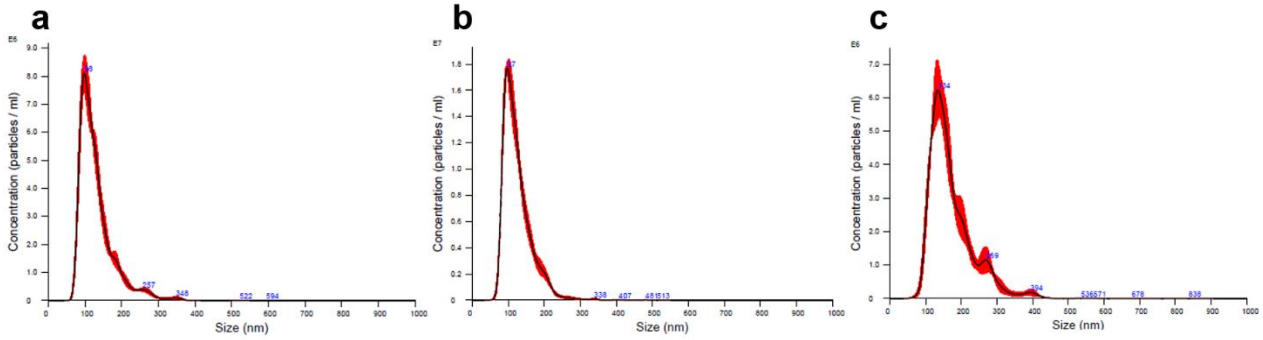

Figure 1. Nanoparticle tracking analysis, size and concentration of EVs purified from plasma of dogs with (a) non-metastatic/pre-metastatic (HN0-1) MCT, (b) early-metastatic/overt-metastatic (HN2-3) MCT and (c) healthy sample by SEC.

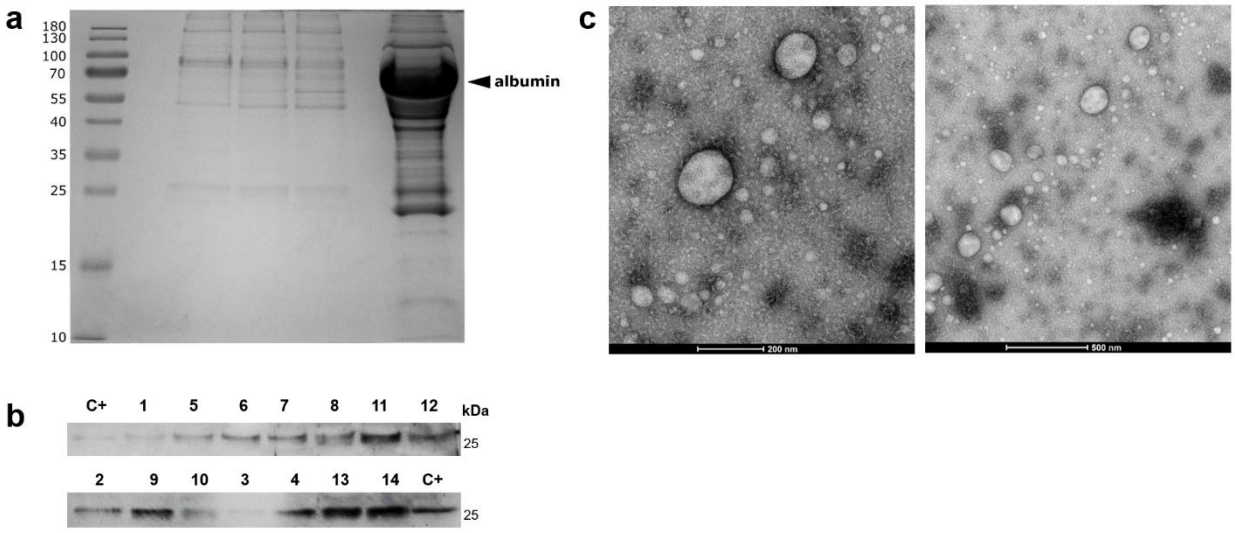

Figure 2. (a) Blue Coomassie staining of the three SEC fractions and of the whole plasma, (b) visualization of the reactive bands of the exosome marker (CD9) by Western Blot analysis and (c) transmission electron microscopy of the exosomes purified from plasma of dogs with MCT by SEC with a lower (200 nm) and a higher (500 nm) magnification. The number of the wells in the western blot are referred to the samples ID reported in Table 1.

Tables:

ID	Breed	Gender	Age (years)	Tumor location	Site	Grade		Lymph node*
						Patnaik	Kiupel	
1	Labrador	Male	10	Scrotum	Cutaneous	II	Low	HN0-1
2	Dachshund	Female	9	Tail	Cutaneous	II	Low	HN0-1
3	Mixed breed	Female	10	Shoulder	Cutaneous	II	Low	HN0-1
4	Mixed breed	Female	9	Limb	Cutaneous	II	Low	HN0-1
5	Golden Retriever	Female	7	Shoulder	Cutaneous	II	Low	HN2-3
6	Tosa Inu	Male	4	Foreskin	Cutaneous	II	Low	HN2-3
7	Boxer	Male	8	Limb	Cutaneous	II	Low	HN2-3
8	Golden Retriever	Female	11	Limb	Cutaneous	I	Low	HN2-3
9	Pitbull	Female	5	Limb	Subcutaneous	-	-	HN2-3
10	English setter	Female	10	Limb	Subcutaneous	-	-	HN2-3
11	Spinone italiano	Female	8	-	-	-	-	Healthy
12	Pointer	Female	9	-	-	-	-	Healthy
13	Mixed breed	Male	8.5	-	-	-	-	Healthy
14	Labrador	Female	6	-	-	-	-	Healthy

*classification system proposed by Weishaar and colleagues (2014). HN= histological node

Table 1. Clinical and histopathological data of dogs enrolled in the study.

ID	Particles/mL	Size (nm)	NH
1	1.37E+10 +/- 1.15e+07	102.5 +/- 3.7	HN0-1
2	3.98E+10 +/- 2.28e+07	66.6 +/- 0.4	HN0-1
3	2.84E+10 +/- 1.06e+07	104.7 +/- 5.5	HN0-1
4	2.54E+10 +/- 2.29e+07	124.5 +/- 5.3	HN0-1
5	8.95E+09 +/- 1.18e+07	90 +/- 4.9	HN2-3
6	1.41E+10 +/- 1.33e+07	99.8 +/- 3.2	HN2-3
7	1.24E+10 +/- 1.16e+07	105.3 +/- 4.0	HN2-3
8	5.95E+10 +/- 2.47e+07	98.9 +/- 3.3	HN2-3
9	2.03E+10 +/- 1.71e+07	107.6 +/- 2.6	HN2-3
10	5.85E+10 +/- 3.34e+07	108.3 +/- 7.7	HN2-3
11	2.07E+10 +/- 4.42e+06	110.4 +/- 4.7	Healthy
12	2.24E+10 +/- 1.15e+07	122.6 +/- 4.3	Healthy
13	6.13E+10 +/- 1.12e+07	143.8 +/- 8.1	Healthy
14	2.40E+10 +/- 1.92e+07	119.1 +/- 7.1	Healthy

Plasma derived EVs from MCT affected dogs (mean +/− standard error)

* HN= histological node. Classification system proposed by Weishaar and colleagues (2014).

Table 2. EVs concentration and size in the purified samples by SEC.

Supplementary materials:

ID	Protein concetration (ug/mL)	Lymph node*
1	408.3	HN0-1
2	257.6	HN0-1
3	295.8	HN0-1
4	105.0	HN0-1
5	240.5	HN2-3
6	302.7	HN2-3
7	295.8	HN2-3
8	427.6	HN2-3
9	347.6	HN2-3
10	604.0	HN2-3
11	512.9	Healthy
12	524.8	Healthy
13	631.0	Healthy
14	389.0	Healthy

* HN= histological node. Classification system proposed by Weishaar and colleagues (2014)

Supplementary Table 1. Protein concentration in the samples purified by SEC.

Oncology–Original Article

MicroRNA Expression in Formalin-Fixed, Paraffin-Embedded Samples of Canine Cutaneous and Oral Melanoma by RT-qPCR

Veterinary Pathology
2019, Vol. 56(6) 848-855

DOI: 10.1177/0300985819868646
journals.sagepub.com/home/vet

Valentina Zamarian[1], Carlotta Catozzi[1], Lorenzo Ressel[2], Riccardo Finotello[3], Fabrizio Ceciliani[1], Miguel Vilafranca[4], Jaume Altimira[4], and Cristina Lecchi[1]

Veterinary Pathology, 2019, doi: 10.1177/0300985819868646

MicroRNA expression in formalin-fixed-paraffin-embedded samples of canine cutaneous and oral melanoma by RT-qPCR

Valentina Zamarian[1], Carlotta Catozzi[1], Lorenzo Ressel[2], Riccardo Finotello[3], Fabrizio Ceciliani[1], Miguel Vilafranca [4], Jaume Altimira [4], Cristina Lecchi [1*].

[1] *Dipartimento di Medicina Veterinaria, Università degli Studi di Milano, via Celoria 10, Milano, Italy.*

[2] *Department of Veterinary Pathology and Public Health Institute of Veterinary Science, University of Liverpool, CH64 7TE, Neston, United Kingdom*

[3] *Department of Small Animal Clinical Science, Institute of Veterinary Science, University of Liverpool, CH64 7TE, Neston, United Kingdom*

[4]*HISTOVET Veterinary Diagnostic Service , Avda. Països Catalans, 12D, 08192 Sant Quirze del Vallès, Barcelona , Spain.*

* Corresponding author: Cristina Lecchi.

Address: via Celoria 10, Milan 20133 – Italy

Telephone number: +390250318100

Fax number: +390250318095

Email: cristina.lecchi@unimi.it

Abstract

MicroRNAs (miRNAs) are a class of small, non-coding RNA that post-transcriptionally regulate protein expression. miRNAs are emerging as clinical biomarkers of many diseases including tumors. The aim of this study was to investigate whether miRNA expression could vary in melanoma samples derived from formalin-fixed-paraffin-embedded (FFPE) tissues.The study included four groups: a) 9 samples of oral canine malignant melanoma; b) 10 samples of cutaneous malignant melanoma; c) 5 samples of healthy oral mucosa; d) 7 samples of healthy skin. The expression levels of six miRNAs–miR-145, miR-146a, miR-425-5p, miR-223, miR-365 and miR-134–were detected and assessed by RT-qPCR using TaqMan probes. Cutaneous canine malignant melanoma showed a decrease of the expression level of miR-145 and miR-365 and an increase of miR-146a and miR-425-5p compared to control samples. MiR-145 was also down-regulated in oral canine malignant melanoma. The miRNAs with decreased expression may regulate genes involved in RAS, Rap1 and TGF-beta signaling pathways, and up-regulated genes associated with phosphatidylinositol signaling system, adherens junction and RAS signalling pathways. In conclusion, miR-145, miR-365, miR-146a and miR-425-5p were differentially expressed in canine malignant melanoma and healthy FFPE samples, suggesting that they may play a role in canine malignant melanoma pathogenesis.

Key words: canine, cutaneous melanoma, dog, microRNAs, oral melanoma, RT-qPCR.

Melanocytic tumors are relatively common in dogs and can arise at different sites, although they mainly affect the oral mucosa and the dermis. [17,28] Among melanocytic neoplasms, malignant melanoma prevails in the oral cavity of dogs, accounting also for the most common oral canine malignant tumor.[42] Oral canine malignant melanoma has often an aggressive biological behavior, characterized by rapid invasion of neighboring structures, high propensity for regional and distant metastasis, and is therefore associated with a poor long-term prognosis.[28,42] Oral canine malignant melanoma resembles human malignant mucosal melanomas of the head and neck, which represent a fatal malignancy.[28] Conventional treatment for oral canine malignant melanoma involves surgical resection and/or radiation of the primary tumor often resulting in efficient local tumor control,[5,32] while treatment of metastatic disease has shown little promise.[34, 45, 6]

Cutaneous malignant melanoma is the third most common malignant skin tumor in dogs[49] representing 27% of all canine malignant melanomas.[15] Cutaneous malignant melanoma is thought to have a less aggressive behaviour than those of humans, although metastases are reported in up to 30-75% of the cases, potentially resulting in a poor prognosis. [7, 43] Surgical excision with wide margins represent the treatment of choice.[8]

Previous studies have investigated the correlation between patient survival and the clinicopathological variables, and suggested that clinical tumor staging, location, completeness of excision, adjunctive treatment, mitotic index, Ki-67 index, level of infiltration and cell pigmentation have a prognostic impact; however, results have been sometimes conflicting.[37,43,41,9,48,18,40] The molecular profile of canine melanoma has been only recently investigated. Comparison of the transcriptome profiles of canine cutaneous melanocytoma and melanoma identifyied 60 differentially expressed genes involved in collagen metabolism and extracellular matrix remodelling.[10,20]

MicroRNAs (miRNAs) are a group of small RNAs, with around 19 to 25 nucleotides, resulting from cleavage of larger non-coding RNAs. They act as post-transcriptional regulators of gene expression.[4] MiRNAs have been associated with several molecular pathways including modulation of proliferation, apoptosis, differentiation, and cell cycle regulation; thus dysregulation of their expression may contribute to a variety of diseases, and disrupt pathways of fundamental importance in development of neoplasia.[11] During tumorigenesis, some miRNAs that negatively regulate oncoproteins (i.e. tumor-suppressor miRNAs) are down-regulated, while those negatively regulating tumor suppressor genes (i.e. oncogenic miRNAs, or oncomiRNAs) are up-regulated.[27,46] The involvement of miRNAs in melanoma pathogenesis has been demonstrated in both humans [1,13,19,39] and dogs.[30,31,29,44] The identification of miRNAs associated with oral and uveal canine malignant melanoma has been investigated by Noguchi and colleagues[29] and Starkey and colleagues,[44] respectively, using a microarray hybridization approach. To the best of authors' knowledge, few data are available on the expression patterns of miRNA in oral and cutaneous canine malignant melanoma when compared to healthy controls. The aims of the present study were 1) to screen by RT-qPCR the expression of a panel of miRNAs, previously demonstrated to be related to melanoma (miR-425-5p, miR-134, miR-145, miR-146a, miR-223-3p and miR-365),[30,39,2,22,51,36,26,35] in a cohort of oral and cutaneous malignant melanoma; 2) to carry out functional enrichment analysis of target genes and functional interaction network analysis, to identify pathways affected by the differentially expressed miRNAs.

Materials and methods

Study population

Histopathology samples of cutaneous (non-digital) and oral mucosal malignant melanoma was computer searched including records from January 2012 to December 2013. Cases were considered

eligible only if blocks were available for review and tumors had positive staining for Melan A and PNL-2 antibodies with immunohistochemistry (IHC). Patient data were collected both from the pathology submission forms and via telephone calls to the referring veterinarians. The formalin-fixed paraffin embedded samples (FFPEs) that satisfied these criteria (19; 9 oral, 10 cutaneous) were enrolled and were subsequently divided into two groups: Cutaneous malignant melanoma and Oral malignant melanoma. Sample details are described in Supplemental Table S1.

Histology and Immunohistochemistry

Cases selected were re-examined by a board-certified pathologist (LR) using hematoxylin and eosin stained slides under a brightfield microscope. Tumors were examined for quality of fixation and for areas of necrosis, inflammation or hemorrhage. The mitotic index (MI) was calculated as the total number of mitotic figures in 10, tumor-representative, 400× (Ocular FN: 22; Objective 40x/0.65) high-power fields (HPFs). For IHC, sections were dewaxed and subjected to antigen retrieval in Dako PT buffer high/low pH (Agilent Technologies Ltd) using a computer controlled antigen retrieval workstation (PT Link; Agilent Technologies Ltd) for 20 min at 98°C. Sections were then immunolabelled in an automated immunostainer (Link 48; Agilent Technologies Ltd), using primary antibodies against Melan A (mouse anti human Melan A, clone A103, Santa Cruz Biotechnology Ltd; 1:500), and PNL-2 (mouse anti human Melanoma marker PNL-2), Agilent Technologies Ltd (A4502); 1:400), as previously suggested.[38] This was followed by a 30 min incubation at RT with the secondary antibody and polymer peroxidase-based detection system (Anti Mouse/Rabbit Envision Flex+, Agilent Technologies Ltd). The reaction was visualized with diaminobenzidine (Agilent Technologies Ltd). Consecutive sections were incubated with murine subclass-matched unrelated monoclonal antibody, which served as a negative control. The positive reaction was represented by a distinct brown cytoplasmic reaction. A canine melanoma known to express Melan A and PNL-2 was used as

positive control. Only melanomas with more than 10% of positive cells with either Melan A or PNL-2 were included in the study (Supplemental Figure 1).[41]

Control population

FFPEs of normal skin and oral mucosa originating from post mortem cases were used as negative controls representative for oral mucosa. Cases with no oral pathology and with non-tumor related cause of death were included.

MiRNA extraction and real-time quantitative PCR

Upon observation with a brightfield microscope, a 2mm diameter area representative of neoplastic growth, with no areas of necrosis, hemorrhage or inflammation was selected and labelled on the histological slide (Supplemental Figure2a). The same area was then identified in the wax block and labelled (Supplemental Figure 2b). Using a disposable 2mm diameter biopsy punch with plunger (Miltex) the area of interest was sampled and extracted from the block (Supplemental Figure 2c); this tissue core specimen was subsequently placed in an Eppendorf tube (Supplemental Figure 2d) and used to extract small RNA.

Small RNAs were extracted from the core tissue specimens using miRNeasy Kit for FFPE blocks (Qiagen, catalog number 217504). The *Caenorhabditis elegans* miRNA cel-miR-39 (25 fmol final concentration) (Qiagen, catalog number 219610) was used as synthetic spike-in control due to the lack of sequence homology to canine miRNAs. The RNA extraction was then carried out according to the manufacturer's instruction. The reverse transcription was performed using the TaqMan MicroRNA Reverse Transcription Kit (Applied Biosystems, catalog number 4366596) using miRNA-specific stem-loop RT primers, according to the manufacturer's instructions. Reverse transcription reactions were performed in 15 µl volume reactions containing 1.5 µl 10X miRNA RT buffer, 1 µl MultiScribe reverse transcriptase (50 U/µl), 0.30 µl 100 mM dNTP mix, 0.19 µl RNase Inhibitor (20 U/µl), 6 µl of custom RT primer pool and 3.01 µl of nuclease-free water. The custom RT primer pool

was prepared combining 10 µl of each individual 5X RT primer to a final volume of 1000 µl; the final concentration of each primer in the RT primer pool was 0.05X each. Three µl of RNA were added to each RT reaction. Every RT reaction mixture was incubated on ice for 5 min, 16°C for 30 min, 42°C for 30 min and then 85°C for 5 min.

The qPCR experiments were designed following the MIQE guidelines. Small RNA TaqMan assays were performed according to manufacturer's instruction. The selection of miRNAs was based on previous publications in which these miRNAs were correlated to melanoma in dogs or humans. The selected primer/probe assays (Life Technologies) included cel-miR-39-3p (assay ID000200), hsa-miR-425-5p (assay ID001516), mmu-miR-134 (assay ID001186), hsa-miR-145 (assay ID002278), hsa-miR-146a (assay ID000468), hsa-miR-365 (assay ID001020) and hsa-miR-223-3p (assay ID002295).[30,39,2,22,51,36,26,35] Quantitative reactions were performed in duplicate in scaled-down (12 µl) reaction volumes using 6 µl TaqMan 2X Universal Master Mix II (Applied Biosystems, catalog number 4440044), 0.6 µl miRNA specific TaqMan Assay 20X and 1 µl of the RT product per reaction on Eco Real Time PCR detection System (Illumina). The standard cycling program was 50°C for 2 min, 95°C for 10 min and 40 cycles of 95°C for 15 sec and 60°C for 60 sec. Data were normalized relative to the expression of cel-miR-39. MiRNAs expression levels were presented in terms of fold change normalized to cel-miR-39 expression using the formula $2^{-\Delta\Delta Cq}$.[24] Predicted targets consisting of significant up- or down-regulated miRNAs were computationally retrieved from the TargetScan (http://www.targetscan.org/vert_71/) and miRWalk (http://mirwalk.umm.uni-heidelberg.de/) databases. The predicted targets of either up- or down-regulated miRNAs identified by both databases were examined using DAVID bioinformatic tool (https://david.ncifcrf.gov/), in order to perform functional annotation and biological pathway enrichment.

Statistical analysis

Statistical analysis was performed using XLStat (AddinSoft, Inc., NY, USA). Statistical significance was accepted at $P \leq 0.05$. Data were tested for normality and homogeneity of variance using the Kolmogorov-Smirnov test. As data were not normally distributed, non-parametric statistical tests were applied. Kruskal-Wallis test was used to assess differences in miRNA concentrations between malignant melanoma groups and control groups. *P* values were adjusted using Bonferroni correction. Linear regression was used to investigate any relationship between differentially expressed -miRNAs and age. Spearman's rho test was performed to evaluate possible correlations among miRNA expression levels, mitoses, melanophages and melanocytes rates. Principal component analysis was performed to evaluate single correlations among miRNAs.

Results

Study Population and Tumor Histology

The 9 oral and 10 cutaneous malignant melanoma were from dogs with a median age of 9 years (range 6-13), and predominantly of mixed breed (n=4), with Rottweiler (n=2), Cocker Spaniel (n=2) overrepresented among other breeds. Median mitotic index was 2.5 (range: 0.8 – 11.4).

miRNAs Expression

To characterize the differences between groups, principal components analysis (PCA) on control and malignant melanoma groups was performed (Figure 1). Data points with a higher correlation had a smaller degree of separation within the chart; a probable correlation was predicted if the factors were within 45° of each other. Healthy samples were separated from malignant melanoma groups in both skin (figure 1a) and oral (figure 1b) samples and were well correlated to each another. Cutaneous malignant melanoma samples were positively correlated; in oral malignant melanoma samples, miR365a and miR-145 were negatively correlated and no correlation was observed between miR-146a and miR-425.

The selected miRNAs were detected in all samples. Among these, miR-145-5p, miR-146a, miR-365 and miR-425-5p exhibited statistically significant differences among the malignant melanoma and control groups (Figure 2). Compared to the corresponding non-neoplastic tissue, miR-145 (figure 2a) was down-regulated in both cutaneous (P = 0.0076; ratio of cutaneous malignant melanoma/healthy skin = -5.7) and oral malignant melanoma (P < 0.0028; ratio of oral malignant melanoma /healthy oral mucosae=-7.6), miR-146a (figure 2b) and miR-425-5p (figure 2d) were up-regulated and miR-365 (figure 2c) was down-regulated in cutaneous malignant melanoma (miR-146a: P = 0.02, ratio of malignant melanoma/healthy skin= 9.6; miR-425-5p: P = 0.04, ratio of malignant melanoma/healthy skin= 4.9; miR-365: P = 0.0087, ratio of malignant melanoma/healthy= -5.9), while there were no differences between oral malignant melanoma and control groups for these miRNAs. The expression levels of miR-223-3p and miR-134 were not different in malignant melanoma compared to healthy skin (figure 2e and f). The levels of differentially expressed miRNAs were not affected by the age of the dog (linear regression, P > 0.05). To test the possible collinearity, Spearman correlation analysis of miRNAs was performed, suggesting that there was a positive correlation among miR-145, miR-146a, miR-365 and miR-425-5p relative concentration (data not shown). No correlation was observed between miRNAs and mitotic count.

miRNA target prediction and pathway enrichment

To investigate the relevance to tumor development, predicted targets of either significantly up- or down- regulated miRNAs were computationally identified by using TargetScan and miRWalk databases. The number of predicted targets shared by both databases included 602 for miR-145, 95 for miR-365, 103 for miR-146a and 98 for miR-425-5p. The mRNA enrichment was performed using the DAVID bioinformatic tool. The Gene Ontology analysis was carried out using DAVID at three different levels: molecular function, cellular component and biological process (Figure 3). Most Gene Ontology molecular function items mainly included genes involved in the regulation of

transcription and serine/threonine kinase activity for both up- and down-regulated miRNAs. The enriched Gene Ontology terms in cellular component converged on genes associated with the cytosol, nucleus and nucleoplasm for both up- and down-regulated miRNAs. Down-regulated miRNAs may modulate ruffle and focal adhesion, which are involved in cell migration, whereas up-regulated miRNAs may regulate activin responsive complex, which is activated by TGF-beta and acts primarily through SMADs. The biological process items focused on the modulation of protein binding and transcriptional activator activity for both sets of miRNAs. The down-regulated miRNAs influence genes involved in the SMAD binding, RNA polymerase and DNA binding activity; up-regulated miRNAs genes are involved in the regulation of transcription. The KEGG pathway analysis was separately performed on the targets of the two sets of miRNAs. The most significantly enriched pathways were RAS, Rap1 and TGF-beta signaling pathways for downregulated miRNAs and phosphatidylinositol signaling system, adherens junction and RAS signaling pathway for upregulated miRNAs (Figure 4).

Discussion

The role of miRNAs in canine malignant melanoma is only beginning to be defined. Using microarray and qPCR, Noguchi and colleagues[30] analyzed the expression pattern of miRNAs in oral canine malignant melanoma and observed that miR-520c-3p was up-regulated and that six other miRNAs (miR-126, miR-200a, miR-203, miR-205, miR-527b and miR-713) were down-regulated compared to healthy oral mucosa. Moreover, they demonstrated an association between the down-regulation of miR-203 and shorter survival times. A recent study by Starkey and colleagues[44] identified nine miRNAs able to discriminate between metastatic or non- metastatic canine uveal melanomas, therefore suggesting their potential in predicting biological behavior. The present study investigated the expression of six miRNAs in FFPE-samples of oral and cutaneous canine malignant melanoma,

and results suggest that specific miRNAs are differentially expressed in neoplastic versus normal tissue samples. Differentially expressed -miRNAs identified herein have previously been implicated in human melanoma and other neoplastic conditions, as molecular regulators of tumor development and progression; a similar mechanism of action is hypothesized from the result of our study. MiR-145 was down-regulated in both oral and cutaneous malignant melanoma, and so was miR-365 in cutaneous malignant melanoma. These were considered as potential onco-suppressor miRNAs in accordance to the knowledge from the human oncology literature. It has been demonstrated that miR-145 and miR-365 modulate tumor cell growth, invasion and metastasis by targeting *NRAS*[23] and *c-MYC,*[30,33] and *neuropilin1*,[2] respectively. The Gene Ontology and pathway analysis would suggest that miR-145 and miR-365 modulate cell migration and cell growth, influencing the RAS and RAP1 signaling pathways, among others.[3,23] Liu and co-workers[23] demonstrated that expression level of miR-145 is lower in melanoma tissues than those in the matched adjacent normal tissues; conversely, *NRAS* levels are higher. A previous study also demonstrated that miR-365 influences the development of melanoma by targeting *BCL2* and *Cyclin D1,* which are respectively involved in apoptosis and cell cycle progression.[53] We could speculate that the lack of regulatory miR-145 and miR-365 observed in oral and cutaneous malignant melanoma samples, may be involved in a different aggressive behavior, which can be influenced by other molecular regulators.

MiR-425 and miR-146a were over-expressed in samples of cutaneous malignant melanoma. The Gene Ontology and pathway analysis showed that these miRNAs may target genes associated with cell proliferation, cell-cell adherens junction, TGF-beta signaling pathway and protein ubiquitination, which can contribute to tumor development and progression. In human medicine, miR-425 over-expression is associated with cell migration and invasion by targeting *CYLD*[50] and cell proliferation in gastric cancer,[52] hepatocellular carcinoma[16] and esophageal squamous cell

carcinoma.[22] The function of miR-425 in melanoma is still debated; Chen and colleagues[12] demonstrated that the over-expression of miR-425/489 plays a pivotal role in the melanoma progression by activating the PI3K-Akt pathway. On contrary, Liu and co-workers[21] suggested that miR-425 inhibits cell proliferation and metastasis, and promotes apoptosis. The role of miR-146a has mainly been investigated in the context of immune response[47] while its role in human melanoma is still controversial. MiR-146a has been proposed as a negative regulator of immune response activation in melanoma by targeting *STAT1* and *IFN-gamma* in mice models, affecting melanoma migration, proliferation, and mitochondrial function as well as *PD-L1* levels.[25] A recent study reported that miR-146a directly targets *SMAD4*, promoting cell metastasis and invasion;[35] Forloni and colleagues[14] concluded that miR-146a plays a central role in the initiation and progression of melanoma by targeting *NUMB*, a suppressor of Notch signaling. Nonetheless, Raimo and colleagues[36] hypothesized that miR-146a has two synchronous but distinctive functions in human melanoma, the enhancement of tumor growth and the suppression of cell metastasis.

Brachelente and colleagues[10] characterized the transcriptome profiles of canine cutaneous melanocytoma and melanoma using a transcriptomic approach, identifying 60 differentially expressed -genes. The comparison between this list and the list of genes potentially modulated by differentially expressed -miRNAs identified in the present study, showed that four genes (*ADAM metallopeptidase with thrombospondin type 1 motif 2* (*ADAMTS2*), *Coiled-Coil Domain Containing 80* (*CCDC80*), *Lysyl Oxidase* (*LOX*) and *Cysteine Rich Secretory Protein LCCL Domain Containing 2* (*CRISPLD2*)) may be potentially modulated by miR-145 and miR-365, and one (*SH3 Domain GRB2 Like Endophilin Interacting Protein 1* (*SGIP1*)) by miR-146a and miR-425-5p. The RNA-seq results[10] showed that *ADAMTS2, CCDC80, LOX and CRISPLD2* are up-regulated in cutaneous malignant melanoma, while *SGIP1* is down-expressed; these results are consistent with the reduced or

increased expression of molecular modulators, such as miR-145 and miR-365 and miR-146a and 425-5p, respectively.

In conclusion, the present study suggests that miR-145, miR-365, miR-146a and miR-425 are abnormally expressed in cutaneous and oral malignant melanoma, potentially modulating pathways involved in cell proliferation. Further studies are needed in order to elucidate the real molecular targets of these miRNAs and to identify candidate targets for molecular therapies in the treatment of canine malignant melanoma

Conflict of Interest Statement

The authors declare no competing interests.

References

1. Babapoor S, Wu R, Kozubek J, Auidi D, Grant-Kels JM, Dadras SS. Identification of microRNAs associated with invasive and aggressive phenotype in cutaneous melanoma by next-generation sequencing. *Lab Invest*. 2017; 97:636–648.

2. Bai J, Zhang Z, Li X, Liu H. MicroRNA-365 inhibits growth, invasion and metastasis of malignant melanoma by targeting NRP1 expression. 2015; 15:599–608.

3. Banerjee R, Russo N, Liu M, Van Tubergen E, D'Silva NJ. Rap1 and its regulatory proteins: the tumor suppressor, oncogene, tumor suppressor gene axis in head and neck cancer. *Small GTPases*. 2012; 3:192–197.

4. Bartel DP. MicroRNAs: genomics, biogenesis, mechanism, and function. *Cell*. 2004; 116:281–297.

5. Barutello G, Rolih V, Arigoni M, et al. Strengths and Weaknesses of Pre-Clinical Models for Human Melanoma Treatment: Dawn of Dogs' Revolution for Immunotherapy. *Int J Mol Sci*. 2018; 19:799.

6. Bergman PJ. Veterinary Oncology Immunotherapies. *Vet Clin North Am Small Anim Pract*. 2018; 48:257–277.

7. Bolon B, Calderwood Mays MB, Hall BJ. Characteristics of canine melanomas and comparison of histology and DNA ploidy to their biologic behavior. *Vet Pathol*. 1990 Mar; 27:96–102.

8. Bongiovanni L, D'Andrea A, Porcellato I, et al. Canine cutaneous melanocytic tumours: significance of β-catenin and survivin immunohistochemical expression. *Vet Dermatol*. 2015; 26:270-e59.

9. Boston SE, Lu X, Culp WTN, et al. Efficacy of systemic adjuvant therapies administered to dogs after excision of oral malignant melanomas: 151 cases (2001-2012). *J Am Vet Med Assoc*. 2014; 245:401–407.

10. Brachelente C, Cappelli K, Capomaccio S, et al. Transcriptome Analysis of Canine Cutaneous Melanoma and Melanocytoma Reveals a Modulation of Genes Regulating Extracellular Matrix Metabolism and Cell Cycle. *Sci Rep*. 2017; 7:6386.

11. Bracken CP, Scott HS, Goodall GJ. A network-biology perspective of microRNA function and dysfunction in cancer. *Nat Rev Genet*. 2016; 17:719–732.

12. Chen X, Dong H, Liu S, et al. Long noncoding RNA MHENCR promotes melanoma progression via regulating miR-425/489-mediated PI3K-Akt pathway. *Am J Transl Res*. 2017; 9:90–102.

13. Fattore L, Costantini S, Malpicci D, et al. MicroRNAs in melanoma development and resistance to target therapy. *Oncotarget*. 2017; 8:22262–22278.

14. Forloni M, Dogra SK, Dong Y, et al. miR-146a promotes the initiation and progression of melanoma by activating Notch signaling. *Elife*. 2014; 3:e01460.

15. Gillard M, Cadieu E, De Brito C, et al. Naturally occurring melanomas in dogs as models for

non-UV pathways of human melanomas. *Pigment Cell Melanoma Res*. 2014; 27:90–102.

16. He B, Li T, Guan L, et al. CTNNA3 is a tumor suppressor in hepatocellular carcinomas and is inhibited by miR-425. *Oncotarget*. 2016; 7:8078–8089.

17. Hernandez B, Adissu HA, Wei B-R, Michael HT, Merlino G, Simpson RM. Naturally Occurring Canine Melanoma as a Predictive Comparative Oncology Model for Human Mucosal and Other Triple Wild-Type Melanomas. *Int J Mol Sci*. 2018; 19:394.

18. Kawabe M, Mori T, Ito Y, et al. Outcomes of dogs undergoing radiotherapy for treatment of oral malignant melanoma: 111 cases (2006-2012). *J Am Vet Med Assoc*. 2015 Nov; 247:1146–1153.

19. Latchana N, Ganju A, Howard JH, Carson WE. MicroRNA dysregulation in melanoma. *Surg Oncol*. 2016; 25:184–189.

20. Lindblad-Toh K, Wade CM, Mikkelsen TS, et al. Genome sequence, comparative analysis and haplotype structure of the domestic dog. *Nature*. 2005; 438:803–819.

21. Liu L, Zhao Z, Zhou W, Fan X, Zhan Q, Song Y. Enhanced Expression of miR-425 Promotes Esophageal Squamous Cell Carcinoma Tumorigenesis by Targeting SMAD2. *J Genet Genomics*. 2015; 42:601–611.

22. Liu P, Hu Y, Ma L, Du M, Xia L, Hu Z. miR-425 inhibits melanoma metastasis through repression of PI3K-Akt pathway by targeting IGF-1. *Biomed Pharmacother*. 2015; 75:51–57.

23. Liu S, Gao G, Yan D, et al. Effects of miR-145-5p through NRAS on the cell proliferation, apoptosis, migration, and invasion in melanoma by inhibiting MAPK and PI3K/AKT pathways. *Cancer Med*. 2017; 6:819–833.

24. Livak KJ, Schmittgen TD. Analysis of relative gene expression data using real-time quantitative PCR and the 2(-Delta Delta C(T)) Method. *Methods*. 2001;c25:402–408.

25. Mastroianni J, Stickel N, Andrlova H, et al. miR-146a Controls Immune Response in the Melanoma Microenvironment. *Cancer Res*. 2019; 79:183–195.

26. Mathsyaraja H, Thies K, Taffany DA, et al. CSF1-ETS2-induced microRNA in myeloid cells promote metastatic tumor growth. *Oncogene*. 2015; 34:3651–3661.

27. Mocellin S, Pasquali S, Pilati P. Oncomirs: from tumor biology to molecularly targeted anticancer strategies. *Mini Rev Med Chem*. 2009; 9:70–80.

28. Nishiya A, Massoco C, Felizzola C, et al. Comparative Aspects of Canine Melanoma. *Vet Sci*. 2016; 3:7.

29. Noguchi S, Mori T, Hoshino Y, Yamada N, Maruo K, Akao Y. MicroRNAs as tumour suppressors in canine and human melanoma cells and as a prognostic factor in canine melanomas. *Vet Comp Oncol*. 2013; 11:113–123.

30. Noguchi S, Mori T, Hoshino Y, et al. Comparative study of anti-oncogenic microRNA-145 in canine and human malignant melanoma. *J Vet Med Sci*. 2012; 74:1–8.

31. Noguchi S, Mori T, Nakagawa T, Itamoto K, Haraguchi T, Mizuno T. DNA methylation

contributes toward silencing of antioncogenic microRNA-203 in human and canine melanoma cells. *Melanoma Res*. 2015; 25:390–398.

32. Piras LA, Riccardo F, Iussich S, et al. Prolongation of survival of dogs with oral malignant melanoma treated by *en bloc* surgical resection and adjuvant CSPG4-antigen electrovaccination. *Vet Comp Oncol*. 2017; 15:996–1013.

33. Poorman K, Borst L, Moroff S, et al. Comparative cytogenetic characterization of primary canine melanocytic lesions using array CGH and fluorescence in situ hybridization. *Chromosome Res*. 2015; 23:171–186.

34. Proulx DR, Ruslander DM, Dodge RK, et al. A retrospective analysis of 140 dogs with oral melanoma treated with external beam radiation. *Vet Radiol Ultrasound.* 2003; 44:352–359.

35. Pu W, Shang Y, Shao Q, Yuan X. miR-146a promotes cell migration and invasion in melanoma by directly targeting SMAD4. *Oncol Lett*. 2018; 15:7111–7117.

36. Raimo M, Orso F, Grassi E, et al. miR-146a Exerts Differential Effects on Melanoma Growth and Metastatization. *Mol Cancer Res*. 2016; 14:548–562.

37. Ramos-Vara JA, Beissenherz ME, Miller MA, et al. Retrospective study of 338 canine oral melanomas with clinical, histologic, and immunohistochemical review of 129 cases. *Vet Pathol*. 2000; 37:597–608.

38. Ramos-Vara JA. Principles and Methods of Immunohistochemistry. In: Vol. 691, *Methods in molecular biology (Clifton, N.J.)*. 2011:83–96.

39. Sand M, Skrygan M, Sand D, et al. Comparative microarray analysis of microRNA expression profiles in primary cutaneous malignant melanoma, cutaneous malignant melanoma metastases, and benign melanocytic nevi. *Cell Tissue Res*. 2013; 351:85–98.

40. Sarowitz BN, Davis GJ, Kim S. Outcome and prognostic factors following curative-intent surgery for oral tumours in dogs: 234 cases (2004 to 2014). *J Small Anim Pract*. 2017; 58:146–153.

41. Smedley RC, Spangler WL, Esplin DG, et al. Prognostic markers for canine melanocytic neoplasms: a comparative review of the literature and goals for future investigation. *Vet Pathol*. 2011; 48:54–72.

42. Smith SH, Goldschmidt MH, McManus PM. A comparative review of melanocytic neoplasms. *Vet Pathol*. 2002; 39:651–678.

43. Spangler WL, Kass PH. The histologic and epidemiologic bases for prognostic considerations in canine melanocytic neoplasia. *Vet Pathol*. 2006; 43:136–149.

44. Starkey MP, Compston-Garnett L, Malho P, Dunn K, Dubielzig R. Metastasis-associated microRNA expression in canine uveal melanoma. *Vet Comp Oncol*. 2018; 16:81–89.

45. Suckow MA. Cancer vaccines: Harnessing the potential of anti-tumor immunity. *Vet J*. 2013; 198:28–33.

46. Sun V, Zhou WB, Majid S, Kashani-Sabet M, Dar AA. MicroRNA-mediated regulation of melanoma. *Br J Dermatol*. 2014; 171:234–241.

47. Testa U, Pelosi E, Castelli G, Labbaye C. miR-146 and miR-155: Two Key Modulators of Immune Response and Tumor Development. *Non-coding RNA*. 2017; 3:22.

48. Tuohy JL, Selmic LE, Worley DR, Ehrhart NP, Withrow SJ. Outcome following curative-intent surgery for oral melanoma in dogs: 70 cases (1998-2011). *J Am Vet Med Assoc*. 2014; 245:1266–1273.

49. Villamil JA, Henry CJ, Bryan JN, et al. Identification of the most common cutaneous neoplasms in dogs and evaluation of breed and age distributions for selected neoplasms. *J Am Vet Med Assoc*. 2011; 239:960–965.

50. Yan Y-F, Gong F-M, Wang B-S, Zheng W. MiR-425-5p promotes tumor progression via modulation of CYLD in gastric cancer. *Eur Rev Med Pharmacol Sci*. 2017; 21:2130–2136.

51. Yuan S-M, Li H, Yang M, et al. High intensity focused ultrasound enhances anti-tumor immunity by inhibiting the negative regulatory effect of miR-134 on CD86 in a murine melanoma model. *Oncotarget*. 2015; 6:37626–37637.

52. Zhang Z, Wen M, Guo J, et al. Clinical value of miR-425-5p detection and its association with cell proliferation and apoptosis of gastric cancer. *Pathol Res Pract*. 2017; 213:929–937.

53. Zhu Y, Wen X, Zhao P. MicroRNA-365 Inhibits Cell Growth and Promotes Apoptosis in Melanoma by Targeting BCL2 and Cyclin D1 (CCND1). *Med Sci Monit*. 2018; 24:3679–3692.

Figures:

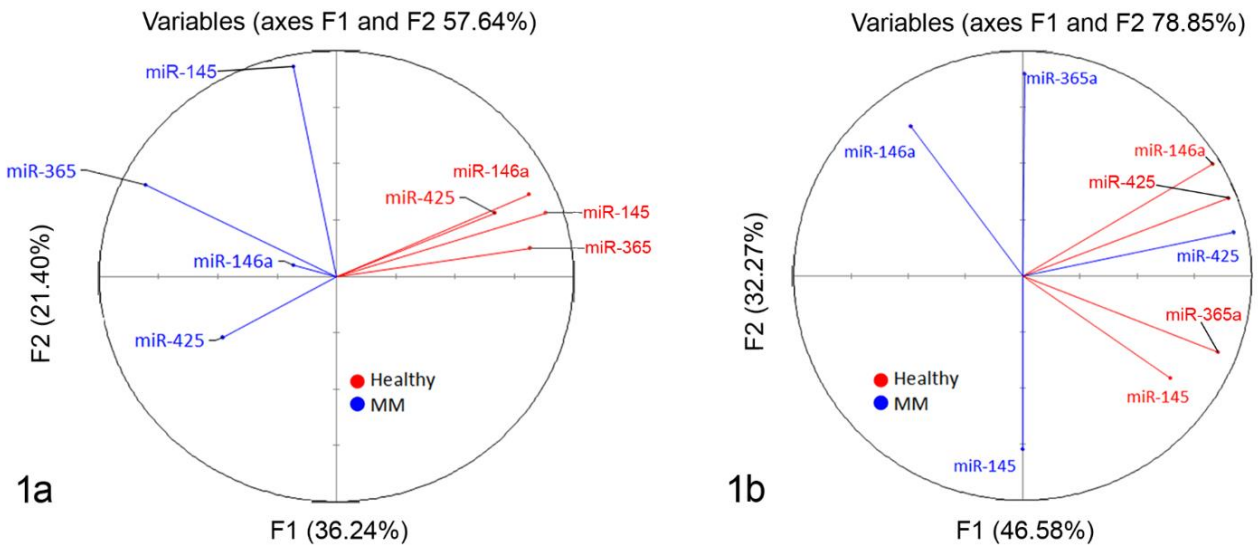

Figure 1. Principal components analysis of miRNA expression in canine malignant melanoma. The correlation circle shows the correlations between the miRNAs in (a) healthy skin and cutaneous canine malignant melanoma (MM) samples, and (b) healthy oral mucosa and oral canine malignant melanoma samples. Variables with a higher correlation have a smaller degree of separation within the chart; a probable correlation can be predicted if the factors are within 45°. If two variables are far from the center and close to each other, they are significantly positively correlated; orthogonal variables are not correlated; and variables on the opposite side of the center line are negatively correlated.

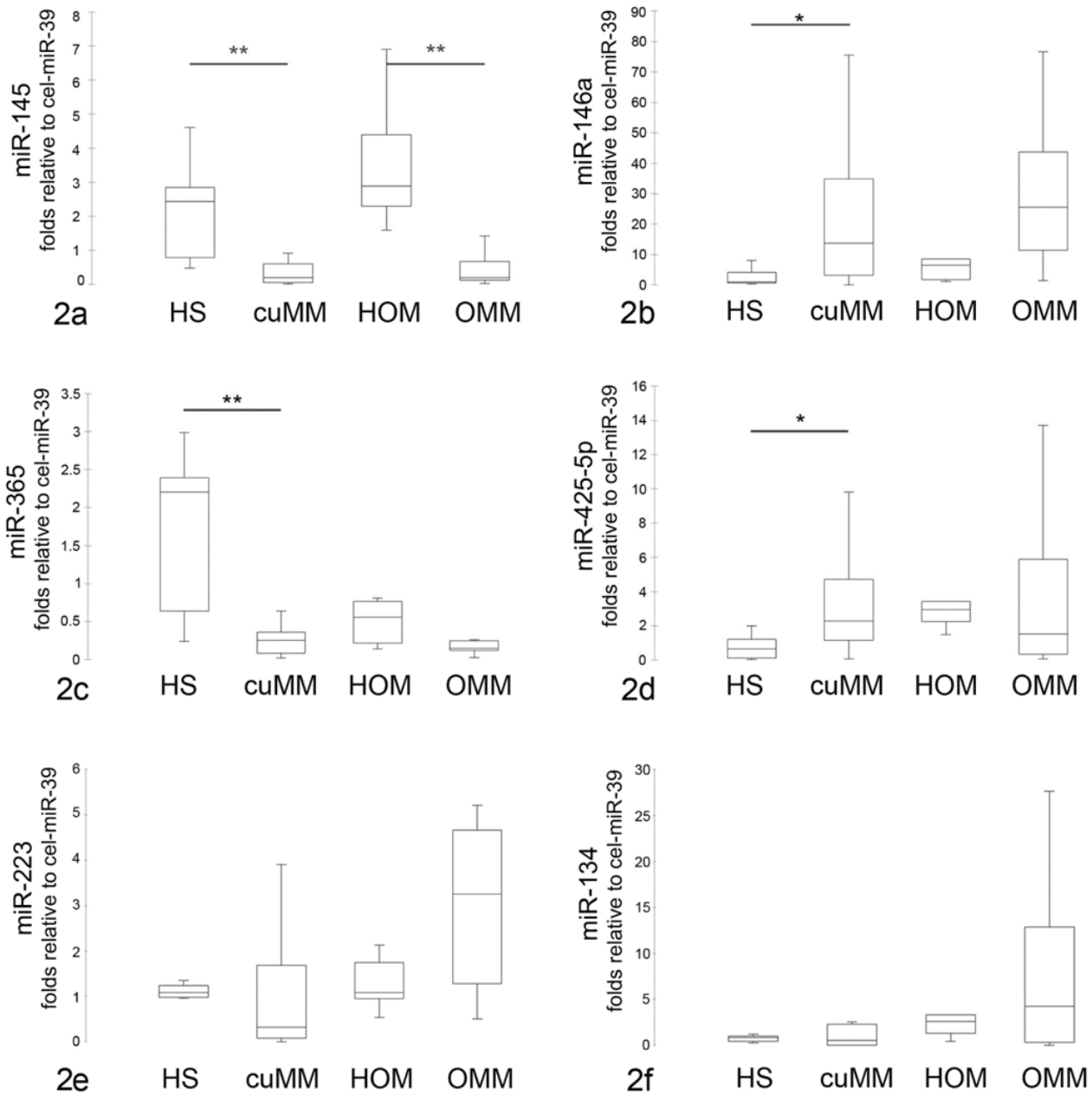

Figure 2. Expression of miRNAs in canine malignant melanoma. qPCR results were normalized using cel-miR-39 as reference miRNA and the formula $2^{-\Delta\Delta Cq}$. Expression levels of miR-145 (a), miR-146a-5p (b), miR-365 (c), miR-425-5p (d), miR-223 (e) and miR-134 (f) in healthy skin (HS), cutaneous malignant melanoma (cuMM); healthy oral mucosa (HOM), and oral malignant melanoma (OMM). The boxes outline the quartiles, the horizontal line shows the median, and the whiskers show the range. *= $P < 0.05$, **= $P < 0.01$.

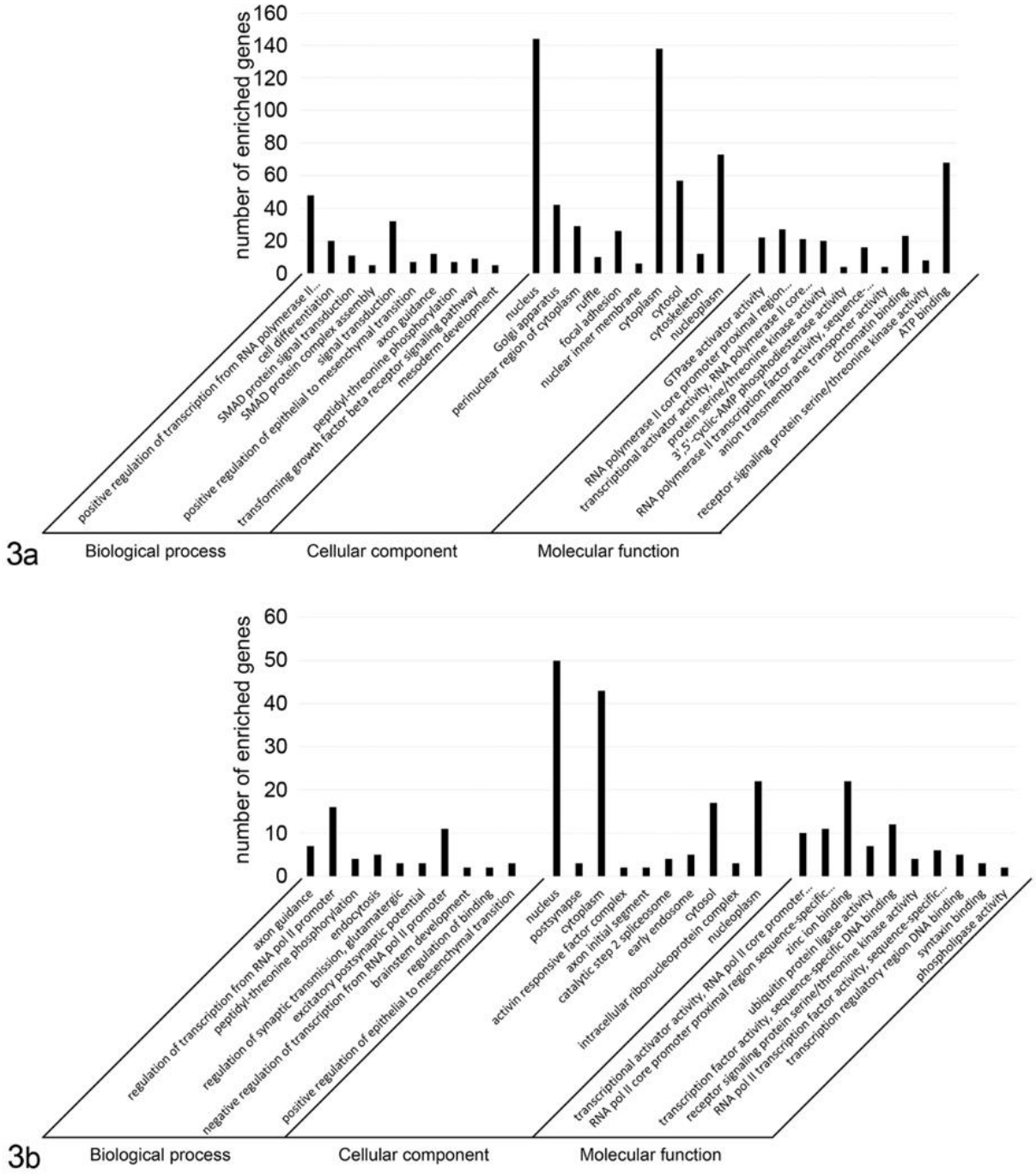

Figure 3. Gene Ontology annotation of genes predicted to be regulated by miRNAs that were found to have significantly lower or higher expression in canine malignant melanoma samples compared to the corresponding healthy control tissues. The targeted genes were annotated by DAVID tool at three levels, including biological process, cellular component and molecular function. (a) Gene

Ontology annotation of genes regulated by down-regulated miR-145 and miR-365. (b) Gene Ontology annotation of genes regulated by up-regulated miR-146a-5p and miR-425-5p.

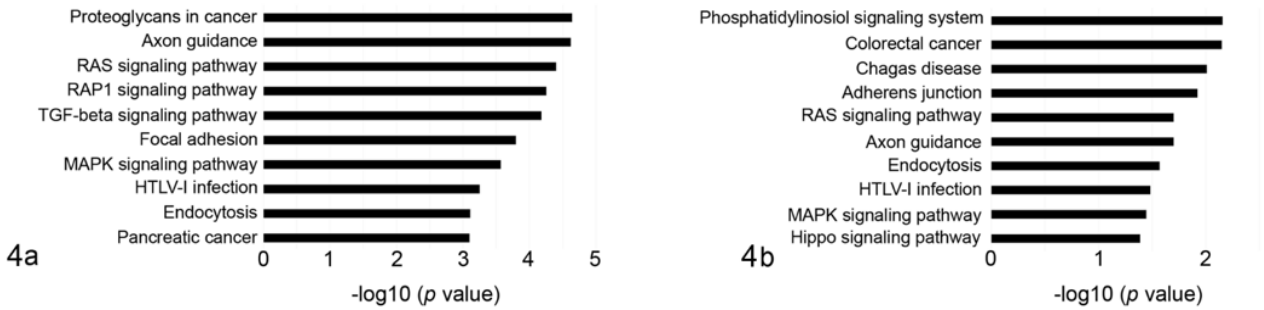

Figure 4. Pathway enrichment for miRNAs that were found to have significantly lower or higher expression in canine malignant melanoma samples compared to the corresponding healthy control tissues. Genes were retrieved and enriched in KEGG pathway with DAVID tools. (a) Pathway enrichment for genes targeted by down-regulated miR-145 and miR-365. (b) Pathway enrichment for genes targeted by up-regulated miR-146a-5p and miR-425-5p. The statistical significance level shown is the negative of the logarithm (base 10) of the P value.

Supplementary materials:

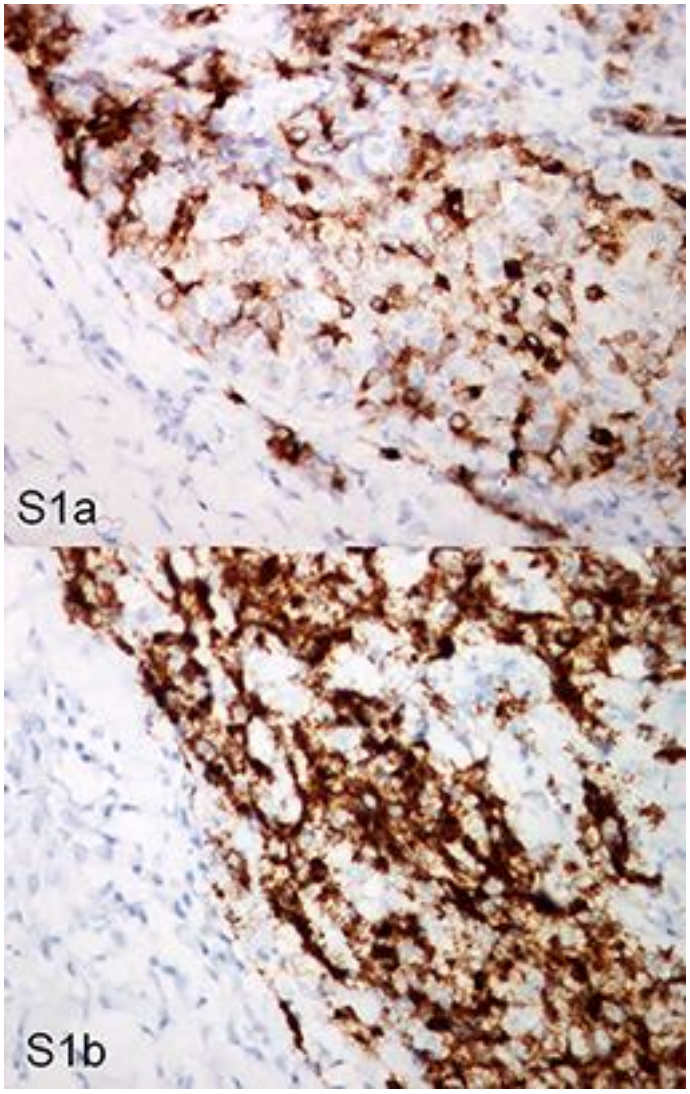

Supplemental Figure S1. Melanoma, oral mucosa, dog. Cytoplasmic granular multifocal immunolabeling expression of Melan-A (a) and PNL-2 (b) in neoplastic cells.

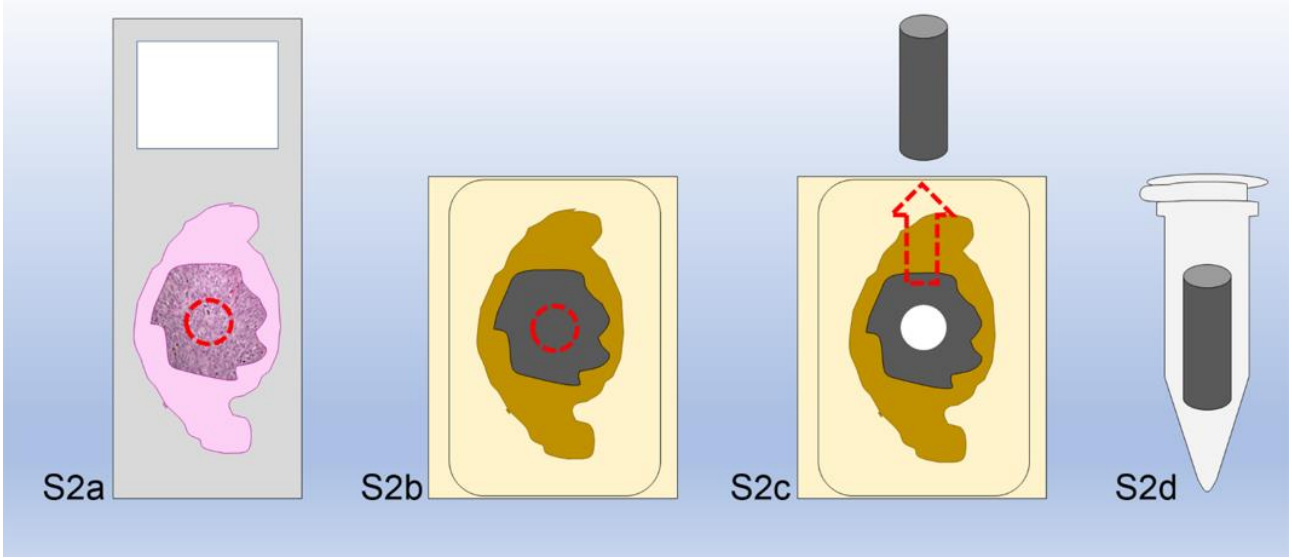

Supplemental Figure S2. Tissue sampling from formalin-fixed-paraffin-embedded samples (FFPEs) schematic drawing. The area of interest (red dotted circle) is identified under the microscope (a) and in the corresponding area of the FFPE block (b). A disposable biopsy punch is used to sample the area (c) subsequently submitted for microRNA extraction (d).

Case number	Location	Age	Breed	Site
1	oral	12	Poodle	gingiva
2	oral	14	Cocker Spaniel	gingiva
3	oral	12	Teckel	gingiva
4	skin	7	Rotweiler	axila
5	oral	13	Teckel	lip
6	oral	13	Cocker Spaniel	gingiva
7	skin	7	Mixed Breed	thorax
8	oral	NG	Mixed Breed	palate
9	skin	8	Boxer	scrotum
10	skin	11	Giant Schnautzer	scrotum
11	skin	5	West Highland White Terrier	digit
12	oral	9	Kerry Blue	gingiva
13	oral	NG	Golden Retriever	gingiva
14	skin	13	Rotweiler	digit
15	skin	9	Mixed Breed	abdomen
16	oral	8	British Bull dog	palate
17	skin	9	Scottish Terrier	limb
18	skin	7	Mixed Breed	face
19	skin	6	Hound	ear
Control 1	skin	8	Mixed Breed	abdomen
Control 2	skin	10	Mixed Breed	face
Control 3	skin	4	Boxer	neck
Control 4	skin	6	Scottish Terrier	digit
Control 5	skin	3	Golden Retriever	forelimb
Control 6	skin	NG	Mixed Breed	abdomen
Control 7	skin	7	Golden Retriever	thorax
Control 8	oral mucosa	7	Mixed Breed	oral mucosa
Control 9	oral mucosa	10	boxer	oral mucosa
Control 10	oral mucosa	5	Mixed Breed	oral mucosa
Control 11	oral mucosa	8	Weimaraner	oral mucosa
Control 12	oral mucosa	4	Mixed Breed	oral mucosa
NG=not given				

Supplemental Table 1. Clinical data of tumor affected and control dogs.

Chapter 7. Discussion and conclusion

This thesis addressed for the first time the molecular modifications of canine mast cell tumor using different omics approaches. Moreover, a targeted approach was applied to quantify miRNAs in oral and cutaneous malignant melanoma of dogs.

Specifically, the miRNomic and the microbiomic profiles were assessed in canine mast cell tumor and the deregulation of specifics target miRNAs was evaluated in canine malignant melanoma. In addition, a protocol for plasmatic exosome purification from MCT affected dogs reliable for further proteomic analysis, that is still ongoing due to the pandemic situation, was set up.

Skin tumors are very common in dogs. Mast cell tumor, among all skin associated neoplasms, is one of the most frequent with a prevalence of 16.8% (Hauck, 2012). Since canine MCT is not a model in human oncology, the pathogenesis and etiology are poorly investigated and described. MCT adopts variable behavior making the prognosis uncertain (Blackwood et al., 2012). Although some studies have recently investigated the deregulation of miRNAs using a targeted approach (Fenger et al., 2014; Heishima et al., 2017) and the transcriptomic profile (Pulz et al., 2019) associated with the neoplasm, no data were available on miRNome of MCT. To cover this gap, we adopted a multistep approach, using miRNomics as a first step to identifying differentially expressed miRNAs in MCT primary tumor mass, then validated them by a quantitative PCR (qPCR) to identify reliable candidate biomarkers in both primary masses and in a non-invasive matrix, the saliva.

The validation step revealed that five miRNAs -miR-21, miR-379, miR-885, miR-338 and miR-92a- were dysregulated in the primary tumor masses. The diagnostic potential of this miRNA panel was assessed testing their ability in discriminating the metastatic (draining lymph node involved) from the non-metastatic tumors. The data demonstrated that miR-21, miR-379, and miR-885 had a higher diagnostic potential since they can discriminate metastasizing from non-metastasizing tumors (AUC= 0.8923) with a sensitivity and a specificity of 92.3% and 80.0%, respectively. The results

suggest the potential role as biomarkers of the panel to support the clinical decision-making process. It has been previously reported that miR-21, recognized as oncomiRNA, was up-regulated in several cancers (Javanmardi et al., 2017); the upregulation of miR-379 exerts and onco-suppressor activity targeting pathways involved in cells proliferation, migration, and invasion (Zhao and Chu, 2018). The role of down-regulated miRNAs is still debated. MiR-92a (cluster miR-17-92) and miR-338 are dysregulated in different cancers playing a dual role as onco-miRNA (Long et al., 2018; Li et al., 2019) or tumor-suppressor miRNA (Ottman et al., 2016; Wang and Qin, 2018); miR-885 acts as tumor suppressor miRNA (Zhang et al., 2016).

The identification and quantification of the same three miRNAs in the saliva of MC- affected dogs, highlighted that two of them, miR-21 and miR-885, were dysregulated. These miRNAs can discriminate dogs affected by MCT from the healthy ones. Moreover, miR-885 showed a good diagnostic potential in recognizing the lymph node involvement, proving its potential as a reliable salivary biomarker. The gene ontology analysis suggested that dysregulated DE-miRNAs may be involved in tumor progression and metastasis, by regulating pathways involved in tumor growth, cell proliferation, and survival.

The tumors can interfere also with the host-microbial population. The bacterial population inhabiting a specific body district interacts with the host cells and the immune system, i.e by producing specific metabolites (Xavier et al., 2020b). The involvement and the changes correlated with the microbiota have been studied in some human tumors, including gastric and intestinal cancers (Plummer et al., 2016; Wong and Yu, 2019), pancreatic cancer (Zhang et al., 2020), lung cancer (Ramírez-Labrada et al., 2020) and skin cancer (Egert and Simmering, 2016; Mrázek et al., 2019). Studies on microbiota in multicentric lymphoma (Gavazza et al., 2018) and colorectal epithelial tumor (Herstad et al., 2018) have been carried out, but this field is moving its first steps in veterinary oncology. To partially cover this gap, the skin and dermal microbiota associated with

canine MCT were assessed to identify any changes in the bacterial population. First of all, a reduction of taxa was observed on the tumor skin surface with an increase of the Firmicutes phylum and *Corynebacteriaceae* family when compared to the healthy contralateral part. These differences in microbiota population are reflected in beta diversity, which takes into account the dissimilarities between the samples, as shifting from the healthy to the tumor skin surface microbiota. Secondly, a microbiota population was found also in the tumor dermis, which presented a reduction of taxa compared with the overlying skin surface, reflecting differences also in beta diversity.

The core microbiota of the tumor and healthy skin surface and dermis revealed that the healthy skin microbiota were composed of more bacterial types (27 ASVs) compared to the tumor skin (12 ASVs) and dermis (16 ASVs). This study demonstrated that the presence of the tumor induces changes in the microbiota composition of skin and dermis due to the presence of mast cells and other immune cells (Valent et al., 2001; Kovalszki and Weller, 2014; Mezouar et al., 2018). A reduction of taxa is usually linked with an unhealthy status (Sanford and Gallo, 2013; Zeeuwen et al., 2013). Therefore, our data may suggest that there is a relationship between the skin microbiota and the presence of the tumor and that its characterization may increase the knowledge about tumor behavior and development. The changes in microbial population over the tumor site, highlight as an alteration in the host organism trigger changes to the associated bacterial community. Further analysis involving more animals is required to confirm the data on skin microbiota and for further investigate the microbiota of the dermis. As future perspective, study the influence that these bacteria can have against the immunity cells could be a starting point to better understand the connection between the host and the residing microbes.

A new source of biomarkers is exosomes (Vasconcelos et al., 2019). Exosomes which are present in different body fluids carrying a precious cargo suitable for cancer monitoring and characterization (Caby et al., 2005; Admyre et al., 2007; Gonzales et al., 2010; Palanisamy et al., 2010). In this thesis,

a feasible protocol for exosome purification from the plasma of dogs suitable for proteomic downstream analysis was set up. Using the SEC purification approach, which depletes plasmatic proteins, an exosome population with the right size range (mean= 107.4 nm), good vesicles (mean= 2.92E+10 particle/ml) and protein (mean= 381.6 µg/ml) concertation and with a good degree of purity was isolated. To profile exosome proteins and identify cancer-associated proteins, proteomic analysis, which we would have done in spring 2020, is still running.

The dysregulation of miRNAs - miR-145, miR-146a, miR-365 and miR-425-5p- in canine cutaneous and oral malignant melanoma, which ranked in the top ten of the most common skin tumors in dogs (Hauck, 2012), was investigated as well. The results suggested that miR-145 and miR-365 were down-regulated and miR-146a and miR-425-5p were up-regulated in cutaneous malignant melanoma comparing to the healthy skin, while miR-145 was down-regulated in oral malignant melanoma compared to the healthy oral mucosa. Both miR-145 and miR-365 have a potential role as onco-suppressors modulating cell growth and invasion in canine cutaneous and oral melanoma modulating tumor invasion, metastasis and cell proliferation by targeting *c-MYC* (Noguchi et al., 2012; Poorman et al., 2015), neuropilin (Bai et al., 2015; Babapoor et al., 2017) and *NRAS* (Liu et al., 2017). Studies in human melanoma demonstrated the involvement of miR-145 (Liu et al., 2017) and miR-365 (Zhu et al., 2018) in the tumor progression, targeting *NRAS*, *BCL2,* and *Cyclin D1* genes.
The up-regulation of miR-146 and miR-425 in cutaneous melanoma may exert as tumor promoters, but their roles are still debated. MiR-146a has been described in different studies and its role includes the negative regulation of immune response (Mastroianni et al., 2019), the promotion of cell metastasis and invasion (Pu et al., 2018), and the enhancement of tumor progression (Forloni et al., 2014). The role of miR-146a has been defined as dual, enhancing tumor growth and suppressing cell metastasis (Raimo et al., 2016). MiR-425 can activate the *PI3K-Akt* pathway, acting as an onco-miRNA (Chen et al., 2017), or promote apoptosis and inhibit cell proliferation and

metastasis as tumor-suppressor (Liu et al., 2015). Intersecting our results with the transcriptomic profile of canine cutaneous melanoma and malanocytoma (Brachelente et al., 2017), four genes - *ADAM metallopeptidase with thrombospondin type 1 motif 2* [*ADAMTS2*], *coiled-coil domain containing 80* [*CCDC80*], *lysyl oxidase* [*LOX*], and *cysteine rich secretory protein LCCL domain containing 2* [*CRISPLD2*])- are potentially modulated by miR-145 and miR-365.

In conclusion, the results suggest that miR-145, miR-365, miR-146 and miR-425 are modulated in canine malignant cutaneous and oral melanoma compared to the healthy tissues and the gene ontology suggests that these miRNAs are involved in tumor progression modulating pathways correlated with cell proliferation.

This thesis will hopefully provide a step forward in the knowledge of the molecular alteration associated with the onset of canine mast cell tumors and malignant melanoma. The findings highlight how a neoplastic proliferation can induce changes in miRNomic profile and also affect the host-microbiota population. Additionally, these alterations can be monitored in different and less-invasive and repeatable over time biological matrices. MiRNAs deregulation in the tumor microenvironment and other biological fluids is a starting point to better understand the tumorigenic strategies, as they are directly linked with the transcripts regulation. This point opens the way to the identification of possible target mRNAs which could be crucial kay points in tumor progression and therefore potential targets for new therapeutic approaches.

In conclusion, the results obtained allow to define the molecular changes that occur in canine mast cell tumor. The identification of specific tumor-associated miRNAs in tumor tissue and saliva will hopefully improve the tumor characterization, and offer a more personalized diagnosis and therapy. On the other hand, the characterization of the microbiota that inhabited the tumor site could increase the knowledge about the connection existing between host immunity and bacterial and to

better understand the tumor behavior. To conclude, the characterization of the exosome proteome will provide information about the tumor communication and dissemination strategies.

Bibliography

Abdallah, F., Mijouin, L., and Pichon, C. (2017). Skin Immune Landscape: Inside and Outside the Organism. *Mediators Inflamm.* 2017:5095293. doi: 10.1155/2017/5095293

Admyre, C., Johansson, S. M., Qazi, K. R., Filén, J.-J., Lahesmaa, R., Norman, M., et al. (2007). Exosomes with Immune Modulatory Features Are Present in Human Breast Milk. *J. Immunol.* 179, 1969–1978. doi:10.4049/jimmunol.179.3.1969.

Asada, H., Tomiyasu, H., Uchikai, T., Ishihara, G., Goto-Koshino, Y., Ohno, K., et al. (2019). Comprehensive analysis of miRNA and protein profiles within exosomes derived from canine lymphoid tumour cell lines. *PLoS One* 14, e0208567. doi:10.1371/journal.pone.0208567.

Atherton, M. J., Morris, J. S., McDermott, M. R., and Lichty, B. D. (2016). Cancer immunology and canine malignant melanoma: A comparative review. *Vet. Immunol. Immunopathol.* 169, 15–26. doi:10.1016/j.vetimm.2015.11.003.

Babapoor, S., Wu, R., Kozubek, J., Auidi, D., Grant-Kels, J. M., and Dadras, S. S. (2017). Identification of microRNAs associated with invasive and aggressive phenotype in cutaneous melanoma by next-generation sequencing. *Lab. Investig.* 97, 636–648. doi:10.1038/labinvest.2017.5.

Bachem, A., Makhlouf, C., Binger, K. J., de Souza, D. P., Tull, D., Hochheiser, K., et al. (2019). Microbiota-Derived Short-Chain Fatty Acids Promote the Memory Potential of Antigen-Activated CD8+ T Cells. *Immunity* 51, 285-297.e5. doi:10.1016/j.immuni.2019.06.002.

Bai, J., Zhang, Z., Li, X., and Liu, H. (2015). MicroRNA-365 inhibits growth, invasion and metastasis of malignant melanoma by targeting NRP1 expression. *Cancer Biomarkers* 15, 599–608. doi:10.3233/CBM-150500.

Baranyai, T., Herczeg, K., Onódi, Z., Voszka, I., Módos, K., Marton, N., et al. (2015). Isolation of

exosomes from blood plasma: Qualitative and quantitative comparison of ultracentrifugation and size exclusion chromatography methods. *PLoS One* 10, e0145686. doi:10.1371/journal.pone.0145686.

Bartel, D. P. (2004). MicroRNAs: Genomics, Biogenesis, Mechanism, and Function. *Cell* 116, 281–297. doi:10.1016/S0092-8674(04)00045-5.

Bergman, P. J. (2007). Canine Oral Melanoma. *Clin. Tech. Small Anim. Pract.* 22, 55–60. doi:10.1053/j.ctsap.2007.03.004.

Blacklock, K. B., Birand, Z., Biasoli, D., Fineberg, E., Murphy, S., Flack, D., et al. (2018). Identification of molecular genetic contributants to canine cutaneous mast cell tumour metastasis by global gene expression analysis. *PLoS One* 13, e0208026. doi:10.1371/journal.pone.0208026.

Blackwood, L., Murphy, S., Buracco, P., De Vos, J. P., De Fornel-Thibaud, P., Hirschberger, J., et al. (2012). European consensus document on mast cell tumours in dogs and cats. *Vet. Comp. Oncol.* 10, e1–e29. doi:10.1111/j.1476-5829.2012.00341.x.

Böing, A. N., van der Pol, E., Grootemaat, A. E., Coumans, F. A. W., Sturk, A., and Nieuwland, R. (2014). Single-step isolation of extracellular vesicles by size-exclusion chromatography. *J. Extracell. Vesicles* 3. doi:10.3402/jev.v3.23430.

Bonfanti, U., Bertazzolo, W., Gracis, M., Roccabianca, P., Romanelli, G., Palermo, G., et al. (2015). Diagnostic value of cytological analysis of tumours and tumour-like lesions of the oral cavity in dogs and cats: A prospective study on 114 cases. *Vet. J.* 205, 322–327. doi:10.1016/j.tvjl.2014.10.022.

Boria, P. A., Murry, D. J., Bennett, P. F., Glickman, N. W., Snyder, P. W., Merkel, B. L., et al. (2004). Evaluation of cisplatin combined with piroxicam for the treatment of oral malignant

melanoma and oral squamous cell carcinoma in dogs. *J. Am. Vet. Med. Assoc.* 224, 388–394. doi:10.2460/javma.2004.224.388.

Boukouris, S., and Mathivanan, S. (2015). Exosomes in bodily fluids are a highly stable resource of disease biomarkers. *Proteomics - Clin. Appl.* 9, 358–367. doi:10.1002/prca.201400114.

Bowlt Blacklock, K. L., Birand, Z., Selmic, L. E., Nelissen, P., Murphy, S., Blackwood, L., et al. (2019). Genome-wide analysis of canine oral malignant melanoma metastasis-associated gene expression. *Sci. Rep.* 9, 6511. doi:10.1038/s41598-019-42839-x.

Brachelente, C., Cappelli, K., Capomaccio, S., Porcellato, I., Silvestri, S., Bongiovanni, L., et al. (2017). Transcriptome Analysis of Canine Cutaneous Melanoma and Melanocytoma Reveals a Modulation of Genes Regulating Extracellular Matrix Metabolism and Cell Cycle. *Sci. Rep.* 7, 6386. doi:10.1038/s41598-017-06281-1.

Bradley, C. W., Morris, D. O., Rankin, S. C., Cain, C. L., Misic, A. M., Houser, T., et al. (2016). Longitudinal Evaluation of the Skin Microbiome and Association with Microenvironment and Treatment in Canine Atopic Dermatitis. *J. Invest. Dermatol.* 136, 1182–1190. doi:10.1016/j.jid.2016.01.023.

Brady, J. V., Troyer, R. M., Ramsey, S. A., Leeper, H., Yang, L., Maier, C. S., et al. (2018). A Preliminary Proteomic Investigation of Circulating Exosomes and Discovery of Biomarkers Associated with the Progression of Osteosarcoma in a Clinical Model of Spontaneous Disease. *Transl. Oncol.* 11, 1137–1146. doi:10.1016/j.tranon.2018.07.004.

Bulkowska, M., Rybicka, A., Senses, K. M., Ulewicz, K., Witt, K., Szymanska, J., et al. (2017). MicroRNA expression patterns in canine mammary cancer show significant differences between metastatic and non-metastatic tumours. *BMC Cancer* 17, 728. doi:10.1186/s12885-017-3751-1.

Bullman, S., Pedamallu, C. S., Sicinska, E., Clancy, T. E., Zhang, X., Cai, D., et al. (2017). Analysis of Fusobacterium persistence and antibiotic response in colorectal cancer. *Science* 358, 1443–1448. doi:10.1126/science.aal5240.

Caby, M.-P., Lankar, D., Vincendeau-Scherrer, C., Raposo, G., and Bonnerot, C. (2005). Exosomal-like vesicles are present in human blood plasma. *Int Immunol.* 17, 879–887. doi: 10.1093/intimm/dxh267.

Calderón-González, K. G., Hernández-Monge, J., Herrera-Aguirre, M. E., and Luna-Arias, J. P. (2016). "Bioinformatics tools for proteomics data interpretation," in *Advances in Experimental Medicine and Biology* (Springer New York LLC), 281–341. doi:10.1007/978-3-319-41448-5_16.

Calin, G. A., Sevignani, C., Dumitru, C. D., Hyslop, T., Noch, E., Yendamuri, S., et al. (2004). Human microRNA genes are frequently located at fragile sites and genomic regions involved in cancers. *Proc. Natl. Acad. Sci. U. S. A.* 101, 2999–3004. doi:10.1073/pnas.0307323101.

Chait, B. T. (2006). Chemistry. Mass spectrometry: bottom-up or top-down? *Science*. 314, 65–66. doi: 10.1126/science.1133987.

Chakraborty, S., Hosen, M. I., Ahmed, M., and Shekhar, H. U. (2018). Onco-Multi-OMICS Approach: A New Frontier in Cancer Research. *Biomed Res. Int.* 2018, 9836256. doi:10.1155/2018/9836256.

Chen, W., Wang, H., Chen, H., Liu, S., Lu, H., Kong, D., et al. (2014). Clinical significance and detection of microRNA-21 in serum of patients with diffuse large B-cell lymphoma in Chinese population. *Eur. J. Haematol.* 92, 407–412. doi:10.1111/ejh.12263.

Chen, X., Dong, H., Liu, S., Yu, L., Yan, D., Yao, X., et al. (2017). Long noncoding RNA MHENCR

promotes melanoma progression via regulating miR-425/489-mediated PI3K-Akt pathway. *Am. J. Transl. Res.* 9, 90–102.

Cho, W. C. S. (2007). Contribution of oncoproteomics to cancer biomarker discovery. *Mol. Cancer* 6, 25. doi:10.1186/1476-4598-6-25.

Clarridge, J. E. (2004). Impact of 16S rRNA gene sequence analysis for identification of bacteria on clinical microbiology and infectious diseases. *Clin. Microbiol. Rev.* 17, 840–862. doi:10.1128/CMR.17.4.840-862.2004.

Condrat, C. E., Thompson, D. C., Barbu, M. G., Bugnar, O. L., Boboc, A., Cretoiu, D., et al. (2020). miRNAs as Biomarkers in Disease: Latest Findings Regarding Their Role in Diagnosis and Prognosis. *Cells* 9, 276. doi:10.3390/cells9020276.

Coumans, F. A. W., Brisson, A. R., Buzas, E. I., Dignat-George, F., Drees, E. E. E., El-Andaloussi, S., et al. (2017). Methodological guidelines to study extracellular vesicles. *Circ. Res.* 120, 1632–1648. doi:10.1161/CIRCRESAHA.117.309417.

Craig, K. K. L., Wood, G. A., Keller, S. M., Mutsaers, A. J., and Wood, R. D. (2019). MicroRNA profiling in canine multicentric lymphoma. *PLoS One* 14, e0226357. doi:10.1371/journal.pone.0226357.

Cufaro, M. C., Pieragostino, D., Lanuti, P., Rossi, C., Cicalini, I., Federici, L., et al. (2019). Extracellular Vesicles and Their Potential Use in Monitoring Cancer Progression and Therapy: The Contribution of Proteomics. *J. Oncol.* 2019. doi:10.1155/2019/1639854.

Cui, M., Wang, H., Yao, X., Zhang, D., Xie, Y., Cui, R., et al. (2019). Circulating MicroRNAs in Cancer: Potential and Challenge. *Front. Genet.* 10, 626. doi:10.3389/fgene.2019.00626.

da Sacco, L., and Masotti, A. (2013). Recent insights and novel bioinformatics tools to understand

the role of MicroRNAs binding to 5' untranslated region. *Int. J. Mol. Sci.* 14, 480–495. doi:10.3390/ijms14010480.

Dai, J., Su, Y., Zhong, S., Cong, L., Liu, B., Yang, J., et al. (2020). Exosomes: key players in cancer and potential therapeutic strategy. *Signal Transduct. Target. Ther.* 5, 145. doi:10.1038/s41392-020-00261-0.

Danielson, K. M., Estanislau, J., Tigges, J., Toxavidis, V., Camacho, V., Felton, E. J., et al. (2016). Diurnal variations of circulating extracellular vesicles measured by nano flow cytometry. *PLoS One* 11. doi:10.1371/journal.pone.0144678.

Davies, D. R., Wyatt, K. M., Jardine, J. E., Robertson, I. D., and Irwin, P. J. (2004). Vinblastine and prednisolone as adjunctive therapy for canine cutaneous mast cell tumors. *J. Am. Anim. Hosp. Assoc.* 40, 124–130. doi:10.5326/0400124.

de Anda-Jáuregui, G., and Hernández-Lemus, E. (2020). Computational Oncology in the Multi-Omics Era: State of the Art. *Front. Oncol.* 10, 423. doi:10.3389/fonc.2020.00423.

Di Leva, G., Garofalo, M., and Croce, C. M. (2014). miRNA in cancer. *Annu. Rev. Pathol.* 9, 287–314. doi: 10.1146/annurev-pathol-012513-104715.

Dobson, J. M., and Scase, T. J. (2007). Advances in the diagnosis and management of cutaneous mast cell tumours in dogs. *J. Small Anim. Pract.* 48, 424–431. doi:10.1111/j.1748-5827.2007.00366.x.

Domínguez-Vigil, I. G., Moreno-Martínez, A. K., Wang, J. Y., Roehrl, M. H. A., and Barrera-Saldaña, H. A. (2018). The dawn of the liquid biopsy in the fight against cancer. *Oncotarget* 9, 2912–2922. doi:10.18632/oncotarget.23131.

Egert M., Simmering R. (2016) The Microbiota of the Human Skin. In: Schwiertz A. (eds) Microbiota

of the Human Body. Advances in Experimental Medicine and Biology, vol 902. Springer, Cham. https://doi.org/10.1007/978-3-319-31248-4_5.

Fenger, J. M., Bear, M. D., Volinia, S., Lin, T. Y., Harrington, B. K., London, C. A., et al. (2014). Overexpression of miR-9 in mast cells is associated with invasive behavior and spontaneous metastasis. *BMC Cancer* 14, 84. doi:10.1186/1471-2407-14-84.

Fernández-Lázaro, D., Hernández, J. L. G., García, A. C., Martínez, A. C., Mielgo-Ayuso, J., and Cruz-Hernández, J. J. (2020). Liquid biopsy as novel tool in precision medicine: Origins, properties, identification and clinical perspective of cancer's biomarkers. *Diagnostics (Basel).* 10, 215. doi:10.3390/diagnostics10040215.

Fish, E. J., Irizarry, K. J., DeInnocentes, P., Ellis, C. J., Prasad, N., Moss, A. G., et al. (2018). Malignant canine mammary epithelial cells shed exosomes containing differentially expressed microRNA that regulate oncogenic networks. *BMC Cancer* 18, 832. doi:10.1186/s12885-018-4750-6.

Forloni, M., Dogra, S. K., Dong, Y., Conte, D., Ou, J., Zhu, L. J., et al. (2014). miR-146a promotes the initiation and progression of melanoma by activating Notch signaling. *Elife* 3, e01460. doi: 10.7554/eLife.01460.

Forshew, T., Murtaza, M., Parkinson, C., Gale, D., Tsui, D. W. Y., Kaper, F., et al. (2012). Noninvasive identification and monitoring of cancer mutations by targeted deep sequencing of plasma DNA. *Sci. Transl. Med.* 4, 136ra68. doi:10.1126/scitranslmed.3003726.

Franchina, T., Amodeo, V., Bronte, G., Savio, G., Ricciardi, G. R. R., Picciotto, M., et al. (2014). Circulating miR-22, miR-24 and miR-34a as Novel Predictive Biomarkers to Pemetrexed-Based Chemotherapy in Advanced Non-Small Cell Lung Cancer. *J. Cell. Physiol.* 229, 97–99. doi:10.1002/jcp.24422.

Gaines, P. J., Powell, T. D., Walmsley, S. J., Estredge, K. L., Wisnewski, N., Stinchcomb, D. T., et al. (2007). Identification of serum biomarkers for canine B-cell lymphoma by use of surface-enhanced laser desorption-ionization time-of-flight mass spectrometry. *Am. J. Vet. Res.* 68, 405–410. doi:10.2460/ajvr.68.4.405.

Gandham, S., Su, X., Wood, J., Nocera, A. L., Alli, S. C., Milane, L., et al. (2020). Technologies and Standardization in Research on Extracellular Vesicles. *Trends Biotechnol.* 38, 1066–1098. doi:10.1016/j.tibtech.2020.05.012.

Ganti, S., Taylor, S. L., Aboud, O. A., Yang, J., Evans, C., Osier, M. V., et al. (2012). Kidney tumor biomarkers revealed by simultaneous multiple matrix metabolomics analysis. *Cancer Res.* 72, 3471–3479. doi:10.1158/0008-5472.CAN-11-3105.

Garrett, L. (2014). Canine mast cell tumors: diagnosis, treatment, and prognosis. *Vet. Med. Res. Reports* 5, 49-58. doi:10.2147/vmrr.s41005.

Gavazza, A., Rossi, G., Lubas, G., Cerquetella, M., Minamoto, Y., and Suchodolski, J. S. (2018). Faecal microbiota in dogs with multicentric lymphoma. *Vet. Comp. Oncol.* 16, E169–E175. doi:10.1111/vco.12367.

Gerlinger, M., Rowan, A. J., Horswell, S., Math, M., Larkin, J., Endesfelder, D. et al. (2012). Intratumor Heterogeneity and Branched Evolution Revealed by Multiregion Sequencing. *N. Engl. J. Med.* 366, 883–892. doi:10.1056/NEJMoa1113205.

Giantin, M., Vascellari, M., Morello, E. M., Capello, K., Vercelli, A., Granato, A., et al. (2012). c-KIT messenger RNA and protein expression and mutations in canine cutaneous mast cell tumors: Correlations with post-surgical prognosis. *J. Vet. Diagnostic Investig.* 24, 116–126. doi:10.1177/1040638711425945.

Giovannetti, E., Erozenci, A., Smit, J., Danesi, R., and Peters, G. J. (2012). Molecular mechanisms underlying the role of microRNAs (miRNAs) in anticancer drug resistance and implications for clinical practice. *Crit. Rev. Oncol. Hematol.* 81, 103–122. doi:10.1016/j.critrevonc.2011.03.010.

Goodwin, S., McPherson, J. D. and McCombie, W. R. (2016). Coming of age: ten years of nextgeneration sequencing technologies. *Nat. Rev. Genet.* 17, 333–351. doi:10.1038/nrg.2016.49.

Goldschmidt MH, Dunstan RW, Stannard AA, et al: Histological classification of epithelial and melanocytic tumors of the skin. In Schulman FY, editor: Worldwide reference for comparative oncology, ed 2, Washington, 1998, Armed Forces Institute for Pathology.

Gong, J., Jaiswal, R., Mathys, J. M., Combes, V., Grau, G. E. R., and Bebawy, M. (2012). Microparticles and their emerging role in cancer multidrug resistance. *Cancer Treat. Rev.* 38, 226–234. doi:10.1016/j.ctrv.2011.06.005.

Gonzales, P. A., Zhou, H., Pisitkun, T., Wang, N. S., Star, R. A., Knepper, M. A., et al. (2010). Isolation and purification of exosomes in urine. *Methods Mol. Biol.* 641, 89–99. doi:10.1007/978-1-60761-711-2_6.

Gregorich, Z. R., Ge, Y. (2014). Top-down proteomics in health and disease: Challenges and opportunities. *Proteomics.* 14, 1195–1210. doi: 10.1002/pmic.201300432.

Gross TL, Ihrke P, Walder EJ, Affolter VK. Mast cell tumors. Skin Diseases of the Dog and Cat Clinical and Histopathologic Diagnosis, 2nd edn. Oxford, UK: Blackwell Science Ltd, 2005: 853–65.

Grüntzig, K., Graf, R., Hässig, M., Welle, M., Meier, D., Lott, G., et al. (2015). The Swiss canine

cancer registry: A retrospective study on the occurrence of tumours in dogs in Switzerland from 1955 to 2008. *J. Comp. Pathol.* 152, 161–171. doi:10.1016/j.jcpa.2015.02.005.

Guo, S. C., Tao, S. C., and Dawn, H. (2018). Microfluidics-based on-a-chip systems for isolating and analysing extracellular vesicles. *J. Extracell. Vesicles* 7, 1508271. doi:10.1080/20013078.2018.1508271.

Hauck, M. L. (2012). "Tumors of the Skin and Subcutaneous Tissues," in *Withrow and MacEwen's Small Animal Clinical Oncology: Fifth Edition* (Elsevier Inc.), 305–320. doi:10.1016/B978-1-4377-2362-5.00018-9.

Heishima, K., Ichikawa, Y., Yoshida, K., Iwasaki, R., Sakai, H., Nakagawa, T., et al. (2017). Circulating microRNA-214 and -126 as potential biomarkers for canine neoplastic disease. *Sci. Rep.* 7,2301. doi:10.1038/s41598-017-02607-1.

Helwa, I., Cai, J., Drewry, M. D., Zimmerman, A., Dinkins, M. B., Khaled, M. L., et al. (2017). A comparative study of serum exosome isolation using differential ultracentrifugation and three commercial reagents. *PLoS One* 12, e0170628. doi:10.1371/journal.pone.0170628.

Hendrick, MJ, Mahaffrey, EA, Moore FM. Histological Classification of Mesenchymal Tumors of Skin and Soft Tissues of Domestic Animals. American Registry of Pathology, 1998 (2nd edition).

Herstad, K. M. V., Moen, A. E. F., Gaby, J. C., Moe, L., and Skancke, E. (2018). Characterization of the fecal and mucosa-associated microbiota in dogs with colorectal epithelial tumors. *PLoS One* 13, e0198342. doi:10.1371/journal.pone.0198342.

Hong, C. S., Funk, S., Muller, L., Boyiadzis, M., and Whiteside, T. L. (2016). Isolation of biologically active and morphologically intact exosomes from plasma of patients with cancer. *J. Extracell.*

Vesicles 5, 29289. doi:10.3402/jev.v5.29289.

Huang, T., and Deng, C. X. (2019). Current progresses of exosomes as cancer diagnostic and prognostic biomarkers. *Int. J. Biol. Sci.* 15, 1–11. doi:10.7150/ijbs.27796.

Ilyinskaya, G. V., Mukhina, E. V., Soboleva, A. V., Matveeva, O. V., and Chumakov, P. M. (2018). Oncolytic sendai virus therapy of canine mast cell tumors (A pilot study). *Front. Vet. Sci.* 5, 116. doi:10.3389/fvets.2018.00116.

Jacob, N. K., Cooley, J. V., Yee, T. N., Jacob, J., Alder, H., Wickramasinghe, P., et al. (2013). Identification of Sensitive Serum microRNA Biomarkers for Radiation Biodosimetry. *PLoS One* 8, e57603. doi:10.1371/journal.pone.0057603.

Javanmardi, S., Aghamaali, M. R., Abolmaali, S. S., Mohammadi, S., and Tamaddon, A. M. (2017). miR-21, An Oncogenic Target miRNA for Cancer Therapy: Molecular Mechanisms and Recent Advancements in Chemo and Radio-resistance. *Curr. Gene Ther.* 16, 375–389. doi:10.2174/1566523217666170102105119.

Jeyaram, A., and Jay, S. M. (2017). Preservation and Storage Stability of Extracellular Vesicles for Therapeutic Applications. *AAPS J.* 20, 1. doi:10.1208/s12248-017-0160-y.

Johnson, J. S., Spakowicz, D. J., Hong, B. Y., Petersen, L. M., Demkowicz, P., Chen, L., et al. (2019). Evaluation of 16S rRNA gene sequencing for species and strain-level microbiome analysis. *Nat. Commun.* 10, 5029. doi:10.1038/s41467-019-13036-1.

Kawabe, M., Baba, Y., Tamai, R., Yamamoto, R., Komori, M., Mori, T., et al. (2015). Profiling of plasma metabolites in canine oral melanoma using gas chromatographymass spectrometry. *J. Vet. Med. Sci.* 77, 1025–1028. doi:10.1292/jvms.14-0641.

Kent, M. S., Collins, C. J., and Ye, F. (2009). Activation of the AKT and mammalian target of

rapamycin pathways and the inhibitory effects of rapamycin on those pathways in canine malignant melanoma cell lines. *Am. J. Vet. Res.* 70, 263–269. doi:10.2460/ajvr.70.2.263.

Kiupel, M., and Camus, M. (2019). Diagnosis and Prognosis of Canine Cutaneous Mast Cell Tumors. *Vet. Clin. North Am. Small Anim. Pract.* 49, 819–836. doi:10.1016/j.cvsm.2019.04.002.

Kiupel, M., Webster, J. D., Bailey, K. L., Best, S., DeLay, J., Detrisac, C. J., et al. (2011). Proposal of a 2-tier histologic grading system for canine cutaneous mast cell tumors to more accurately predict biological behavior. *Vet. Pathol.* 48, 147–155. doi:10.1177/0300985810386469.

Klopfleisch, R., Klose, P., Weise, C., Bondzio, A., Multhaup, G., Einspanier, R., et al. (2010). Proteome of metastatic canine mammary carcinomas: Similarities to and differences from human breast cancer. *J. Proteome Res.* 9, 6380–6391. doi:10.1021/pr100671c.

Klose, P., Weise, C., Bondzio, A., Multhaup, G., Einspanier, R., Gruber, A. D., et al. (2011). Is there a malignant progression associated with a linear change in protein expression levels from normal canine mammary gland to metastatic mammary tumors? *J. Proteome Res.* 10, 4405–4415. doi:10.1021/pr200112q.

Kogure, A., Kosaka, N., and Ochiya, T. (2019). Cross-talk between cancer cells and their neighbors via miRNA in extracellular vesicles: An emerging player in cancer metastasis. *J. Biomed. Sci.* 26, 7. doi:10.1186/s12929-019-0500-6.

Konoshenko, M. Y., Lekchnov, E. A., Vlassov, A. V., and Laktionov, P. P. (2018). Isolation of Extracellular Vesicles: General Methodologies and Latest Trends. *Biomed Res. Int.* 2018, 8545347. doi:10.1155/2018/8545347.

Kormelink, T. G., Arkesteijn, G. J. A., Nauwelaers, F. A., van den Engh, G., Nolte-'t Hoen, E. N. M., and Wauben, M. H. M. (2016). Prerequisites for the analysis and sorting of extracellular

vesicle subpopulations by high-resolution flow cytometry. *Cytometry A.* 89, 135–147. doi:10.1002/cyto.a.22644.

Kovalszki, A., and Weller, P. F. (2014). Eosinophilia in mast cell disease. *Immunol. Allergy Clin. North Am.* 34, 357–364. doi:10.1016/j.iac.2014.01.013.

Krol, J., Loedige, I., and Filipowicz, W. (2010). The widespread regulation of microRNA biogenesis, function and decay. *Nat. Rev. Genet.* 11, 597–610. doi:10.1038/nrg2843.

Kusuma, G. D., Barabadi, M., Tan, J. L., Morton, D. A. V., Frith, J. E., and Lim, R. (2018). To protect and to preserve: Novel preservation strategies for extracellular vesicles. *Front. Pharmacol.* 9, 1199. doi:10.3389/fphar.2018.01199.

Lane, R. E., Korbie, D., Trau, M., and Hill, M. M. (2019). Optimizing Size Exclusion Chromatography for Extracellular Vesicle Enrichment and Proteomic Analysis from Clinically Relevant Samples. *Proteomics* 19, e1800156. doi:10.1002/pmic.201800156.

Lässer, C. (2012). Exosomal RNA as biomarkers and the therapeutic potential of exosome vectors. *Expert Opin Biol Ther* 1, S189-97. doi: 10.1517/14712598.2012.680018.

Lee, R. C., Feinbaum, R. L., and Ambros, V. (1993). The C. elegans heterochronic gene lin-4 encodes small RNAs with antisense complementarity to lin-14. *Cell* 75, 843–854. doi:10.1016/0092-8674(93)90529-Y.

Leroy, B. E., Painter, A., Sheppard, H., Popiolek, L., Samuel-Foo, M., and Andacht, T. M. (2007). Protein expression profiling of normal and neoplastic canine prostate and bladder tissue. *Vet. Comp. Oncol.* 5, 119–130. doi:10.1111/j.1476-5829.2006.00121.x.

Letard, S., Yang, Y., Hanssens, K., Palmérini, F., Leventhal, P. S., Guéry, S., et al. (2008). Gain-of-function mutations in the extracellular domain of KIT are common in canine mast cell tumors.

Mol. Cancer Res. 6, 1137–1145. doi:10.1158/1541-7786.MCR-08-0067.

Li, J., Guan, X., Fan, Z., Ching, L. M., Li, Y., Wang, X., et al. (2020). Non-invasive biomarkers for early detection of breast cancer. *Cancers (Basel).* 12, 2767. doi:10.3390/cancers12102767.

Li, X., Guo, S., Min, L., Guo, Q., and Zhang, S. (2019). miR-92a-3p promotes the proliferation, migration and invasion of esophageal squamous cell cancer by regulating PTEN. *Int. J. Mol. Med.* 44, 973–981. doi:10.3892/ijmm.2019.4258.

Liga, A., Vliegenthart, A. D. B., Oosthuyzen, W., Dear, J. W., and Kersaudy-Kerhoas, M. (2015). Exosome isolation: A microfluidic road-map. *Lab Chip* 15, 2388–2394. doi:10.1039/c5lc00240k.

Linares, R., Tan, S., Gounou, C., Arraud, N., and Brisson, A. R. (2015). High-speed centrifugation induces aggregation of extracellular vesicles. *J. Extracell. vesicles* 4. doi:10.3402/JEV.V4.29509.

Liu, C. J., Lin, S. C., Yang, C. C., Cheng, H. W., and Chang, K. W. (2012). Exploiting salivary miR-31 as a clinical biomarker of oral squamous cell carcinoma. *Head Neck* 34, 219–224. doi:10.1002/hed.21713.

Liu, L., Zhao, Z., Zhou, W., Fan, X., Zhan, Q., and Song, Y. (2015). Enhanced Expression of miR-425 Promotes Esophageal Squamous Cell Carcinoma Tumorigenesis by Targeting SMAD2. *J. Genet. Genomics* 42, 601–611. doi:10.1016/j.jgg.2015.09.010.

Liu, S., Gao, G., Yan, D., Chen, X., Yao, X., Guo, S., et al. (2017). Effects of miR-145-5p through NRAS on the cell proliferation, apoptosis, migration, and invasion in melanoma by inhibiting MAPK and PI3K/AKT pathways. *Cancer Med.* 6, 819–833. doi:10.1002/cam4.1030.

Lobb, R. J., Becker, M., Wen, S. W., Wong, C. S. F., Wiegmans, A. P., Leimgruber, A., et al. (2015).

Optimized exosome isolation protocol for cell culture supernatant and human plasma. *J. Extracell. Vesicles* 4, 27031. doi:10.3402/jev.v4.27031.

Lobb, R. J., Lima, L. G., and Möller, A. (2017). Exosomes: Key mediators of metastasis and pre-metastatic niche formation. *Semin. Cell Dev. Biol.* 67, 3–10. doi:10.1016/j.semcdb.2017.01.004.

London, C. A., Galli, S. J., Yuuki, T., Hu, Z. Q., Helfand, S. C., and Geissler, E. N. (1999). Spontaneous canine mast cell tumors express tandem duplications in the proto-oncogene c-kit. *Exp. Hematol.* 27, 689–697. doi:10.1016/S0301-472X(98)00075-7.

Long, J., Luo, J., and Yin, X. (2018). MiR-338-5p promotes the growth and metastasis of malignant melanoma cells via targeting CD82. *Biomed. Pharmacother.* 102, 1195–1202. doi:10.1016/j.biopha.2018.03.075.

Lu, M., and Zhan, X. (2018). The crucial role of multiomic approach in cancer research and clinically relevant outcomes. *EPMA J.* 9, 77–102. doi:10.1007/s13167-018-0128-8.

Lucchetti, D., Tenore, C. R., Colella, F., and Sgambato, A. (2020). Extracellular vesicles and cancer: A focus on metabolism, cytokines, and immunity. *Cancers (Basel).* 12, 171. doi:10.3390/cancers12010171.

Ludwig, N., Hong, C. S., Ludwig, S., Azambuja, J. H., Sharma, P., Theodoraki, M. N., et al. (2019a). Isolation and Analysis of Tumor-Derived Exosomes. *Curr. Protoc. Immunol.* 127, e91. doi:10.1002/cpim.91.

Ludwig, N., Whiteside, T. L., and Reichert, T. E. (2019b). Challenges in exosome isolation and analysis in health and disease. *Int. J. Mol. Sci.* 20, 4684. doi:10.3390/ijms20194684.

Ma, C., Han, M., Heinrich, B., Fu, Q., Zhang, Q., Sandhu, M., et al. (2018). Gut microbiome–

mediated bile acid metabolism regulates liver cancer via NKT cells. *Science* 360, eaan5931. doi: 10.1126/science.aan5931.

Ma, Y., Longley, B. J., Wang, X., Blount, J. L., Langley, K., and Caughey, G. H. (1999). Clustering of activating mutations in c-KIT's juxtamembrane coding region in canine mast cell neoplasms. *J. Invest. Dermatol.* 112, 165–170. doi:10.1046/j.1523-1747.1999.00488.x.

Maia, J., Caja, S., Strano Moraes, M. C., Couto, N., and Costa-Silva, B. (2018). Exosome-based cell-cell communication in the tumor microenvironment. *Front. Cell Dev. Biol.* 6, 18. doi:10.3389/fcell.2018.00018.

Mardamshina, M., and Geiger, T. (2017). Next-Generation Proteomics and Its Application to Clinical Breast Cancer Research. *Am. J. Pathol.* 187, 2175–2184. doi:10.1016/j.ajpath.2017.07.003.

Mastroianni, J., Stickel, N., Andrlova, H., Hanke, K., Melchinger, W., Duquesne, S., et al. (2019). MiR-146a Controls Immune Response in the Melanoma Microenvironment. *Cancer Res.* 79, 183–195. doi:10.1158/0008-5472.CAN-18-1397.

McCaw, D. L., Chan, A. S., Stegner, A. L., Mooney, B., Bryan, J. N., Turnquist, S. E., et al. (2007). Proteomics of canine lymphoma identifies potential cancer-specific protein markers. *Clin. Cancer Res.* 13, 2496–2503. doi:10.1158/1078-0432.CCR-06-2699.

McCormack, A. L. (2005). Mass spectrometry in proteomics. *Methods* 35, 209–210. doi:10.1016/j.ymeth.2004.08.012.

Mezouar, S., Chantran, Y., Michel, J., Fabre, A., Dubus, J. C., Leone, M., et al. (2018). Microbiome and the immune system: From a healthy steady-state to allergy associated disruption. *Hum. Microbiome J.* 10, 11–20. doi:10.1016/j.humic.2018.10.001.

Mikiewicz, M., Paździor-Czapula, K., Gesek, M., Lemishevskyi, V., and Otrocka-Domagała, I. (2019). Canine and Feline Oral Cavity Tumours and Tumour-like Lesions: a Retrospective Study of 486 Cases (2015–2017). *J. Comp. Pathol.* 172, 80–87. doi:10.1016/j.jcpa.2019.09.007.

Misra, B. B., Langefeld, C. D., Olivier, M., and Cox, L. A. (2018). Integrated omics: Tools, advances and future approaches. *J. Mol. Endocrinol.* JME-18-0055. doi:10.1530/JME-18-0055.

Modiano, J. F., Ritt, M. G., and Wojcieszyn, J. (1999). The molecular basis of canine melanoma: pathogenesis and trends in diagnosis and therapy. *J. Vet. Intern. Med.* 13, 167-174. doi: 10.1892/0891-6640(1999)013<0163:tmbocm>2.3.co;2.

Morgan, X. C., and Huttenhower, C. (2012). Chapter 12: Human Microbiome Analysis. *PLoS Comput. Biol.* 8, e1002808. doi:10.1371/journal.pcbi.1002808.

Morris, J. S. (2016). Genomic and proteomic profiling for cancer diagnosis in dogs. *Vet. J.* 215, 101–109. doi:10.1016/j.tvjl.2016.01.003.

Mrázek, J., Mekadim, C., Kučerová, P., Švejstil, R., Salmonová, H., et al. (2019). Melanoma-related changes in skin microbiome. *Folia Microbiol. (Praha).* 64, 435–442. doi: 10.1007/s12223-018-00670-3.

Mullins, M. N., Dernell, W. S., Withrow, S. J., Ehrhart, E. J., Thamm, D. H., and Lana, S. E. (2006). Evaluation of prognostic factors associated with outcome in dogs with multiple cutaneous mast cell tumors treated with surgery with and without adjuvant treatment: 54 cases (1998–2004). *J. Am. Vet. Med. Assoc.* 228, 91–95. doi:10.2460/javma.228.1.91.

Murakami, A., Mori, T., Sakai, H., Murakami, M., Yanai, T., Hoshino, Y., et al. (2011). Analysis of KIT expression and KIT exon 11 mutations in canine oral malignant melanomas. *Vet. Comp. Oncol.* 9, 219–224. doi:10.1111/j.1476-5829.2010.00253.x.

Naik, S., Bouladoux, N., Wilhelm, C., Molloy, M. J., Salcedo, R., Kastenmuller, W., et al. (2012). Compartmentalized control of skin immunity by resident commensals. *Science* 337, 1115–1119. doi:10.1126/science.1225152.

Newman, S. J., Jankovsky, J. M., Rohrbach, B. W., and LeBlanc, A. K. (2012). C-kit Expression in Canine Mucosal Melanomas. *Vet. Pathol.* 49, 760–765. doi:10.1177/0300985811414032.

Nishiya, A. T., Massoco, C. O., Felizzola, C. R., Perlmann, E., Batschinski, K., Tedardi, M. V., et al. (2016). Comparative aspects of canine melanoma. *Vet. Sci.* 3, 7. doi:10.3390/vetsci3010007.

Noguchi, S., Mori, T., Hoshino, Y., Yamada, N., Nakagawa, T., Sasaki, N., et al. (2012). Comparative study of anti-oncogenic MicroRNA-145 in canine and human malignant melanoma. *J. Vet. Med. Sci.* 74, 1–8. doi:10.1292/jvms.11-0264.

O'Connell, K., and Thomson, M. (2013). Evaluation of prognostic indicators in dogs with multiple, simultaneously occurring cutaneous mast cell tumours: 63 cases. *Vet. Comp. Oncol.* 11, 51–62. doi:10.1111/j.1476-5829.2011.00301.x.

Ohashi, H., Hasegawa, M., Wakimoto, K., and Miyamoto-Sato, E. (2015). Next-generation technologies for multiomics approaches including interactome sequencing. *Biomed Res. Int.* 2015, 104209. doi:10.1155/2015/104209.

Ortiz-Quintero, B. (2016). Cell-free microRNAs in blood and other body fluids, as cancer biomarkers. *Cell Prolif.* 49, 281–303. doi:10.1111/cpr.12262.

Ottman, R., Levy, J., Grizzle, W. E., and Chakrabarti, R. (2016). The other face of miR-17-92a cluster, exhibiting tumor suppressor effects in prostate cancer. *Oncotarget* 7, 73739–73753. doi:10.18632/oncotarget.12061.

Owen, L. N, World Health Organization. Veterinary Public Health Unit & WHO Collaborating Center

for Comparative Oncology. (1980). TNM Classification of Tumours in Domestic Animals/ edited by L.N. Owen. World Health Organization. https://apps.who.int/iris/handle/10665/68618

Palanisamy, V., Sharma, S., Deshpande, A., Zhou, H., Gimzewski, J., and Wong, D. T. (2010). Nanostructural and transcriptomic analyses of human saliva derived exosomes. *PLoS One* 5, e8577. doi:10.1371/journal.pone.0008577.

Palviainen, M., Saraswat, M., Varga, Z., Kitka, D., Neuvonen, M., Puhka, M., et al. (2020). Extracellular vesicles from human plasma and serum are carriers of extravesicular cargo—Implications for biomarker discovery. *PLoS One* 15. doi:10.1371/journal.pone.0236439.

Pardanani, A., Wieben, E. D., Spelsberg, T. C., and Tefferi, A. (2002). Primer on medical genomics part IV: Expression proteomics. *Mayo Clin. Proc.* 77, 1185–1196. doi:10.4065/77.11.1185.

Patnaik, A. K., Ehler, W. J., and MacEwen, E. G. (1984). Canine Cutaneous Mast Cell Tumor: Morphologic Grading and Survival Time in 83 Dogs. *Vet. Pathol.* 21, 469–474. doi:10.1177/030098588402100503.

Pietrowska, M., Wlosowicz, A., Gawin, M., and Widlak, P. (2019). MS-Based Proteomic Analysis of Serum and Plasma: Problem of High Abundant Components and Lights and Shadows of Albumin Removal. *Adv. Exp. Med. Biol.* 1073, 57–76. doi:10.1007/978-3-030-12298-0_3.

Pisamai, S., Roytrakul, S., Phaonakrop, N., Jaresitthikunchai, J., and Suriyaphol, G. (2018). Proteomic analysis of canine oral tumor tissues using MALDI-TOF mass spectrometry and in-gel digestion coupled with mass spectrometry (GeLC MS/MS) approaches. *PLoS One* 13, e0200619. doi:10.1371/journal.pone.0200619.

Ploypetch, S., Roytrakul, S., Jaresitthikunchai, J., Phaonakrop, N., Krobthong, S., and Suriyaphol, G.

(2019). Salivary proteomics of canine oral tumors using MALDI-TOF mass spectrometry and LC-tandem mass spectrometry. *PLoS One* 14, e0219390. doi:10.1371/journal.pone.0219390.

Plummer, M., de Martel, C., Vignat, J., Ferlay, J., Bray, F., and Franceschi, S. (2016). Global burden of cancers attributable to infections in 2012: a synthetic analysis. *Lancet Glob. Heal.* 4, e609–e616. doi:10.1016/S2214-109X(16)30143-7.

Poorman, K., Borst, L., Moroff, S., Roy, S., Labelle, P., Motsinger-Reif, A., et al. (2015). Comparative cytogenetic characterization of primary canine melanocytic lesions using array CGH and fluorescence in situ hybridization. *Chromosom. Res.* 23, 171–186. doi:10.1007/s10577-014-9444-6.

Prescott, S. L., Larcombe, D. L., Logan, A. C., West, C., Burks, W., Caraballo, L., et al. (2017). The skin microbiome: Impact of modern environments on skin ecology, barrier integrity, and systemic immune programming. *World Allergy Organ. J.* 10, 29. doi:10.1186/s40413-017-0160-5.

Prouteau, A., and André, C. (2019). Canine melanomas as models for human melanomas: Clinical, histological, and genetic comparison. *Genes (Basel).* 10, 501. doi:10.3390/genes10070501

Pu, W., Shang, Y., Shao, Q., and Yuan, X. (2018). miR-146a promotes cell migration and invasion in melanoma by directly targeting SMAD4. *Oncol. Lett.* 15, 7111–7117. doi:10.3892/ol.2018.8172.

Pulz, L. H., Barra, C. N., Alexandre, P. A., Huete, G. C., Cadrobbi, K. G., Nishiya, A. T., et al. (2019). Identification of two molecular subtypes in canine mast cell tumours through gene expression profiling. *PLoS One* 14, e0217343. doi:10.1371/journal.pone.0217343.

Rahman, M. M., Lai, Y. C., Husna, A. A., Chen, H. W., Tanaka, Y., Kawaguchi, H., et al. (2019). Micro

RNA transcriptome profile in canine oral melanoma. *Int. J. Mol. Sci.* 20, 4832. doi:10.3390/ijms20194832.

Raimo, M., Orso, F., Grassi, E., Cimino, D., Penna, E., De Pittà, C., et al. (2016). MiR-146a exerts differential effects on melanoma growth and metastatization. *Mol. Cancer Res.* 14, 548–562. doi:10.1158/1541-7786.MCR-15-0425-T.

Ramírez-Labrada, A. G., Isla, D., Artal, A., Arias, M., Rezusta, A., Pardo, J., et al. (2020). The Influence of Lung Microbiota on Lung Carcinogenesis, Immunity, and Immunotherapy. *Trends in Cancer* 6, 86–97. doi:10.1016/j.trecan.2019.12.007.

Ramos-Vara, J. A., Beissenherz, M. E., Miller, M. A., Johnson, G. C., Pace, L. W., Fard, A., et al. (2000). Retrospective study of 338 canine oral melanomas with clinical, histologic, and immunohistochemical review of 129 cases. *Vet. Pathol.* 37, 597–608. doi:10.1354/vp.37-6-597.

Rapado-González, Ó., Majem, B., Muinelo-Romay, L., Álvarez-Castro, A., Santamaría, A., Gil-Moreno, A., et al. (2018). Human salivary microRNAs in Cancer. *J. Cancer* 9, 638–649. doi:10.7150/jca.21180.

Rassnick, K. M., Ruslander, D. M., Cotter, S. M., Al-Sarraf, R., Bruyette, D. S., Gamblin, R. M., et al. (2001). Use of carboplatin for treatment of dogs with malignant melanoma: 27 cases (1989-2000). *J. Am. Vet. Med. Assoc.* 218, 1444–1448. doi:10.2460/javma.2001.218.1444.

Ratcliffe, L., Mian, S., Slater, K., King, H., Napolitano, M., Aucoin, D., et al. (2009). Proteomic identification and profiling of canine lymphoma patients. *Vet. Comp. Oncol.* 7, 92–105. doi:10.1111/j.1476-5829.2009.00165.x.

Reinert, T., Schøler, L. V., Thomsen, R., Tobiasen, H., Vang, S., Nordentoft, I., et al. (2016). Analysis

of circulating tumour DNA to monitor disease burden following colorectal cancer surgery. *Gut* 65, 625–634. doi:10.1136/gutjnl-2014-308859.

Revenfeld, A. L. S., Bæk, R., Nielsen, M. H., Stensballe, A., Varming, K., and Jørgensen, M. (2014). Diagnostic and prognostic potential of extracellular vesicles in peripheral blood. *Clin. Ther.* 36, 830–846. doi:10.1016/j.clinthera.2014.05.008.

Rivera, R. S., Nagatsuka, H., Gunduz, M., Cengiz, B., Gunduz, E., Siar, C. H., et al. (2008). C-kit protein expression correlated with activating mutations in KIT gene in oral mucosal melanoma. *Virchows Arch.* 452, 27–32. doi:10.1007/s00428-007-0524-2.

Roccabianca, P. (2018). Canine Skin Cancer and the Art of Classifications. *Vet. Pathol.* 55, 770–771. doi:10.1177/0300985818790783.

Rosenfeld, N., Aharonov, R., Meiri, E., Rosenwald, S., Spector, Y., Zepeniuk, M., et al. (2008). MicroRNAs accurately identify cancer tissue origin. *Nat. Biotechnol.* 26, 462–469. doi:10.1038/nbt1392.

Roy, S., Lin, H. Y., Chou, C. Y., Huang, C. H., Small, J., Sadik, N., et al. (2019). Navigating the landscape of tumor extracellular vesicle heterogeneity. *Int. J. Mol. Sci.* 20. doi:10.3390/ijms20061349.

Rupaimoole, R., Calin, G. A., Lopez-Berestein, G., and Sood, A. K. (2016). miRNA Deregulation in Cancer Cells and the Tumor Microenvironment. *Cancer Discov.* 6, 235–246. doi:10.1158/2159-8290.CD-15-0893.

Quick, J., and N. Loman. . Thar she blows! Ultra long read method for nanopore sequencing - Oral presentation at London Calling 2017 by Oford Nanopore Technology. Page.

Sahabi, K., Selvarajah, G. T., Abdullah, R., Cheah, Y. K., and Tan, G. C. (2018). Comparative aspects

of microRNA expression in canine and human cancers. *J. Vet. Sci.* 19, 162–171. doi:10.4142/jvs.2018.19.2.162.

Salazar, C., Nagadia, R., Pandit, P., Cooper-White, J., Banerjee, N., Dimitrova, N., et al. (2014). A novel saliva-based microRNA biomarker panel to detect head and neck cancers. *Cell. Oncol. (Dordr).* 37, 331–338. doi:10.1007/s13402-014-0188-2.

Sanford, J. A., and Gallo, R. L. (2013). Functions of the skin microbiota in health and disease. *Semin. Immunol.* 25, 370–377. doi:10.1016/j.smim.2013.09.005

Schlieben, P., Meyer, A., Weise, C., Bondzio, A., Einspanier, R., Gruber, A. D., et al. (2012). Differences in the proteome of high-grade versus low-grade canine cutaneous mast cell tumours. *Vet. J.* 194, 210–214. doi:10.1016/j.tvjl.2012.04.002.

Schwartzberg, L. S., Horinouchi, H., Chan, D., Chernilo, S., Tsai, M. L., Isla, D., et al. (2020). Liquid biopsy mutation panel for non-small cell lung cancer: analytical validation and clinical concordance. *NPJ Precis. Oncol.* 4, 15. doi:10.1038/s41698-020-0118-x.

Schwarzenbach, H., Hoon, D. S. B., and Pantel, K. (2011). Cell-free nucleic acids as biomarkers in cancer patients. *Nat. Rev. Cancer* 11, 426–437. doi:10.1038/nrc3066.

Shahi, S. K., Freedman, S. N., and Mangalam, A. K. (2017). Gut microbiome in multiple sclerosis: The players involved and the roles they play. *Gut Microbes* 8, 607–615. doi:10.1080/19490976.2017.1349041.

Sharma, P., Ludwig, S., Muller, L., Hong, C. S., Kirkwood, J. M., Ferrone, S., et al. (2018). Immunoaffinity-based isolation of melanoma cell-derived exosomes from plasma of patients with melanoma. *J. Extracell. Vesicles* 7, 1435138. doi:10.1080/20013078.2018.1435138.

Si, W., Shen, J., Zheng, H., and Fan, W. (2019). The role and mechanisms of action of microRNAs in

cancer drug resistance. *Clin. Epigenetics* 11, 25. doi:10.1186/s13148-018-0587-8.

Sitar, S., Kejžar, A., Pahovnik, D., Kogej, K., Tušek-Žnidarič, M., Lenassi, M., et al. (2015). Size Characterization and Quantification of Exosomes by Asymmetrical-Flow Field-Flow Fractionation. *Anal. Chem.* 87, 9225–9233. doi:10.1021/acs.analchem.5b01636.

Sivan, A., Corrales, L., Hubert, N., Williams, J. B., Aquino-Michaels, K., Earley, Z. M., et al. (2015). Commensal Bifidobacterium promotes antitumor immunity and facilitates anti-PD-L1 efficacy. *Science* 350, 1084–1089. doi:10.1126/science.aac4255.

Śmiech, A., Lsopuszyński, W., Ślaska, B., Bulak, K., and Jasik, A. (2019). Occurrence and distribution of canine cutaneous mast cell tumour characteristics among predisposed breeds. *J. Vet. Res.* 63, 141–148. doi:10.2478/jvetres-2019-0002.

Sódar, B. W., Kittel, Á., Pálóczi, K., Vukman, K. V., Osteikoetxea, X., Szabó-Taylor, K., et al. (2016). Low-density lipoprotein mimics blood plasma-derived exosomes and microvesicles during isolation and detection. *Sci. Rep.* 6, 24316. doi:10.1038/srep24316.

Soung, Y. H., Ford, S., Zhang, V., and Chung, J. (2017). Exosomes in cancer diagnostics. *Cancers (Basel).* 9, 8. doi:10.3390/cancers9010008.

Srivastava, A., Amreddy, N., Pareek, V., Chinnappan, M., Ahmed, R., Mehta, M., et al. (2020). Progress in extracellular vesicle biology and their application in cancer medicine. *Wiley Interdiscip. Rev. Nanomedicine Nanobiotechnology* 12. doi:10.1002/wnan.1621.

Stanclift, R. M., and Gilson, S. D. (2008). Evaluation of neoadjuvant prednisone administration and surgical excision in treatment of cutaneous mast cell tumors in dogs. *J. Am. Vet. Med. Assoc.* 232, 53–62. doi:10.2460/javma.232.1.53.

Stranska, R., Gysbrechts, L., Wouters, J., Vermeersch, P., Bloch, K., Dierickx, D., et al. (2018).

Comparison of membrane affinity-based method with size-exclusion chromatography for isolation of exosome-like vesicles from human plasma. *J. Transl. Med.* 16, 1. doi:10.1186/s12967-017-1374-6.

Stückrath, I., Rack, B., Janni, W., Jäger, B., Pantel, K., and Schwarzenbach, H. (2015). Aberrant plasma levels of circulating miR-16, miR-107, miR-130a and miR-146a are associated with lymph node metastasis and receptor status of breast cancer patients. *Oncotarget* 6, 13387–13401. doi:10.18632/oncotarget.3874.

Takeuchi, Y., Fujino, Y., Watanabe, M., Takahashi, M., Nakagawa, T., Takeuchi, A., et al. (2013). Validation of the prognostic value of histopathological grading or c-kit mutation in canine cutaneous mast cell tumours: A retrospective cohort study. *Vet. J.* 196, 492–498. doi:10.1016/j.tvjl.2012.11.018.

Takov, K., Yellon, D. M., and Davidson, S. M. (2018). Comparison of small extracellular vesicles isolated from plasma by ultracentrifugation or size-exclusion chromatography: yield, purity and functional potential. *J. Extracell. Vesicles* 8, 1560809. doi:10.1080/20013078.2018.1560809.

Tamlin, V. S., Bottema, C. D. K., and Peaston, A. E. (2020). Comparative aspects of mast cell neoplasia in animals and the role of KIT in prognosis and treatment. *Vet. Med. Sci.* 6, 3–18. doi:10.1002/vms3.201.

Taylor, D. D., and Shah, S. (2015). Methods of isolating extracellular vesicles impact down-stream analyses of their cargoes. *Methods* 87, 3–10. doi:10.1016/j.ymeth.2015.02.019.

Théry, C., Witwer, K. W., Aikawa, E., Alcaraz, M. J., Anderson, J. D., Andriantsitohaina, R., et al. (2018). Minimal information for studies of extracellular vesicles 2018 (MISEV2018): a position statement of the International Society for Extracellular Vesicles and update of the MISEV2014

guidelines. *J. Extracell. Vesicles* 7, 1535750. doi:10.1080/20013078.2018.1535750.

Tominaga, N., Katsuda, T., and Ochiya, T. (2015). Micromanaging of tumor metastasis by extracellular vesicles. *Semin. Cell Dev. Biol.* 40, 52–59. doi:10.1016/j.semcdb.2015.02.016.

Turri-Zanoni, M., Medicina, D., Lombardi, D., Ungari, M., Balzarini, P., Rossini, C., et al. (2013). Sinonasal mucosal melanoma: Molecular profile and therapeutic implications from a series of 32 cases. *Head Neck* 35, 1066–1077. doi:10.1002/hed.23079.

Ushio, N., Rahman, M. M., Maemura, T., Lai, Y.-C., Iwanaga, T., Kawaguchi, H., et al. (2019). Identification of dysregulated microRNAs in canine malignant melanoma. *Oncol. Lett.* 17, 1080–1088. doi:10.3892/ol.2018.9692.

Vail DM, Thamm DH, Liptak JM. Withrow and MacEwen's Small Animal Clinical Oncology. Elsevier, 2019, 6th Edition.

Valent, P., Horny, H. P., Escribano, L., Longley, B. J., Li, C. Y., Schwartz, L. B., et al. (2001). Diagnostic criteria and classification of mastocytosis: a consensus proposal. *Leuk. Res.* 25, 603–625. doi:10.1016/s0145-2126(01)00038-8.

Van Deun, J., Mestdagh, P., Agostinis, P., Akay, Ö., Anand, S., Anckaert, J., et al. (2017). EV-TRACK: Transparent reporting and centralizing knowledge in extracellular vesicle research. *Nat. Methods* 14, 228–232. doi:10.1038/nmeth.4185.

Vasconcelos, M. H., Caires, H. R., Ābols, A., Xavier, C. P. R., and Linē, A. (2019). Extracellular vesicles as a novel source of biomarkers in liquid biopsies for monitoring cancer progression and drug resistance. *Drug Resist. Updat.* 47, 100647. doi:10.1016/j.drup.2019.100647.

Vasudevan, S., Tong, Y., and Steitz, J. A. (2007). Switching from repression to activation: MicroRNAs can up-regulate translation. *Science* 318, 1931–1934.

doi:10.1126/science.1149460.

Vaswani, K., Koh, Y. Q., Almughlliq, F. B., Peiris, H. N., and Mitchell, M. D. (2017). A method for the isolation and enrichment of purified bovine milk exosomes. *Reprod. Biol.* 17, 341–348. doi:10.1016/j.repbio.2017.09.007.

Veenstra, T. D., Prieto, D. A., and Conrads, T. P. (2004). Proteomic patterns for early cancer detection. *Drug Discov. Today* 9, 889–897. doi:10.1016/S1359-6446(04)03246-5.

Villavicencio-Diaz, T. N., Rodriguez-Ulloa, A., Guirola-Cruz, O., and Perez-Riverol, Y. (2014). Bioinformatics Tools for the Functional Interpretation of Quantitative Proteomics Results. *Curr. Top. Med. Chem.* 14, 435–449. doi:10.2174/1568026613666131204105110.

Wagner, S., Willenbrock, S., Nolte, I., and Escobar, H. M. (2013). Comparison of non-coding RNAs in human and canine cancer. *Front. Genet.* 4, 46. doi:10.3389/fgene.2013.00046.

Wang, K., Zhang, S., Weber, J., Baxter, D., and Galas, D. J. (2010). Export of microRNAs and microRNA-protective protein by mammalian cells. *Nucleic Acids Res.* 38, 7248–7259. doi:10.1093/nar/gkq601.

Wang, Y., and Qin, H. (2018). miR-338-3p targets RAB23 and suppresses tumorigenicity of prostate cancer cells. *Am. J. Cancer Res.* 8, 2564–2574.

Wang, Z., Mascarenhas, N., Eckmann, L., Miyamoto, Y., Sun, X., Kawakami, T., et al. (2017). Skin microbiome promotes mast cell maturation by triggering stem cell factor production in keratinocytes. *J. Allergy Clin. Immunol.* 139, 1205-1216.e6. doi:10.1016/j.jaci.2016.09.019.

Weishaar, K. M., Thamm, D. H., Worley, D. R., and Kamstock, D. A. (2014). Correlation of nodal mast cells with clinical outcome in dogs with mast cell tumour and a proposed classification system for the evaluation of node metastasis. *J. Comp. Pathol.* 151, 329–338.

doi:10.1016/j.jcpa.2014.07.004.

Welle, M. M., Bley, C. R., Howard, J., and Rüfenacht, S. (2008). Canine mast cell tumours: A review of the pathogenesis, clinical features, pathology and treatment. *Vet. Dermatol.* 19, 321–339. doi:10.1111/j.1365-3164.2008.00694.x.

Whiteside, T. L. (2016). Exosomes and tumor-mediated immune suppression. *J. Clin. Invest.* 126, 1216–1223. doi:10.1172/JCI81136.

Wilson, C. R., Regnier, F. E., Knapp, D. W., Raskin, R. E., Andrews, D. A., and Hooser, S. B. (2008). Glycoproteomic profiling of serum peptides in canine lymphoma and transitional cell carcinoma. *Vet. Comp. Oncol.* 6, 171–181. doi:10.1111/j.1476-5829.2008.00158.x.

Wisgrill, L., Lamm, C., Hartmann, J., Preißing, F., Dragosits, K., Bee, A., et al. (2016). Peripheral blood microvesicles secretion is influenced by storage time, temperature, and anticoagulants. *Cytometry A* 89, 663–672. doi:10.1002/cyto.a.22892.

Withrow, S., Vail, D., and Page, R. (2012). *Withrow and MacEwen's Small Animal Clinical Oncology*. 5th Edition. , ed. D. Vail Saunders.

Wong, S. H., and Yu, J. (2019). Gut microbiota in colorectal cancer: mechanisms of action and clinical applications. *Nat. Rev. Gastroenterol. Hepatol.* 16, 690–704. doi:10.1038/s41575-019-0209-8.

Wu, M., Ouyang, Y., Wang, Z., Zhang, R., Huang, P. H., Chen, C., et al. (2017). Isolation of exosomes from whole blood by integrating acoustics and microfluidics. *Proc. Natl. Acad. Sci. U. S. A.* 114, 10584–10589. doi:10.1073/pnas.1709210114.

Xavier, C. P. R., Caires, H. R., Barbosa, M. A. G., Bergantim, R., Guimarães, J. E., and Vasconcelos, M. H. (2020a). The Role of Extracellular Vesicles in the Hallmarks of Cancer and Drug

Resistance. *Cells* 9, 1141. doi:10.3390/cells9051141.

Xavier, J. B., Young, V. B., Skufca, J., Ginty, F., Testerman, T., Pearson, A. T., et al. (2020b). The Cancer Microbiome: Distinguishing Direct and Indirect Effects Requires a Systemic View. *Trends in Cancer* 6, 192–204. doi:10.1016/j.trecan.2020.01.004.

Yang, D., Zhang, W., Zhang, H., Zhang, F., Chen, L., Ma, L., et al. (2020). Progress, opportunity, and perspective on exosome isolation - Efforts for efficient exosome-based theranostics. *Theranostics* 10, 3684–3707. doi:10.7150/thno.41580.

Yarbrough, W. G., Slebos, R. J. C., and Liebler, D. (2006). Proteomics: Clinical applications for head and neck squamous cell carcinoma. *Head Neck* 28, 549–558. doi:10.1002/hed.20357.

Yoshizawa, J. M., Schafer, C. A., Schafer, J. J., Farrell, J. J., Paster, B. J., Wong, D. T. W. (2013). Salivary biomarkers: toward future clinical and diagnostic utilities. *Clin Microbiol Rev.* 26, 781-91. doi: 10.1128/CMR.00021-13.

Yuana, Y., Sturk, A., and Nieuwland, R. (2013). Extracellular vesicles in physiological and pathological conditions. *Blood Rev.* 27, 31–39. doi:10.1016/j.blre.2012.12.002.

Zamani-Ahmadmahmudi, M., Nassiri, S. M., and Rahbarghazi, R. (2014). Serological proteome analysis of dogs with breast cancer unveils common serum biomarkers with human counterparts. *Electrophoresis* 35, 901–910. doi:10.1002/elps.201300461.

Zeeuwen, P. L. J. M., Kleerebezem, M., Timmerman, H. M., and Schalkwijk, J. (2013). Microbiome and skin diseases. *Curr. Opin. Allergy Clin. Immunol.* 13, 514–520. doi:10.1097/ACI.0b013e328364ebeb.

Zhang, D. Y., Ye, F., Gao, L., Liu, X., Zhao, X., Che, Y., et al. (2009). Proteomics, pathway array and signaling network-based medicine in cancer. *Cell Div.* 4,20. doi:10.1186/1747-1028-4-20.

Zhang, X., Liu, Q., Liao, Q., and Zhao, Y. (2020). Pancreatic cancer, gut microbiota, and therapeutic efficacy. *J. Cancer* 11, 2749–2758. doi:10.7150/jca.37445.

Zhang, Z., Yin, J., Yang, J., Shen, W., Zhang, C., Mou, W., et al. (2016). miR-885-5p suppresses hepatocellular carcinoma metastasis and inhibits Wnt/β-catenin signaling pathway. *Oncotarget* 7, 75038-75051. doi:10.18632/oncotarget.12602.

Zhao, X., and Chu, J. (2018). Microrna-379 suppresses cell proliferation, migration and invasion in nasopharyngeal carcinoma by targeting tumor protein D52. *Exp. Ther. Med.* 16, 1232–1240. doi:10.3892/etm.2018.6302.

Zhu, Y., Wen, X., and Zhao, P. (2018). Microrna-365 inhibits cell growth and promotes apoptosis in melanoma by targeting BCL2 and cyclin D1 (CCND1). *Med. Sci. Monit.* 24, 3679–3692. doi:10.12659/MSM.909633.

List of papers published, submitted or in preparation

Published paper

Zamarian, V., Ferrari, R., Stefanello, D., Ceciliani, F., Grieco, V., Minozzi, G., Chiti, L.E., Arigoni, M., Calogero, R., Lecchi, C. (2020). miRNA profiles of canine cutaneous mast cell tumours with early nodal metastasis and evaluation as potential biomarkers. *Sci Rep*. 10(1):18918. doi: 10.1038/s41598-020-75877-x.

Zamarian, V., Catozzi, C., Ressel, L., Finotello, R., Vilafranca, M., Altamira, J., Lecchi, C. (2019). MicroRNA Expression in Formalin-Fixed, Paraffin-Embedded Samples of Canine Cutaneous and Oral Melanoma by RT-qPCR. *Vet. Pathol*. 56:848-855. doi: 10.1177/0300985819868646.

Zamarian V., Catozzi C., Cuscó A., Stefanello D., Ferrari R., Ceciliani F., Francino O., Sánchez A., Grieco V., Zani D., Talenti A., Crepaldi P., Lecchi C. (2020). Characterization of skin surface and dermal microbiota in dogs with mast cell tumor. *Sci Rep*. 10:12634. doi: 10.1038/s41598-020-69572-0.

Manuscripts submitted

Zamarian, V., Stefanello, V., Ferrari, R., Chiti, L.E., Grieco, V., Ceciliani, F., Lecchi, C. Salivary miR-885 as potential minimally invasive biomarker to detect mast cell tumor in dogs. **[Manuscript submitted – Veterinary Pathology – ID: VET-20-FLM-0334]**

Zamarian, V., Stefanello, D., Grieco, V., Ferrari, R., Milanesi, S., Ceciliani, F., Lecchi, C. Set up of a method for purification, quantification and characterization of exosomes from plasma of dogs with mast cell tumor. **[Manuscript submitted – Veterinary Pathology – ID: VET-20-BC-0369]**

Other manuscripts not related to the present thesis project

Bardi, E., Stefano Brizzola, S., Ravasio, G., Romussi, S., Dall'Ara, P., **Zamarian, V.,** Arigoni, M., Calogero, R. A., Lecchi, C. Candidate biomarkers of acute surgical pain and inflammation in turtles: circulating miR-499-3p and miR-203-5p in Trachemys scripta after elective gonadectomy. **[Manuscript submitted – Scientific Reports – ID: 77817749-a32c-47aa-83fa-de0bb3bfaf94]**

Sauerwein, H., Blees, T., **Zamarian, V.,** Catozzi, C., Müller, U., Sadri, H., Dänicke, S., Frahm, J., Ceciliani, F. (2020). Acute phase proteins and markers of oxidative status in water buffalos during

the transition from late pregnancy to early lactation. *Vet Immunol Immunopathol*. 228:110113. doi: 10.1016/j.vetimm.2020.110113.

Webb, L.A., Ghaffari, M.H., Sadri, H., Schuh, K., **Zamarian, V.,** Koch, C., Trakooljul, N., Wimmers, K., Lecchi, C., Ceciliani, F. and Sauerwein, H. (2020). Profiling of circulating microRNA and pathway analysis in normal- versus over-conditioned dairy cows during the dry period and early lactation. *J. Dairy Sci*. 103:9534-9547. doi: 10.3168/jds.2020-18283.

Addis, M.F., Maffioli, E.M., Ceciliani, F., Tedeschi, G., **Zamarian, V.,** Tangorra, F., Albertini, M., Piccinini, R., Bronzo, V. (2020). Influence of subclinical mastitis and intramammary infection by coagulase-negative staphylococci on the cow milk peptidome. *J Proteomics*. 226:103885. doi: 10.1016/j.jprot.2020.103885.

Lecchi, C., **Zamarian, V.,** Borriello, G., Galiero, G., Grilli, G., Caniatti, M., D'Urso, E.S, Roccabianca, P., Perego, R., Minero, M., Legnani, S., Calogero, R., Arigoni, M., Ceciliani, F. (2020). Identification of Altered miRNAs in Cerumen of Dogs Affected by Otitis Externa. *Front Immunol.* 11:914. doi: 10.3389/fimmu.2020.00914.

Lecchi, C., **Zamarian, V.,** Gini, C., Avanzini, C., Polloni, A., Rota Nodari, S., Ceciliani, F. (2020). Salivary microRNAs are potential biomarkers for the accurate and precise identification of inflammatory response after tail docking and castration in piglets. *J Anim Sci*. 98:skaa153. doi: 10.1093/jas/skaa153.

Catozzi, C., Ávila, G., **Zamarian, V.,** Pravettoni, D., Sala, G., Ceciliani, F., Lacetera, N., Lecchi, C. (2020). In-vitro effect of heat stress on bovine monocytes lifespan and polarization. *Immunobiology*. 225:151888. doi: 10.1016/j.imbio.2019.11.023.

Meroni, G., **Zamarian, V.,** Prussiani, C., Bronzo, V., Lecchi, C., Martino, P.A., Ceciliani, F. (2019). The bovine acute phase protein α1-acid glycoprotein (AGP) can disrupt Staphylococcus aureus biofilm. *Vet Microbiol*. 235:93-100. doi: 10.1016/j.vetmic.2019.06.007.

Lecchi, C., Catozzi, C., **Zamarian, V.,** Poggi, G., Borriello, G., Martucciello, A., Vecchio, D., DeCarlo, E., Galiero, G., Ceciliani, F. (2019). Characterization of circulating miRNA signature in water buffaloes (Bubalus bubalis) during Brucella abortus infection and evaluation as potential biomarkers for non-invasive diagnosis in vaginal fluid. *Sci. Rep*. 9. doi:10.1038/s41598-018-38365-x.

Activities during the Ph.D.

Transferable skills	Year	CFU	Notes
Open access/open data e il mondo delle pubblicazioni	2018		
La valutazione della ricerca: indicatori bibliometrici e peer review	2018		
Research integrity	2018		
How to write a research project - Part 1 and 2	2019		
Tutelare e valorizzare sul mercato i risultati della ricerca	2019		
Communication on new media – Part 1 and 2	2020		
Valorizzare creando impresa: fare spin off in Università degli Studi di Milano - fondazione Unimi	2020		
CV e tecniche di selezione	2020		
Sustainability and Innovation	2020		
Data protection e attività di ricerca scientifica	2020		

Courses	Year	CFU	Notes
Statistic for Veterinary and Animal Science 1	2017	4	Approved exam
Digital Imaging	2018	2	Approved exam
Core Training Corse in Molecular Animal Nutrition (MANNA)	2018		Certificate of attendance
Basic and advanced techniques for optical microscopy in biological and preclinical research	2019	2	Approved exam
Pathology of laboratory animals	2019	2	Approved exam
Migliorare la propria capacità di gestire/parteciparea riunioni e gruppi di lavoro (team work techniques)	2019	2	Approved exam
Winter school ISCCA - flow cytometry for beginners	2019		Certificate of attendance
RNAseq Workshop	2019		Certificate of attendance
Summer School in Omics (MANNA)	2019		Certificate of attendance
Cell and tissue culture: from basic principles to advanced technologies	2020	3	Approved exam
Proteomics tutorials under the framework of molecular animal nutrition (MANNA)	2020		Certificate of attendance

Congress	Year	Abstract title	Notes
ASAS-CSAS Annual Meeting & Trade Show	2018 Vancouver, Canada	Profiling peripheral microRNA in normal-versus over-conditioned dairy cows during dry-off and early lactation	Author in the abstract
London Calling - Nanopore Congress	2018 London	Nanopore sequencing of full-length 16S rRNA gene in low-biomass samples: subclinical mastitis in water buffalo	Author in the abstract
International Mastitis Conference	2018 Milano	Comparison between second and third generation sequencing of water buffalo milk microbiota samples	Author in the abstract
SisVet Congress	2018 Torino	Water buffalo subclinical mastitis: changes of milk microbiota after treatment with *Lactobacillus rhamnosus*	Author in the abstract
ESVONC annual congress (poster)	2019 Frankfurt	Identification of Mast Cell Tumour-associated miRNAs through NGS and qPCR techniques	First author
SisVet congress (oral presentation)	2019 Olbia	Differences in micro RNA expression between mast cell tumour and healthy adjacent tissue	First author
SisVet congress	2019 Olbia	Cytokine expression in water buffalo exudate affected by tuberculosis	Author in the abstract
ASPA congress	2019 Sorrento	Effect of heat stress on monocytes and lymphocytes in dairy cattle	Author in the abstract
ESVONC annual congress **Rescheduled to 2021**	Siracusa	Characterization of skin surface and dermal microbiota in dogs with mast cell tumor	First author

Acknowledgments

I want to thank my lab Team. Thanks to my supervisor, Prof. Cristina Lecchi who helped my professional growth giving me the instruments to be independent. Thanks to Prof. Fabrizio Ceciliani to be ever-present and to help me during these three years. A special thanks to my lab colleagues, Carlotta and Gabriela to be firstly my friends and for being a real team with which I shared unforgettable moments. Thanks also to Chiara and Daria to be my friends and for reminding me of the enthusiasm for learning new things.

A special thanks to all my friends. Thanks, Mariangela to be always present with your unique spirit, even if 900 km separate us. Thanks, Alessandra to be always present and remembering the strength of friendship. Thanks, Tatiana for showing the strength and the confidence that all of us should have.

Thanks to my parents. My mum and my dad raised me, independent, open-minded, and strong, giving me the possibility to become who I am. I love you both.

In the end, thanks to my boyfriend, Marco, with who I share all my life. Thanks to being and to be always present and thanks for being able to show me the right way in the moments in which I felt lost.

La vita non ti dà le persone che vuoi, ti dà le persone di cui hai bisogno: per amarti, per odiarti, per formarti, per distruggerti e per renderti la persona che era destino che fossi